



**HAL**  
open science

# Structuration et contrôle de l'architecture de capsules à coeur liquide à base d'hydrogel d'alginate par association de biopolymères

Ghazi Ben Messaoud

► **To cite this version:**

Ghazi Ben Messaoud. Structuration et contrôle de l'architecture de capsules à coeur liquide à base d'hydrogel d'alginate par association de biopolymères. Alimentation et Nutrition. Université de Lorraine, 2015. Français. NNT : 2015LORR0327 . tel-01752334

**HAL Id: tel-01752334**

**<https://hal.univ-lorraine.fr/tel-01752334>**

Submitted on 29 Mar 2018

**HAL** is a multi-disciplinary open access archive for the deposit and dissemination of scientific research documents, whether they are published or not. The documents may come from teaching and research institutions in France or abroad, or from public or private research centers.

L'archive ouverte pluridisciplinaire **HAL**, est destinée au dépôt et à la diffusion de documents scientifiques de niveau recherche, publiés ou non, émanant des établissements d'enseignement et de recherche français ou étrangers, des laboratoires publics ou privés.



## AVERTISSEMENT

Ce document est le fruit d'un long travail approuvé par le jury de soutenance et mis à disposition de l'ensemble de la communauté universitaire élargie.

Il est soumis à la propriété intellectuelle de l'auteur. Ceci implique une obligation de citation et de référencement lors de l'utilisation de ce document.

D'autre part, toute contrefaçon, plagiat, reproduction illicite encourt une poursuite pénale.

Contact : [ddoc-theses-contact@univ-lorraine.fr](mailto:ddoc-theses-contact@univ-lorraine.fr)

## LIENS

Code de la Propriété Intellectuelle. articles L 122. 4

Code de la Propriété Intellectuelle. articles L 335.2- L 335.10

[http://www.cfcopies.com/V2/leg/leg\\_droi.php](http://www.cfcopies.com/V2/leg/leg_droi.php)

<http://www.culture.gouv.fr/culture/infos-pratiques/droits/protection.htm>



UNIVERSITÉ  
DE LORRAINE



UNIVERSITE DE LORRAINE  
École Nationale Supérieure d'Agronomie et des Industries Alimentaires (ENSAIA)  
Laboratoire d'Ingénierie des Biomolécules (LIBio)

## THESE

Pour obtenir le grade de

**Docteur de l'université de Lorraine**

**Spécialité : Procédés Biotechnologiques et Alimentaires**

**École Doctorale : Sciences et Ingénierie Ressources Procédés Produits Environnement (RP2E)**

# **Structuration et contrôle de l'architecture de capsules à cœur liquide à base d'hydrogel d'alginate par association de biopolymères**

Présentée par

**Ghazi BEN MESSAOUD**

Présentée et soutenue publiquement le 29 Octobre 2015

Devant le jury composé de :

<b>Amparo Chiralt</b>	Professeur, IIAD, Universitat Politècnica de Valencia	Rapporteur
<b>Jérôme Bibette</b>	Professeur, LCMD, ESPCI ParisTech	Rapporteur
<b>Denis Poncelet</b>	Professeur, GEPEA, ONIRIS	Président du jury
<b>Stéphane Desobry</b>	Professeur, LIBio, Université de Lorraine	Directeur de thèse
<b>Laura Sanchez-Gonzalez</b>	Docteur, LIBio, Université de Lorraine	Co-Directrice de thèse
<b>Laurent Probst</b>	PDG, COOKAL SAS	Invité

## **Remerciements**

*Cette thèse a été réalisée au sein du laboratoire d'ingénierie des biomolécules (LIbio).*

*Je tiens en premier lieu à remercier **Stéphane** de m'avoir donné l'opportunité d'effectuer cette thèse ! Je vous remercie de votre confiance et présence durant ces années de thèse. J'ai énormément appris à votre contact sur le plan professionnel mais également humain. Un grand merci !*

*Je tiens également à remercier vivement **Laura**, d'avoir accepté de codiriger cette thèse et d'avoir découvert avec moi ces petits objets mystérieux que sont les capsules à cœur liquide ! Je te remercie pour tes nombreux conseils et tes encouragements tout au long de ce projet qu'on a vu évoluer ensemble des technologies douces à l'incorporation de polymères. Encore merci !*

*Ce travail a été financé par la société Cookal dans le cadre d'une convention CIFRE. Je remercie messieurs **Laurent Probst** et **Patrick Karst** pour la confiance qu'ils m'ont accordé.*

*J'adresse également mes remerciements à **Cécile, Faviola** et tout le personnel de l'entreprise, qui ont contribué au bon déroulement de ce travail.*

*Je remercie également monsieur **Alain Giraud** et la société **Gymnokidi** d'avoir cofinancé une partie de cette thèse.*

*Je souhaite remercier l'Association Nationale de la Recherche et de la Technologie (**ANRT**) d'avoir accepté de financer ce travail de thèse.*

*Je tiens à remercier tous les membres du jury.*

*Je remercie vivement les Professeurs **Amparo Chiralt** et **Jérôme Bibette** pour avoir accepté de juger ce travail en qualité de rapporteurs. Je remercie également le Professeur **Denis Poncelet** et Monsieur **Laurent Probst** d'avoir accepté de prendre part à ce jury.*

*Un grand merci également à **Elmira**, pour sa disponibilité, ses conseils, et sa contribution pour mener à bien cette thèse. Merci d'avoir su me remotiver pendant les moments difficiles !*

*Je tiens à remercier tous mes stagiaires : **Elise, Maeva** et **Nicolas** pour leur contribution à l'avancement de ce projet.*

*Je remercie également, d'abord mes collègues de bureau **Adrien, Nadia, Mariam et Rana** sur qui j'ai pu compter pour leur optimisme et leur bonne humeur.*

*Je remercie tous les thésards 'passés' et 'présents' du laboratoire que j'ai eu l'occasion de côtoyer: **Yoana, Hassan, Mouna, Charlotte, Mahmoud, Ange, Magda, Smail, Jennifer, Marie-***

**Celeste, Majid, Citlalli, Justine, PH** et tous ceux que j'ai oublié de citer (Ne soyez pas vexés, je suis en train de rédiger les derniers mots de ce manuscrit et la fatigue commence à se ressentir) !

Je remercie également **la grande et la petite Carole(s)** pour leur bonne humeur et pour nos discussions scientifiques et techniques... mais pas seulement !

Je remercie également **Aurélie** pour son efficacité et sa réactivité au quotidien et surtout lors de mes inscriptions à la dernière minute aux congrès (Euromat 2013 par exemple).

Je remercie tous les membres du LIBio avec qui j'ai passé des moments agréables au cours de ces années. J'ai vécu au sein du laboratoire une expérience très enrichissante aussi bien sur le plan professionnel que sur le plan humain.

Je remercie toute ma famille, mes parents **Rachid** et **Rafika**, mon frère **Sélim** et ma ~~belle~~-sœur **Emna** qui m'ont toujours soutenu et encouragé. Un grand merci à vous ! Vous êtes un peu loin mais toujours présents dans mes pensées. Un grand merci à **Nana** et à toute la famille.

Enfin je remercie ma **Sonia**, qui est toujours présente à mes côtés pour me soutenir et me donner du courage pour aller de l'avant. Je te remercie pour ta présence et ta patience. Je te remercie d'être tout juste 'mon équilibre'.

# Sommaire

Liste des figures hors publications.....	7
Liste des tableaux hors publications .....	8
Liste des publications et communications.....	9
<b>Introduction et objectifs de l'étude</b> .....	11
<b>Chapitre I: Synthèse bibliographique</b> .....	17
1. Encapsulation .....	19
1.1. Définition .....	19
1.2. Etapes de l'encapsulation .....	20
1.3. Techniques d'encapsulation.....	21
1.4. Microcapsules 'intelligentes' .....	22
1.4.2. Stimuli physiques .....	24
1.4.3. Stimuli biologiques .....	26
1.5. Microcapsules ayant des propriétés d'auto-éclatement .....	27
2. Encapsulation dans une matrice d'alginate .....	29
2.1. L'alginate .....	29
2.2. Historique .....	29
2.3. Origine .....	30
2.4. Structure chimique .....	31
2.5. Propriétés .....	32
2.5.1. Solubilité et stabilité .....	32
2.5.2. Viscosité .....	33
2.5.3. Bioadhésion .....	33
2.6. Gélification de l'alginate .....	33
2.6.1. Généralités .....	34
2.6.2. Gélification ionotropique .....	35
2.6.3. Gélification acide .....	38
2.6.4. Différences entre les hydrogels ionotropiques et acides .....	38
2.6.5. Autres méthodes de gélification .....	39
2.7. Applications des hydrogels d'alginate.....	41
2.8. Techniques d'encapsulation avec de l'alginate .....	43
2.9. Capsules d'alginate à coeur liquide .....	45
2.9.1. Nano-capsules d'alginate .....	45
2.9.2. Microcapsules d'alginate .....	46
2.9.3. Capsules millimétriques d'alginate .....	51
3. Capsules millimétriques intelligentes à base d'alginate .....	55
4. Conclusion.....	56
<b>Chapitre II: Influence de l'agent épaississant sur les propriétés physicochimiques des capsules</b> .....	<b>57</b>
<i>Influence of internal composition on physicochemical properties of alginate aqueous-core capsules</i> .....	61
Abstract.....	62
1. Introduction.....	62
2. Materials and methods.....	65
2.1. Materials.....	65
2.2. Solutions preparation and characterization.....	66

2.3. Alginate systems preparation.....	69
2.3.1. Capsules.....	69
2.3.2. Alginate hydrogels.....	69
2.4. Capsules characterizations.....	70
2.4.1. Measurements of capsule dimensions.....	70
2.3.2. Mechanical stability.....	71
2.3.3. Solutes release.....	71
2.3.4. FTIR spectroscopy.....	72
2.4. Hydrogels characterization.....	72
2.5. Statistical analysis.....	72
3. Results and Discussion.....	73
3.1. Capsules dimensions.....	73
3.2. Capsules mechanical stability.....	74
3.3. Solutes release measurements.....	76
3.4. Rheology of plane hydrogels.....	79
3.5. FTIR spectroscopy.....	83
4. Conclusion.....	85
<b>Chapitre III : Contrôle des propriétés physicochimiques des capsules d'alginate par incorporation de polymère dans la membrane pouvant interagir avec la molécule encapsulée.....</b>	<b>87</b>
<i>Alginate/sodium caseinate aqueous-core capsules: a pH-responsive matrix .....</i>	<i>91</i>
Abstract.....	91
1. Introduction.....	92
2. Materials and methods.....	94
2.1. Materials.....	94
2.2. Capsule preparation.....	94
2.3. Characterization of solutions.....	95
2.3.1. NaAlg-NaCas mixture.....	95
2.3.2. Zeta potential of NaCas solution.....	95
2.3.3. Dye-NaCas interaction.....	95
2.4. Characterization of capsules.....	96
2.4.1. Measurements of capsule size and membrane thickness.....	96
2.4.2. Mechanical study.....	97
2.4.3. Release properties.....	97
2.5. Statistical analysis.....	98
3. Results and Discussion.....	98
3.1. Capsules characterization.....	98
3.2. Mechanical stability.....	101
3.3. Capsule release properties.....	104
3.3.1. Kinetics of dye release.....	105
3.3.2. pH-responsive release mechanism.....	107
4. Conclusion.....	113
References.....	114
<i>Composite alginate/sodium caseinate microspheres for anionic dye removal.....</i>	<i>117</i>
Abstract.....	117
1. Introduction.....	118
2. Material and methods.....	120
2.1. Material.....	120

2.2. Microspheres preparation.....	121
2.3. Capsules characterization.....	121
2.3.1. Optical microscopy.....	121
2.3.2. Size.....	122
2.4. Adsorption studies.....	122
2.4.1. Batch experiments.....	122
2.4.2. Kinetic study.....	123
2.4.3. Influence of initial pH.....	123
2.5. Data modeling.....	123
3. Results and discussion.....	123
3.1. Physicochemical characterization of microspheres.....	123
3.2. Adsorption kinetic study.....	125
3.3. Effect of pH.....	129
4. Conclusion.....	131
<b>Chapitre IV: Amélioration des propriétés barrières des capsules par incorporation d'un polymère pH-sensible.....</b>	<b>133</b>
<i>Physico-chemical properties of alginate/shellac aqueous-core capsules: influence of membrane architecture on riboflavin release.....</i>	<i>137</i>
Abstract.....	137
1. Introduction.....	138
2. Materials and methods.....	141
2.1. Materials.....	141
2.2. Samples preparation.....	142
2.2.1. Solutions preparation.....	142
2.2.2. Capsules preparation.....	143
2.3. Characterization of capsules.....	143
2.3.1. Measurements of capsule size and membrane thickness.....	143
2.3.2. Release properties.....	144
2.4. ATR-FTIR spectroscopy.....	144
2.5. Scanning electronic Microscopy.....	145
3. Results and Discussion.....	145
3.1. Feasibility of shellac incorporation into alginate matrix.....	145
3.2. Capsules structure.....	146
3.3. FTIR spectroscopy.....	154
3.4. Release properties.....	156
4. Conclusion.....	160
<b>Conclusion générale et perspectives.....</b>	<b>161</b>
<b>Références bibliographiques.....</b>	<b>165</b>





## *Liste des figures hors publications*

<b>Figure 1.</b> Représentation schématique d'une microsphère (à gauche) et d'une microcapsule (à droite).....	20
<b>Figure 2.</b> Image futuriste d'une microcapsule multifonctionnelle intelligente.....	22
<b>Figure 3.</b> Illustration schématique de stimuli potentiels qui peuvent influencer la libération à partir des microcapsules.....	23
<b>Figure 4.</b> Evolution d'une microcapsule lors de la dégradation du microgel interne jusqu'à son auto-éclatement. Représentation schématique (a), observation sous microscope confocal laser (b).....	28
<b>Figure 5.</b> Structure chimique de l'alginate de sodium: monomères d'acides uroniques(a), conformation des chaînes (b) et distribution des blocs(c).....	32
<b>Figure 6.</b> Mécanisme de gélification de l'alginate en présence d'ions calcium.....	36
<b>Figure 7.</b> Les points de jonction possibles dans un hydrogel d'alginate. Jonctions GG / GG (a), jonctions GG/MG (b), et jonctions MG/MG (c).....	37
<b>Figure 8.</b> Exemple de biomatériaux développés à partir d'un hydrogel d'alginate. Capsules millimétriques à cœur liquide avec une fine membrane d'alginate(a), microspheres d'alginate obtenues par émulsification (b), nanocapsules d'alginate (c), photo de capsules anisotrope en forme de champignon (d), microfibre pleine (e)et microfibre creuse (f).....	42
<b>Figure 9.</b> Représentation schématique de la formation de nanocapsules d'alginate. Solution d'alginate (a). Incorporation de la phase d'huile contenant le principe actif dissout dans la solution d'alginate (b). Addition de $\text{CaCl}_2$ et formation de la membrane d'alginate à l'interface des gouttelettes d'huile (c). Elimination du solvant, lavage et dispersion des nanocapsules (d).....	46
<b>Figure 10.</b> Schéma de la formation de capsule par polymérisation multicouches. Des couches successives sont déposées à la surface d'un colloïde exposé alternativement à des polymères de charges opposées. La matrice du colloïde est ensuite dissoute pour former une capsule à cœur liquide.....	47
<b>Figure 11.</b> Préparation de microcapsules par microfluidique. Illustration schématique du dispositif microfluidique capillaire (a), photo de la double émulsion H/E/H (b) et structure des capsules à cœur d'huile.....	49
<b>Figure 12.</b> Etapes de préparation de microcapsules d'alginate par émulsification et gélification à l'interface.....	50
<b>Figure 13.</b> Principe de l'encapsulator BUCHI B-395 Pro(a) et photo du jet à la sortie de la buse coaxiale.....	51
<b>Figure 14.</b> Principe de l'électro-coextrusion (a) et de la coextrusion (b).....	52
<b>Figure 15.</b> Etapes de préparation de capsules d'alginate à cœur liquide par polymérisation multicouches.....	53
<b>Figure 16.</b> Principe de l'encapsulation par sphérification inverse.....	54
<b>Figure 17.</b> Exemple de perles gastronomiques Cookal à base de vinaigre balsamique.....	55

*Liste des tableaux hors publications*

<b>Tableau 1.</b> Similitudes et différences entre gels acides et gels ionotropiques.....	39
<b>Tableau 2.</b> Synthèse des méthodes actuelles de production de particules à base d'hydrogel d'alginate.....	44

## Liste des publications et communications

### Articles scientifiques :

- **G. Ben Messaoud**, L. Sánchez-González, L. Probst, C. Jeandel, E. Arab-Tehrany, S. Desobry. Physico-chemical properties of alginate/shellac aqueous-core capsules: influence of membrane architecture on riboflavin release. *Carbohydrate Polymers* 144 (2016) 428-437.
- **G. Ben Messaoud**, L. Sánchez-González, L. Probst, S. Desobry. Influence of internal composition on physicochemical properties of alginate aqueous-core capsules. *Journal of Colloid and Interface Science* 469 (2016) 120-128.
- **G. Ben Messaoud**, L. Sánchez-González, A. Jacquot, L. Probst, S. Desobry. Alginate/sodium caseinate aqueous-core capsules: a pH-responsive matrix. *Journal of Colloid and Interface Science* 440 (2015) 1-8.
- M. Bekhit, L. Sánchez-González, **G. Ben Messaoud**, S. Desobry. Encapsulation of *Lactococcus lactis* subsp. *lactis* on alginate / pectin microbeads: effect of matrix composition on bacterial survival and nisin release. *Journal of Food Engineering* 180 (2016) 1-9.
- R. Kadri<sup>1</sup>, **G. Ben Messaoud**<sup>1</sup>, A. Tamayol, B. Aliakbarian, H.Y. Zhang, M. Hasan, L. Sánchez-González, E. Arab-Tehrany. Preparation and characterization of nanofunctionalized alginate/methacrylated gelatin hybrid hydrogels. *RSC Advances* 6 (2016), 27879 – 27884.
- M. Bekhit, L. Sánchez-González, **G. Ben Messaoud**, S. Desobry. Design of microcapsules containing *Lactococcus lactis* subsp. *lactis* in alginate shell and xanthan gum with nutrients core. *LWT - Food Science and Technology* 68 (2016) 446-453.
- M. Hasan, **G. Ben Messaoud**, F. Michaux, A. Tamayol, C. Khan, B. N. Belhaj, M. Linder, E. Arab-Tehrany. Chitosan-coated liposomes encapsulating curcumin: Study of lipid-polysaccharide interactions and nanovesicles behavior. *RSC Advances* 6 (2016) 45290 - 45304
- M.A Jmel, **G. Ben Messaoud**, M.N Marzouki, M. Mathlouthi, I. Smaali. Physico-chemical characterization and enzymatic functionalization of *Enteromorpha* sp. cellulose. *Carbohydrate Polymers* 135 (2016) 274-279.
- M. Mathlouthi, **G. Ben Messaoud**, B. Rogé. Role of water in the polymorphic transitions of small carbohydrates. *Food Chemistry* 132 (2012) 1630–1637

### Communications orales :

- **G. Ben Messaoud**, L. Sanchez-Gonzalez, Stephane Desobry (2013). *Influence of the thickening agent on mechanical characteristics and release properties of alginate capsules*. **Euromat**, 8-13 Septembre 2013 Seville, Espagne
- L. Sánchez-González, **G. Ben Messaoud**, S. Desobry (2015). Association of biopolymers in microencapsulation to control the release of active molecules. **Colloque Encapsulation/vectorisation des molécules actives, une stratégie dynamique en agro-alimentaire et en pharmacie**. 22 July 2015 Dijon, France.
- M. Bekhit, L. Sánchez-González, **G. Ben Messaoud**, S. Desobry (2015). *Encapsulation of Lactococcus lactis subsp. lactis on alginate / pectin composite microbeads: effect of matrix composition on bacterial survival and nisin release*. **Innovations in Food Packaging, Shelf Life and Food Safety**, 15-17 Septembre, Munich, Germany.
- M. Mathlouthi., **G. Ben Messaoud** and B. Rogé (2010). *Role of water in the polymorphic transitions of small carbohydrates*. **International conference on Water in Food**, 21-23 Mars 2010 Reims, France.

### Communications écrites (posters):

- **G. Ben Messaoud**, L. Sanchez-Gonzalez, R. Kadri and S. Desobry (2015). *Alginate/caseinate microbeads for anionic dye removal from acidic solutions*, Euromat, 20-24 septembre, Varsovie, Pologne.
- **G. Ben Messaoud**, L. Sanchez-Gonzalez, E. Schnepf, L. Probst and S. Desobry (2015). *Physicochemical properties of pH-responsive alginate/shellac aqueous-core capsules*, **5<sup>th</sup> International colloids conference**, 21-24 juin, Amsterdam, Pays-bas.
- **G. Ben Messaoud**, B. Rogé and M. Mathlouthi (2010). *Extraction, purification and physicochemical characterization of polysaccharides of green algae (Ulva sp. and Enteromorpha sp.)*, **6<sup>th</sup> International Conference on Polysaccharides Glycoscience**, 29 septembre -1 Octobre, Prague, République tchèque.

## ***Introduction et objectifs de l'étude***



Les capsules d'alginate à cœur liquide sont des systèmes biphasique (gel / liquide) de structure complexe. Ces capsules trouvent des applications dans des domaines aussi nombreux que variés, allant de la gastronomie moléculaire à la biotechnologie.

Dans ce contexte, l'entreprise 'COOKAL' développe des perles gastronomiques comme élément de décoration ou d'assaisonnement de plats. Ces perles sont préparées par sphérification inverse qui consiste en une extrusion goutte à goutte d'un mélange (contenant du chlorure de calcium) dans un bain de gélification à base d'alginate. Généralement un agent épaississant doit être ajouté à la solution de  $\text{CaCl}_2$  afin de garantir la formation de capsules sphériques et de limiter leur déformation par le cisaillement du bain de gélification.

La fonctionnalité de ces capsules dépend considérablement de leur perméabilité, stabilité mécanique et chimique. Il est donc essentiel de maîtriser les propriétés physicochimiques du produit fini. En général, le contrôle de ces propriétés peut se faire en premier lieu en jouant sur la transition sol-gel de l'alginate par maîtrise de la cinétique de gélification, à savoir les concentrations en chlorure de calcium et en alginate ou par contrôle du temps de gélification (temps de séjour). Cependant, une augmentation de la concentration en chlorure de calcium ou du temps de gélification affecte les qualités sensorielles du produit fini : formation d'une membrane épaisse, amertume, gout salé. D'un autre côté, une augmentation de la concentration en alginate et donc de la viscosité du bain de gélification affecte l'entrée des gouttes du mélange dans le bain de gélification.

Il existe des approches alternatives qui permettent de renforcer la structure de la membrane d'alginate. En effet, l'incorporation d'un second polymère dans un hydrogel d'alginate, qui peut être soit juste dispersé dans la matrice finale ce qui aboutit à la formation d'un hydrogel semi-interpénétré (semi-IPN), soit réticulé avec le même ou un second agent réticulant et dans ce cas on parle d'un réseau interpénétré (full-IPN). Le second polymère peut être également appliqué comme enrobage ou revêtement externe (coating).



Cette thèse a donc pour objectif d'étudier les propriétés physicochimiques de capsules à cœur liquide à base d'hydrogel d'alginate et de contrôler leur perméabilité et stabilité mécanique par association avec des biopolymères.

Le manuscrit s'organise comme suit :

Dans une première partie, les techniques d'encapsulation et des exemples de microcapsules 'intelligentes' répondant à différents types de stimuli chimiques, physiques ou biologiques sont présentés. S'ensuit une présentation détaillée de la structure chimique, des propriétés et des mécanismes de gélification de l'alginate qui est le polymère utilisé dans les différents travaux d'encapsulation au cours de cette thèse. Enfin, les différentes techniques de préparation de capsules d'alginate à cœur liquide à différentes échelles sont présentées avec un intérêt particulier pour les capsules millimétriques.

Dans une seconde partie, l'influence de la composition du cœur liquide et plus précisément du polymère utilisé pour ajuster la viscosité de la solution de  $\text{CaCl}_2$  sur la perméabilité et la stabilité mécanique de la membrane d'alginate ont été étudiées. Les propriétés mécaniques des capsules et plus précisément de la membrane (module de Young surfacique) ont été corrélées avec les propriétés viscoélastiques d'hydrogels plans d'alginate obtenues par rhéologie oscillatoire aux faibles amplitudes.

Un troisième travail a consisté à élaborer des capsules composites avec une membrane alginate/caséinate de sodium. L'influence de la concentration en caséinate de sodium et du pH de préparation a été étudiée. Les capsules composites ont montré un renforcement des propriétés mécaniques qui peut être expliqué par des interactions entre les groupements carboxyliques du mélange protéique et les cations calcium, mais aussi par des interactions électrostatiques entre les groupements carboxyliques de l'alginate et les groupements amines du caséinate de sodium. La cinétique de diffusion de la rouge cochenille (utilisée comme molécule modèle dans cette

étude) a montré un profil de libération pH-dépendant. Cette libération contrôlée est expliquée par une adsorption membranaire du colorant par des interactions électrostatiques entre les groupements sulfonates et amines du caséinate.

Comme perspective à cette étude, des microsphères (hydrogels sphériques) à base d'alginate et de caséinate de sodium ont été développées en utilisant un équipement basé sur une technologie de buse vibrante combinée à un potentiel électrostatique. Trois types de systèmes ont été synthétisés : microsphères simples (alginate), composites (alginate/caséinate de sodium) et composites enrobées avec une couche de caséinate de sodium. L'efficacité des microsphères pour l'élimination des colorants azoïques (Rouge cochenille et noir amido) a été évaluée. Ce type de système trouve des applications dans l'élimination des colorants à partir des rejets industriels (textile, plasturgie, etc...) par un mécanisme d'adsorption.

Dans une quatrième partie, la gomme laque qui est un additif alimentaire (E904) issu de la sécrétion d'une cochenille asiatique (*Kerria lacca*) a été incorporée dans la membrane d'alginate ou comme revêtement externe. L'influence de la concentration de la gomme laque ainsi que son mécanisme de préparation (précipitation acide ou réticulation avec les ions calcium) a été étudiée. L'optimisation de l'architecture des capsules alginate/gomme laque a permis d'améliorer les propriétés barrières de la membrane d'alginate vis-à-vis des molécules de faible masse moléculaire (riboflavine dans cette étude).

Enfin, une conclusion générale des différentes expériences menées au cours de cette thèse ainsi que les principales perspectives susceptibles d'apporter un complément scientifique à ces travaux sont discutées.



# ***Chapitre I:***

## ***Synthèse bibliographique***



# 1. Encapsulation

## 1.1.Définition

Généralement, l'encapsulation est définie comme un procédé physicochimique ou mécanique de piégeage d'un ou plusieurs objets au sein d'un matériau en vue de son immobilisation, sa protection, sa structuration, sa fonctionnalisation et le contrôle de son transport et de sa libération (Vandamme, Poncelet, & Subra-Paternault, 2007).

L'encapsulation permet de produire des particules d'une taille allant de quelques nanomètres à quelques millimètres. Cette large gamme de taille ainsi que la diversité des matériaux qui peuvent être utilisés pour former la matrice d'encapsulation (protéines, polysaccharides lipides, ...matériaux organique/inorganique, hybrides) offrent une large gamme d'applications et en constante évolution dans plusieurs domaines:

- Alimentaire : Masquage d'odeurs, couleurs et arômes, libération contrôlée de composés actifs, contrôle de réactions d'oxydation (encapsulation d'antioxydants) ; encapsulation d'agents antimicrobiens.
- La biotechnologie : Encapsulation d'ADN, de peptides et surtout de cellules afin de les protéger de l'environnement externe tout en assurant une perméabilité sélective de la matrice d'encapsulation afin de garantir la diffusion des nutriments nécessaires à la prolifération cellulaire vers l'intérieur de la capsules.
- Pharmaceutique : Libération contrôlée de médicaments.
- Cosmétique
- Environnement et énergie : Elimination de colorants et métaux lourds à partir des eaux usées.(Nghah, Teong, & Hanafiah, 2011)

Généralement, deux structures peuvent exister : les microsphères et les microcapsules (Figure 1). Les premières sont formées d'une matrice continue de polymère au sein de laquelle le principe actif est dissout ou dispersé (système matriciel). Les microcapsules sont quant à elles constituées d'un cœur de principe actif sous forme liquide, solide ou éventuellement gazeux, entouré par une membrane de matériau enrobant (système réservoir).

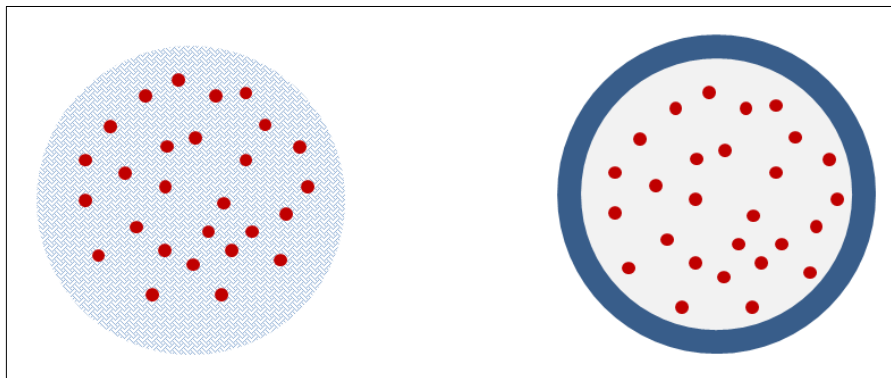


*Figure 1. Représentation schématique d'une microsphère (à gauche) et d'une microcapsule (à droite).*

Selon le domaine d'applications des microparticules, des propriétés de biocompatibilité et/ou de biodégradabilité seront requises. Les lipides (acides gras, alcools gras, glycérides, cholestérol...) seront plutôt utilisés sous forme solide, de même que les cires naturelles ou minérales. D'autres molécules tels que des stabilisants (tensioactifs, dispersants, antimottants...) ou des cryoprotecteurs peuvent être ajoutés à la formulation des microparticules. L'ensemble des composés va intervenir sur le profil de libération de la matière active.

## **1.2. Etapes de l'encapsulation**

D'une manière générale, l'encapsulation se réalise en trois grandes étapes : La première étape consiste à incorporer le principe actif dans le matériau d'encapsulation par dissolution ou

dispersion (cas de liquide) ou par agglomération ou adsorption (cas de poudre). S'ensuit une étape de dispersion ou de pulvérisation des particules contenant le matériau d'encapsulation et le principe actif. Enfin, les microcapsules (microparticules) sont stabilisées par différents types de procédés: chimiques (polymérisation), physicochimiques (gélification, coacervation), ou physiques (évaporation, solidification, coalescence) (Vandamme et al., 2007).

### **1.3. Techniques d'encapsulation**

Il existe plusieurs méthodes de classification des techniques d'encapsulation. En effet les techniques peuvent être classées en fonction de la nature du procédé ou du milieu dispersant utilisé (Madene, 2006) (Legrand et al., 2007):

#### En fonction de la nature du procédé :

- Techniques chimiques : coacervation, co-cristallisation, inclusion moléculaire et polymérisation interfaciale)
- Techniques mécaniques ou physiques : atomisation, lyophilisation, séchage en lit fluidisé, atomisation à froid et extrusion)

#### En fonction de la nature du milieu dispersant utilisé lors de la préparation des capsules :

- En milieu liquide : coacervation, émulsification-évaporation, gélification de gouttes, polycondensation interfaciale et la polymérisation en milieu dispersé.
- En milieu gazeux : enrobage en lit d'air fluidisé « Spray-Coating » et la nébulisation / séchage « Spray-Drying ».
- En milieu supercritique :

En utilisant le fluide supercritique en tant que non-solvant: procédés SFA (Supercritical Fluid Antisolvent) ou en tant que solvant RESS (« Rapid Expansion of Supercritical Solutions »)

- En absence de solvant : extrusion sphéronisation, et congélation de gouttes «spray congealing»



Néanmoins, les techniques d'encapsulation sont très diverses et en constante évolution ce qui rend leur classification parfois ambiguë (Vandamme et al., 2007).

#### 1.4. Microcapsules 'intelligentes'

Le développement de microcapsules 'intelligentes' est un défi important dans le domaine de l'encapsulation. Dans le cas idéal, les capsules devraient ressembler dans leur complexité à une cellule vivante, où les multi-compartiments pourraient interagir, s'échanger des produits chimiques, recevoir de l'énergie, effectuer un travail mécanique, modifier les propriétés chimiques et physiques, tout cela en réponse à des stimuli environnementaux (Figure 2). Cette image pour l'instant futuriste pourrait être réalisable dans un futur pas aussi lointain qu'on puisse l'imaginer grâce notamment aux progrès réalisés dans ce domaine (Motornov, Roiter, Tokarev, & Minko, 2010).

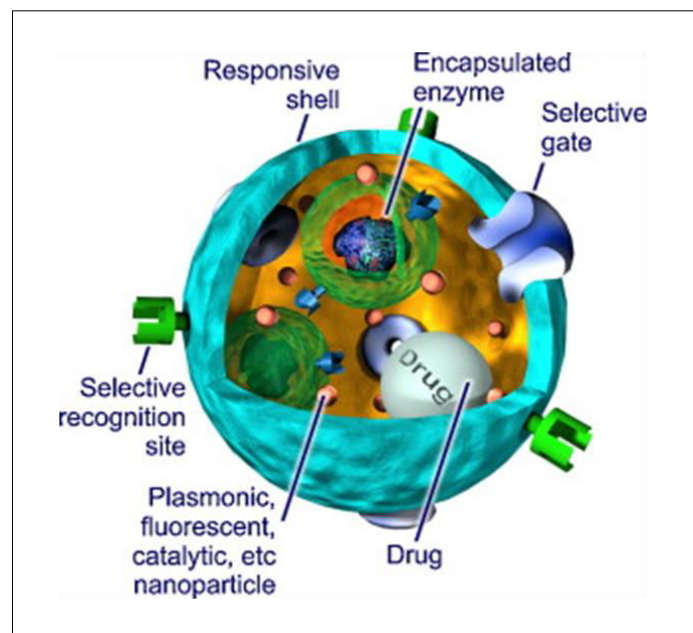


**Figure 2.** Image futuriste d'une microcapsule multifonctionnelle intelligente (Motornov et al., 2010).

Les microcapsules intelligentes présentent un large spectre d'applications surtout dans le domaine médical pour des applications de libération contrôlée (Delcea, Möhwald, & Skirtach, 2011).

L'objectif est de développer des microcapsules intelligentes qui protègent leur contenu contre les influences extérieures et le libèrent uniquement en réponse à certaines conditions environnementales (stimuli). Ces stimuli peuvent être chimiques (pH, force ionique,...), physiques (température, laser, champs magnétiques, stress mécanique, ultrasons,...) ou biologiques (enzyme, récepteurs) (figure 3).

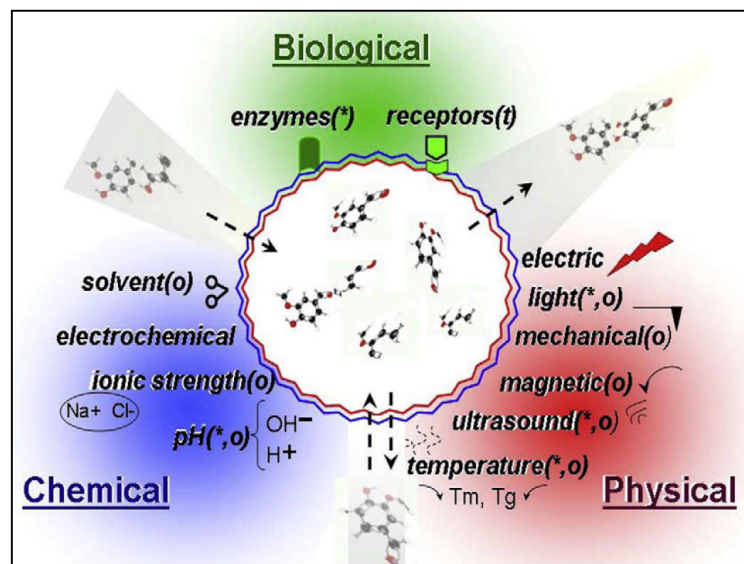


**Figure 3.** Illustration schématique de stimuli potentiels qui peuvent influencer la libération à partir des microcapsules (Delcea et al., 2011).

Les microcapsules dites « intelligentes » peuvent donc réagir à ces stimuli extérieurs et subir des modifications relativement importantes de leur structure et de leurs propriétés telles que la perméabilité ou encore la résistance mécanique.

## **1.4.1. Les stimuli chimiques**

### **1.4.1.1.Le pH**

Ce type de microcapsules comprend généralement des groupements ioniques qui peuvent accepter/donner des protons en réponse à un changement de pH : la variation du degré d'ionisation modifie la charge nette ce qui peut causer des transitions brusques de volume.

Lorsque le pH est modifié par rapport au pKa des polymères constituant la membrane polyélectrolyte de capsules, une protonation / déprotonation des groupements chargés se déroule. La protonation conduit par exemple à une forte répulsion qui se traduit par un gonflement des capsules; cela aboutit à l'augmentation de la perméabilité. D'autre part, la déprotonation provoque le rétrécissement de la membrane et donc une diminution de la perméabilité. Le plus grand avantage de cette adaptation au milieu extérieur est sa réversibilité (Delcea et al., 2011).

### **1.4.1.2.La force ionique**

La force ionique peut influencer la structure des microcapsules et en particulier les microcapsules avec une membrane polyélectrolyte obtenue par polymérisation multicouches. Les modifications de la perméabilité induite par un sel peuvent être expliquées par la réduction des attractions électrostatiques à l'intérieur des multicouches ou par la formation de cavités dans la membrane (Delcea et al., 2011).

## **1.4.2. Stimuli physiques**

### **1.4.2.1.La température**

Les microparticules sensibles à la température sont des systèmes répondant à une diminution ou à une augmentation de la température. Les microgels sphériques physiques subissent une

transition gel-sol à une température critique alors que les microgels chimiques répondent par un changement de volume.

Dans le cas de capsules avec une membrane polyélectrolyte, une réduction significative de la perméabilité accompagne la variation de la température. Elle est due généralement à des forces hydrophobes. Ce phénomène se passe généralement à une température au-dessus de la température de transition vitreuse (Tg) de la membrane polyélectrolytes.

La réduction de volume de la membrane par expulsion de l'eau (déshydratation) est accompagnée par son durcissement et par l'augmentation de sa résistance mécanique (Delcea et al., 2011).

#### **1.4.2.2. Contrainte mécanique**

La rupture de la membrane des microcapsules et la libération de leur contenu peuvent être obtenues par application d'une contrainte mécanique au niveau de la membrane des microcapsules. Dans ce contexte, un groupe de chercheurs a étudié le mécanisme de libération à partir de microcapsules polyélectrolytes soumises à des contraintes mécaniques en combinant la microscopie de fluorescence avec la spectroscopie de force en utilisant la microscopie à force atomique (AFM) (Fernandes, Delcea, Skirtach, Möhwald, & Fery, 2010).

#### **1.4.2.3. Energie Laser**

Le principe est basé sur l'incorporation au niveau de la membrane des microcapsules des nanoparticules de métaux nobles qui absorbent efficacement l'énergie laser pour la convertir en chaleur. En raison du chauffage local autour des nanoparticules, la membrane devient transitoirement mobile ce qui permet de contrôler sa perméabilité d'une manière réversible. En effet, si l'irradiation est arrêtée, la production de chaleur est stoppée et le complexe polymérique autour des nanoparticules refroidit rapidement, revenant la membrane à son état imperméable.

#### **1.4.2.4.Ultrasons**

L'incorporation de nanoparticules de ZnO au niveau des hydrogels et plus particulièrement au niveau de la membrane des microcapsules a montré la possibilité de l'ouverture de microcapsules et de libération de leur contenu sous l'action des ultrasons. Le contrôle donc des propriétés mécaniques et de la sensibilité à un traitement aux ultrasons peut être réalisé en faisant varier la quantité de nanoparticules de ZnO. Néanmoins, le plus grand défi est de pouvoir diminuer l'intensité des ultrasons pour se rapprocher de la limite tolérée en médecine.

#### **1.4.2.5.Champs magnétiques**

Le principe est basé sur l'incorporation de nanoparticules magnétiques au niveau du cœur ou de la membrane de microcapsules. Bien que l'activation magnétique de microcapsules est une piste intéressante surtout pour la libération contrôlée de médicaments, la longue durée d'exposition et la forte intensité du champ magnétique nécessaire pour perméabiliser les capsules conduisent à une augmentation de la température.

### **1.4.3. Stimuli biologiques**

#### **1.4.3.1.Enzymes**

Dans les organismes vivants tous les processus sont contrôlés à un moment ou un autre par des enzymes (Zelzer, Todd, Hirst, McDonald, & Ulijn, 2012). Inspiré par cela, les enzymes sont de plus en plus utilisés comme stimulus pour modifier les propriétés des microcapsules (B. G. De Geest, Vandenbroucke, et al., 2006).

#### **1.4.3.2.Récepteurs**

Une des classes de récepteurs est les anticorps qui peuvent être greffés avec les antigènes correspondant à la surface des microparticules. En présence d'antigènes dans le milieu environnant, les interactions anticorps-antigènes sont affaiblies par échange avec les antigènes libres: les microparticules ou la membrane des microcapsules se perméabilise pour faciliter la libération du contenu des microcapsules (Cortez et al., 2007) (Zhang, Wu, Chen, Zhang, & Lin, 2008).

### **1.5. Microcapsules ayant des propriétés d'auto-éclatement**

Ce type de microcapsules fait également partie de la catégorie des capsules 'intelligentes'.

Ces microcapsules avec des propriétés d'auto-explosion sont des capsules de structure cœur-coque dont le cœur est composé d'un microgel dégradable entouré d'une membrane semi-perméable. Pendant la dégradation du microgel interne dans des conditions bien déterminées (stimuli), et lorsque la pression de gonflement dépasse la résistance mécanique à la traction de la membrane, la microcapsule est rompue et son contenu est libéré rapidement.

Le concept d'auto-éclatement a été introduit par de Geest et son équipe qui ont développé plusieurs types de microcapsules ayant cette capacité (B. G. De Geest et al., 2005) (Bruno G. De Geest et al., 2006) (B. G. De Geest, Déjugnat, et al., 2006) (B. G. De Geest et al., 2007) (Bruno G. De Geest, McShane, Demeester, De Smedt, & Hennink, 2008) (Bruno G. De Geest, De Koker, Demeester, De Smedt, & Hennink, 2009) (Bruno G. De Geest, Koker, Demeester, Smedt, & Hennink, 2010).

En effet, ce type de microcapsules peut carrément éjecter son contenu dans le milieu externe lors de son auto-éclatement (Bruno G. De Geest et al., 2008). Par éjection à partir des microcapsules, les nanoparticules encapsulées peuvent se déplacer avec une vitesse presque 800 fois plus rapide que par le mouvement brownien. Cette fonction pourrait être

particulièrement intéressante dans les situations dans lesquelles le contenu à libérer doit traverser des longues distances dans un temps très court et à travers des milieux visqueux.

L'évolution de ce type de microcapsules au cours de la dégradation du microgel interne jusqu'à leur auto-éclatement est présentée dans la figure 4.

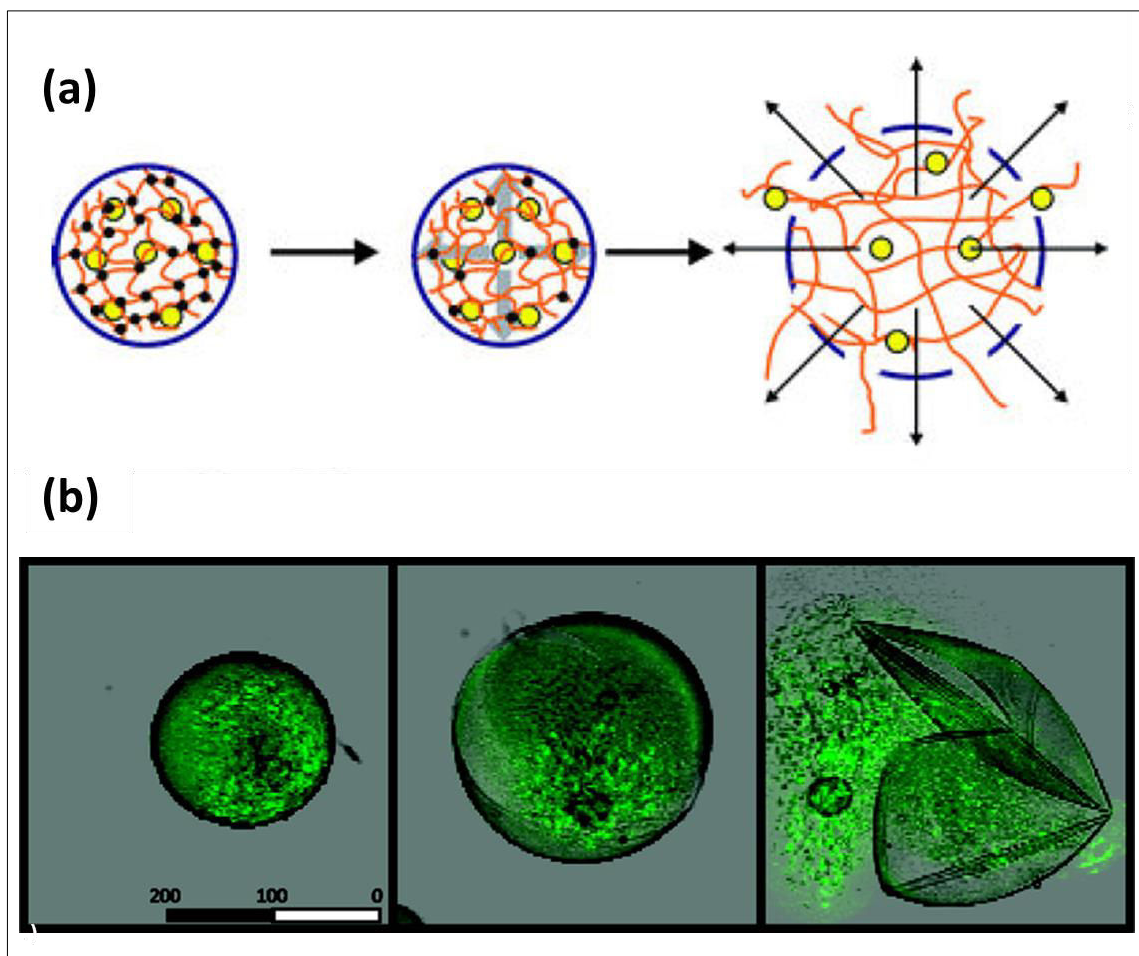


*Figure 4. Evolution d'une microcapsule lors de la dégradation du microgel interne jusqu'à son auto-éclatement. Représentation schématique (a), observation sous microscope confocal laser (b). Adaptée de (Bruno G. De Geest et al., 2008) (Bruno G. De Geest et al., 2010)*

## **2. Encapsulation dans une matrice d'alginate**

### **2.1. L'alginate**

L'alginate est un biopolymère « polyvalent » très utilisé en industrie car il possède de nombreuses propriétés: épaississant, stabilisant, gélifiant et filmogène. Ce polysaccharide est abondant dans la nature. En effet, il s'agit d'un composé structural majeur des algues brunes (jusqu'à 40% de la masse sèche totale) et de capsules bactériennes.

La commercialisation des alginates a démarré en 1927, et la production mondiale a atteint de nos jours 30 000 tonnes/an. Environ 30% de cette production est destinée à l'industrie agro-alimentaire et le reste de la production est répartie sur plusieurs secteurs et plus particulièrement l'industrie pharmaceutique et cosmétique (Ertesvåg & Valla, 1998).

### **2.2. Historique**

Le chimiste britannique E.C.C. Stanford fut le premier à décrire l'alginate dans un brevet daté du 12 Janvier 1881, détaillé par la suite en 1883 (Stanford, 1881) (Stanford, 1883). En effet, Stanford parvint à préparer l'alginate par extraction de l'acide alginique à partir des algues brunes avec du carbonate de sodium puis par précipitation à pH acide. Il pensait que l'alginate contenait de l'azote. En 1926, deux équipes de recherche (Atsuki et Tamoda) et (Schmidt et Vocke) ont constaté la présence de l'acide uronique comme constituant principal de l'alginate (Atsuki & Tomoda, 1926) (Schmidt & Vocke, 1926). Les années suivantes, différentes équipes se sont intéressées à la nature de ces acides uroniques et se sont accordées sur le fait que l'alginate est constitué d'acide D-mannuronique. En 1939, Hirst et *al.*, mit en évidence que la nature des liaisons entre les résidus d'acide mannuronique est de type  $\beta$ -1,4, à l'instar de la cellulose (Hirst, Jones, & Jones, 1939). Cette structure relativement simple fut remise en question par les travaux de Fisher et Dörfel en 1955, basés sur l'utilisation de la chromatographie des acides uroniques et des polyuronides, ils décelèrent la présence d'un second acide uronique présent en quantité non négligeable dans l'alginate: l'acide L-



guluronique (Fischer & Dörfel, 1955). Depuis, l'alginate est considéré comme un copolymère binaire linéaire composé de résidus  $\alpha$ -L-guluronique et  $\beta$ -D-mannuronique. Au cours des années 60-70 Haug, Larsen et Smidsrød ont mis en évidence la structure à blocs de l'alginate ainsi que la corrélation entre structure et propriétés de l'alginate (Haug, 1964) (Haug & Smidsrød, 1965) (Haug, Larsen, & Smidsrød, 1966) (Haug, Larsen, & Smidsrød, 1967b) (Haug, Larsen, & Smidsrød, 1967a) (Haug, Myklestad, Larsen, & Smidsrød, 1967) (Haug et al., 1970).

### **2.3. Origine**

Les alginates sont très abondants dans la nature. Ils peuvent être extraits des parois cellulaires des algues brunes (*phaeophyceae*) essentiellement du genre laminaire (*laminaria*) telles que *Laminaria hyperborea*, *Laminaria digitata*, *Laminaria japonica*, *Ascophyllum nodosum* et *Macrocystis pyrifera* (O. Smidsrød & Skjåk-Braek, 1990).

L'alginate est extrait par traitement alcalin en utilisant de la soude puis filtré et précipité en ajoutant du calcium ou du sodium. Le sel d'alginate obtenu peut être transformé en acide alginique par traitement avec du HCl dilué (Shilpa, Agrawal, & Ray, 2003).

L'alginate peut être également isolé à partir de capsules de bactéries du genre *Pseudomonas* et *Azotobacter* ou produit par fermentation ou par des voies biotechnologiques de biosynthèse (Sabra, Zeng, & Deckwer, 2001). La biosynthèse par voie bactérienne pourrait aboutir à la production d'alginate avec une structure chimique et des propriétés physiques semblables à celle des algues brunes.

Les progrès récents dans la régulation de la biosynthèse de l'alginate dans des bactéries et la modification relativement facile des bactéries pourraient permettre la production d'alginate hautement spécifique pour une large gamme d'applications (K. Y. Lee & Mooney, 2012).

### **2.4. Structure chimique**

L'alginate est un copolymère qui consiste en une alternance d'acide  $\beta$ -D mannuronique (M) et d'acide  $\alpha$ -L guluronique (G) liés en (1 $\rightarrow$ 4). Les molécules d'acide uronique sont réparties le

long de la chaîne de l'alginate sous forme de blocs. Il en existe 3 types (Figure 5) : des séquences homopolymériques ne contenant que des unités d'acide mannuronique (blocs M) ou guluronique (blocs G), ainsi que des blocs hétéropolymériques contenant à la fois des unités d'acide mannuronique et guluronique (blocs MG) (Pawar & Edgar, 2012). La composition et l'organisation des acides uroniques en séquences sont donc très variables en fonction du type d'alginate. A l'échelle moléculaire, à la différence de l'alginate d'origine algale, on note la présence de groupements O-acétyl au niveau du C<sub>2</sub> et/ou C<sub>3</sub> dans l'alginate d'origine bactérienne (Skj, Grasdalen, Larsen, 1986).

En ce qui concerne la conformation des chaînes, l'alginate possède quatre types de liaisons glycosidiques : di-axial (GG), di-équatoriale (MM), axial-équatoriale (GM) et équatoriale-axiale (MG) (Figure 5b).

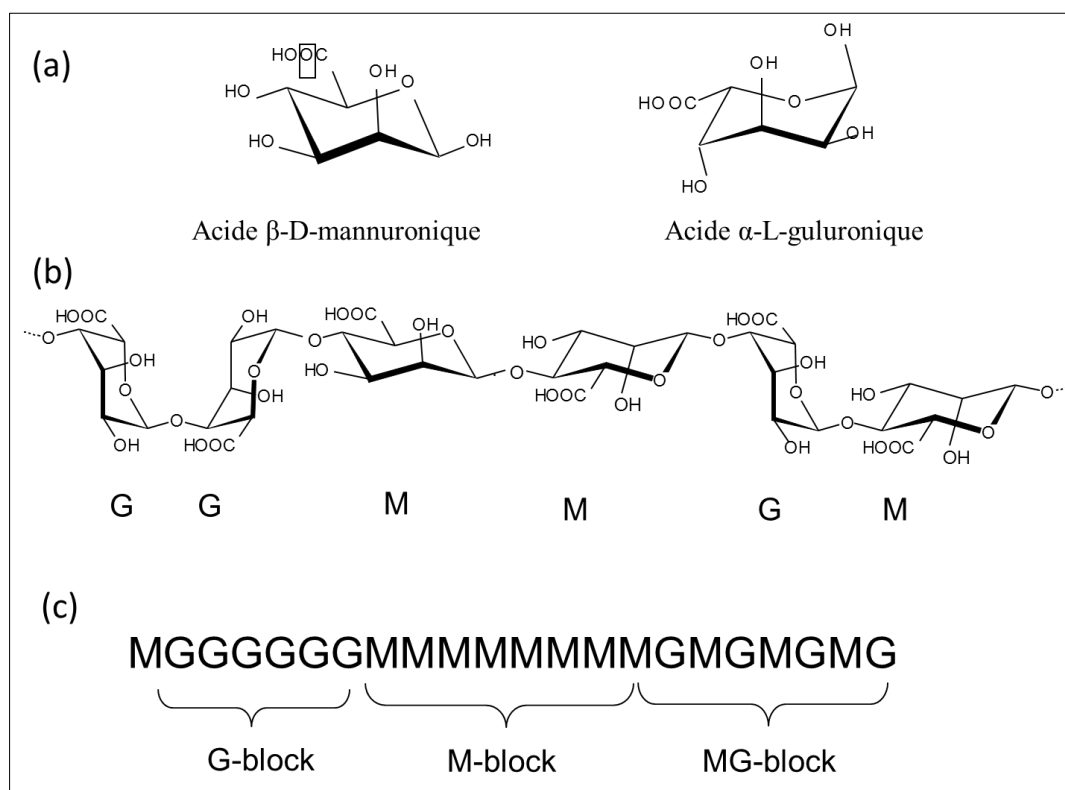


**Figure 5.** Structure chimique de l'alginate de sodium: monomères d'acides uroniques(a), conformation des chaînes (b) et distribution des blocs(c).

## 2.5. Propriétés

Les propriétés physiques de l'alginate ont été très étudiées à partir de 1964 grâce notamment aux travaux de Haug, Larsen et Smidsrød (Haug, 1964)(Haug & Smidsrød, 1965)(Haug et al., 1966) (Haug, Larsen, et al., 1967b)(Haug, Larsen, et al., 1967a)(Haug, Myklestad, et al., 1967)(Haug et al., 1970).

### 2.5.1. Solubilité et stabilité

L'alginate de sodium est hygroscopique; par conséquent, la teneur en humidité s'équilibre rapidement avec l'humidité relative de l'eau. La stabilité au stockage est excellente à sec lorsque la poudre est stockée dans un récipient bien fermé.

L'alginate de sodium est soluble dans l'eau froide formant une solution colloïdale visqueuse. Il est insoluble dans l'alcool et dans les solutions hydro-alcooliques dans lesquels la teneur en alcool est supérieure à 30 % (m/m). Il est également insoluble dans les autres types de solvants organiques (chloroforme, éther...) (Shilpa et al., 2003).

La solubilité de l'alginate dépend de trois paramètres principaux (Kurt Ingar Draget, Smidsrød, & Skjåk-Bræk, 2005) :

- pH du solvant : Il détermine la présence de charges électrostatiques au niveau des acides uroniques. Les valeurs de pKa déterminés par titration potentiométrique des deux résidus composant l'alginate à savoir l'acide  $\beta$ -D-mannuronique et  $\alpha$ -L- guluronique sont de 3,38 et 3,65, respectivement. Le pKa final de l'alginate diffère faiblement du pKa des deux acides uroniques qui le compose.
- La force ionique : Elle agit par la présence de groupements anioniques au niveau du polysaccharide et peut modifier la conformation moléculaire.

- La présence d'ions divalents : Ils peuvent interagir avec les groupements carboxyliques et influencent donc la solubilité de l'alginate. La dureté de l'eau (teneur en  $\text{Ca}^{2+}$ ) par exemple est un facteur important lors de la préparation d'une solution d'alginate.

### **2.5.2. Viscosité**

La composition précise de l'alginate varie en fonction des espèces d'algues et de la saison ce qui engendre des propriétés structurales très variables du polysaccharide.

Il existe donc différents grades d'alginate de sodium donnant une viscosité variant entre 0.02-0.4 Pa.s pour une solution à 1% m / v à 20°C. Les solutions d'alginate présentent généralement un comportement rhéo-fluidifiant avec une diminution de la viscosité en fonction de la vitesse de cisaillement (Lund, 1994).

### **2.5.3. Bioadhésion**

La bioadhésion est définie comme l'adhésion ou le contact entre deux surfaces dont l'une est un substrat biologique. Si l'une des surfaces est une couche de muqueuse, le terme " mucoadhésion " est utilisé.

L'alginate est classé comme polymère naturel avec des propriétés mucoadhésives supérieures à d'autres polymères comme le chitosane, la carboxyméthylcellulose et l'acide polylactique. En effet, des études ont montré que les polymères polyanioniques sont plus efficaces que les polymères polycationiques et non-ioniques (Wee & Gombotz, 1998).

Cette propriété de l'alginate est à l'origine de son utilisation dans le domaine de la bioencapsulation comme matrice d'encapsulation des médicaments administrés par voie orale.

## **2.6. Gélification de l'alginate:**

### **2.6.1. Généralités**

De façon générale, un phénomène de gélification implique une transition sol-gel. L'état « sol » se réfère à un système colloïdal de caractère liquide. En revanche un état « gel » est un système colloïdal de caractère solide dans lequel la substance dispersée forme un réseau continu qui est interpénétré par un système (en général liquide) constitué par des unités plus petites que les entités colloïdales.

Un gel est donc un matériau semi-solide constitué d'au moins deux composants: un réseau tridimensionnel (fraction solide) dans laquelle un solvant (fraction liquide) est immobilisé. Dans le cas où la fraction liquide est constituée par de l'eau, on parle d'un hydrogel.

Le terme hydrogel décrit donc des structures de réseau en trois dimensions obtenues à partir de polymères naturels ou synthétiques hydrophiles qui peuvent absorber et retenir des quantités importantes d'eau. Le caractère insoluble de l'hydrogel dans l'eau est lié à la présence de réticulation chimique ou physique. Les hydrogels peuvent donc être classés en fonction de ces réticulations qui sont à l'origine du maintien de l'intégrité structurale, en hydrogels physiques et chimiques (Rosiak & Yoshii, 1999).

L'intégrité structurale des hydrogels physiques est maintenue par des forces secondaires de type ioniques, Van der Waals, empilement  $\Pi$ - $\Pi$ , hydrophobes ou liaisons hydrogènes. Ces hydrogels sont généralement réversibles. En revanche, les hydrogels dits chimiques sont généralement réticulés de manière covalente et ils sont donc irréversibles ou permanents (Rosiak & Yoshii, 1999).

L'alginate est un gélifiant naturel qui peut former des hydrogels physiques par gélification ionotrope en présence d'ions divalents ou par gélification acide par diminution du pH. D'autres méthodes de gélification ont été développées après modification chimique de l'alginate. Dans la section suivante, les mécanismes de gélification de l'alginate sont détaillés.

### **2.6.2. Gélification ionotrope**

La gélification ionotropique de l'alginate est liée à son affinité pour certains ions par formation de liaisons sélectives (Haug et al., 1970) (Olav Smidsrød, 1974). En effet, les chaînes de polymère d'alginate interagissent avec les cations bivalents ou trivalents ( $\text{Fe}^{3+}$ ,  $\text{Al}^{3+}$ ) pour former des hydrogels. L'affinité de l'alginate vis-à-vis des ions bivalents diminue dans l'ordre suivant:  $\text{Pb} > \text{Cu} > \text{Cd} > \text{Ba} > \text{Sr} > \text{Ca} > \text{Co, Ni, Zn} > \text{Mn}$  (Mørch, Donati, Strand, & Skjåk-Braek, 2006). Un travail relativement récent a démontré que les ions  $\text{Mg}^{2+}$  longtemps considérés comme des ions non gélifiants ou ayant une faible affinité pour l'alginate forment un hydrogel mais avec une cinétique de gélification relativement lente (2-3 heures) et dépendant fortement de la structure chimique de l'alginate. (Topuz, Henke, Richtering, & Groll, 2012)

Le calcium demeure le cation le plus couramment utilisé pour induire la formation de gel d'alginate.

Les étapes de la réticulation ionique de l'alginate sont schématisées dans la figure 6.

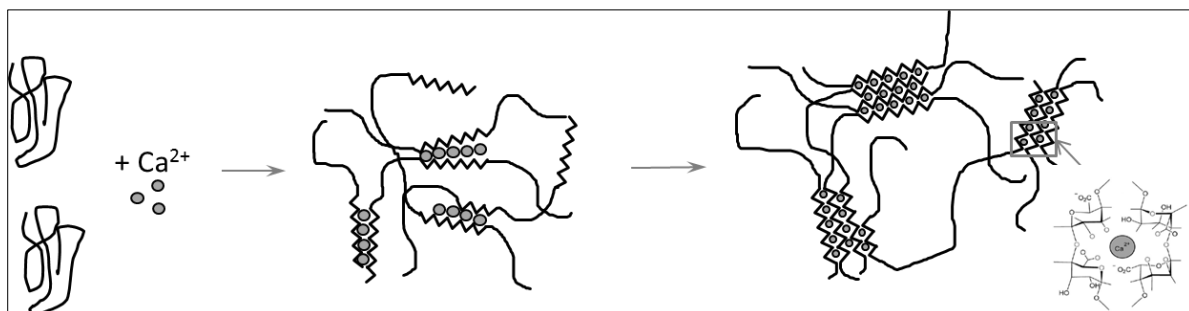


**Figure 6.** Mécanisme de gélification de l'alginate en présence d'ions calcium.

Deux blocs G ou MG de deux chaînes de polymères adjacentes peuvent être réticulés en présence d'un cation bivalent par des interactions électrostatiques entre deux groupements carboxyliques  $\text{COO}^-$  du polysaccharide. Lorsque deux brins de polymère sont face à face, la conformation des blocs G ou MG forment des cavités dans lesquelles viennent se loger les ions  $\text{Ca}^{2+}$ . Cette dimérisation des blocs est appelée structure type "boîte d'œufs" (Grant, Morris, Rees, Smith, & Thom, 1973).

La formation de gel est induite par des interactions entre les blocs G qui s'associent pour former des jonctions fortes en présence de cations bivalents. En plus de blocs G, les blocs MG participent également formant des jonctions plus faibles. Une représentation schématique des trois types de jonctions possibles dans un hydrogel d'alginate est présentée (Figure 7) (Donati et al., 2005).

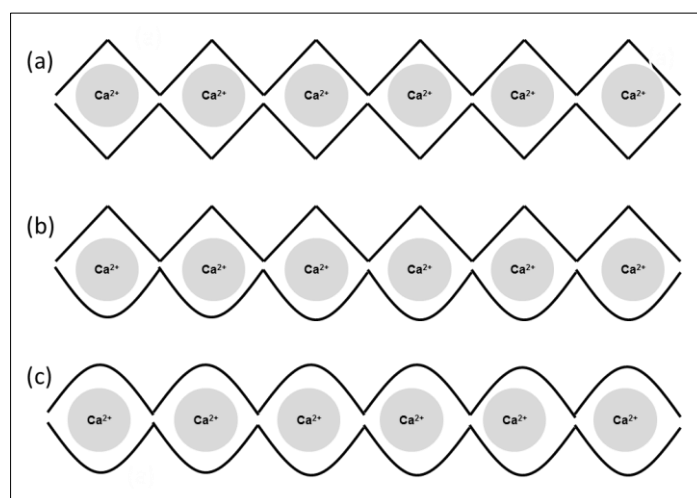


**Figure 7.** Les points de jonction possibles dans un hydrogel d'alginate. Jonctions GG / GG (a), jonctions GG/MG (b), et jonctions MG/MG (c).

Les propriétés mécaniques de l'hydrogel obtenu dépendent du ratio entre les blocs M et les blocs G (ratio M/G) qui compose l'alginate. En effet, les alginates composés d'un ratio (M/G) élevé forment des gels mous et élastiques, alors que les alginates avec un ratio (M/G) faible donnent des gels durs et cassants.

Il existe deux approches de préparation d'hydrogel d'alginate par réticulation ionique :

- Une approche dite par « gélification externe » dans lequel les ions de réticulation diffusent vers la solution d'alginate à partir d'une solution externe. Elle permet une gélification très rapide de la solution d'alginate mais les hydrogels formés ne sont pas homogènes.
- Une approche dite de "gélification interne ou *in situ*", où la source de calcium initialement sous forme insoluble ( $\text{CaCO}_3$ ,  $\text{CaSO}_4$ ,...) est dispersée dans la solution d'alginate. Ces ions sont par la suite libérés de façon contrôlée typiquement par diminution progressive du pH (par solubilisation donc de la source de calcium) qui déclenche la libération des ions dans la solution d'alginate. La diminution progressive du pH est généralement obtenue par ajout de lactones à hydrolyse lente telle que la  $\delta$ -gluconolactone (GDL). Il est également possible de contrôler le pH final du gel d'alginate en maîtrisant le ratio ( $\text{CaCO}_3$ / GDL) (Kuo & Ma, 2001).

### 2.6.3. Gélification acide

Lorsque le pH d'une solution d'alginate est abaissé au-dessous du pKa des acides uroniques, un gel acide d'alginate est formé (King, 1983).

La préparation des gels acides peut se faire par deux méthodes :

La première méthode se base sur une acidification d'une solution d'alginate en dessous du pKa du polymère. L'abaissement du pH doit se faire de manière progressive. En effet une diminution rapide par ajout direct d'un acide par exemple engendre la formation d'un précipité plutôt qu'un gel. Il est donc nécessaire d'abaisser le pH de façon graduelle par ajout de lactones à hydrolyse lente telle que la  $\delta$ -gluconolactone (GDL) (K. I. Draget, Skjåk Bræk, & Smidsrød, 1994).

Dans la seconde méthode, un hydrogel d'alginate préalablement obtenu par réticulation ionique est converti en hydrogel acide par incubation dans une solution acide et échange de protons.

Ce type d'hydrogels est généralement stabilisé par des liaisons de type hydrogène (K. I. Draget, Skjåk-Bræk, Christensen, Gåserød, & Smidsrød, 1996).



#### 2.6.4. Différences entre les hydrogels ionotropiques et acides

Contrairement aux hydrogels d'alginate réticulés ioniquement qui ont été largement étudiés en terme de relation structure/fonction depuis les années 60-70, les hydrogels acides n'ont été caractérisés qu'à partir des années 90 et notamment grâce aux travaux de Draget et son équipe qui ont pu donc déduire les différences entre les deux types de gels (Stokke et al., 2000) (Kurt Ingar Draget, Skjåk-Bræk, & Stokke, 2006).

Les similitudes et les différences entre les deux types de gels sont reportées dans le tableau 1.

**Tableau 1.** Similitudes et différences entre gels acides et gels ionotropiques (Kurt Ingar Draget et al., 2006).

Similitudes	Différences
<ul style="list-style-type: none"><li>- Les blocs G sont les premières structures impliquées dans le mécanisme de gélification.</li><li>- Des processus coopératifs semblent être impliqués dans la formation de la zone de jonction</li><li>- La présence de la zone de jonction multiplicités co-existantes.</li></ul>	<ul style="list-style-type: none"><li>- Contrairement aux gels ionotropiques, les blocs M donnent également des liaisons intermoléculaires stables dans les gels acides.</li><li>- La transition sol-gel des hydrogels acide est de nature d'équilibre thermodynamique.</li><li>- Les plus grandes zones de jonction sont de multiplicité supérieure à celle des plus grandes zones de jonction dans les gels ionotropiques.</li></ul>

### **2.6.5. Autres méthodes de gélification**

La gélification ionotropique est la méthode la plus utilisée pour la formation des gels d'alginate. En effet, c'est une gélification simple à mettre en œuvre dans des conditions relativement douces. Ces gels sont stables dans des conditions de pH neutre ou légèrement acide et sont convertis en gels acides par échange de protons à des pH acides  $< 3-3.5$  (pka de l'alginate). Cependant, dans des solutions faiblement basiques, les gels d'alginate subissent un gonflement suivis par une érosion et éventuellement une désintégration. Le contrôle des propriétés physicochimiques de ce type de biomatériau (propriétés mécaniques, gonflement, dégradation..) est également limité par la perte de cations bivalents dans le milieu environnant par échange d'ions ce qui affecte la stabilité chimique de la matrice.

Par exemple, un hydrogel d'alginate se dégrade en présence de solutions salines (Rolland, Santanach-Carreras, Delmas, Bibette, & Bremond, 2014).

Dans ce contexte, plusieurs équipes se sont intéressées à la préparation de gels en utilisant d'autres méthodes de réticulation après modification chimique de l'alginate.

#### **2.6.5.1. Réticulation covalente**

Birnbaum et *al.*, ont testé trois méthodes de gélification de microsphères d'alginate. Dans la première méthode, des billes d'alginate préalablement formées en présence de polyéthylèneimine sont réticulées avec du glutaraldéhyde. Dans la seconde méthode, une solution d'alginate a été traitée avec du carbodiimide et du N-hydroxysuccinimide (pour former des esters actifs). Les billes obtenues par gélification ionotropique sont ensuite réticulées avec la polyéthylèneimine. Pour la troisième méthode une solution d'alginate traitée avec du periodate (pour former des groupements aldéhydes), est gélifiée dans une solution de  $\text{CaCl}_2$  puis réticulée avec de la polyéthylèneimine (Birnbaum, Pendleton, Larsson, & Mosbach, 1981).

Mooney et son équipe, ont réticulé l'alginate de manière covalente en utilisant du polyéthylène glycol-diamines avec différentes masses moléculaires après activation des groupements carboxyliques avec de 1-éthyl-3-(3-diméthylaminopropyl) carbodiimide et le N-hydroxysuccinimide (Eiselt, Lee, & Mooney, 1999)(K. Y. Lee et al., 2000).

Gattás-Asfura et Stabler, ont modifié l'alginate avec des groupements azide via des liaisons amides stables et des segments de polyéthylène glycol. La ligation de Staudinger a été ensuite utilisée pour former des hydrogels d'alginate réticulés de manière covalente avec des caractéristiques variables, telles que le gonflement et la stabilité mécanique (Gattás-Asfura & Stabler, 2009).

#### **2.6.5.2. Photoréticulation**

Récemment de l'alginate photoréticulé sous UV a été préparé par réaction de l'alginate de sodium et du méthacrylate de 2-aminoéthyle, en présence de 1-éthyl-3-(3-diméthylaminopropyl) carbodiimide et le N-hydroxysuccinimide. L'alginate méthacrylé a été par la suite, photoréticulé sous UV en présence d'un photoinitiateur. L'intérêt de ce type de système est que ses propriétés physicochimiques pourraient être contrôlées en faisant varier le degré de méthacrylation (Jeon, Bouhadir, Mansour, & Alsberg, 2009).

### **2.7. Applications des hydrogels d'alginate**

Les hydrogels d'alginate constituent une classe de biomatériaux avec un large spectre d'applications dans plusieurs domaines : l'alimentaire (Farris, Schaich, Liu, Piergiovanni, & Yam, 2009), nutraceutique (Chen, Remondetto, & Subirade, 2006), environnement et traitement des eaux (Crini, 2005).

Les hydrogels d'alginate connaissent un intérêt grandissant dans le domaine biomédical (Hoffman, 2012).

Cette dernière catégorie regroupe différents domaines d'applications tels que l'ingénierie tissulaire (Drury & Mooney, 2003), l'administration de médicaments (George & Abraham, 2006) et la microfluidique (K. H. Lee, Shin, Park, & Lee, 2009).

L'intérêt des hydrogels à base d'alginate a également donné naissance au développement d'une large gamme de biomatériaux avec différentes architectures tels que des hydrogels plans ou sphériques (billes et capsules), de fibres et des structures anisotropes à l'échelle milli-, micro- et nanométriques (Figure 8).

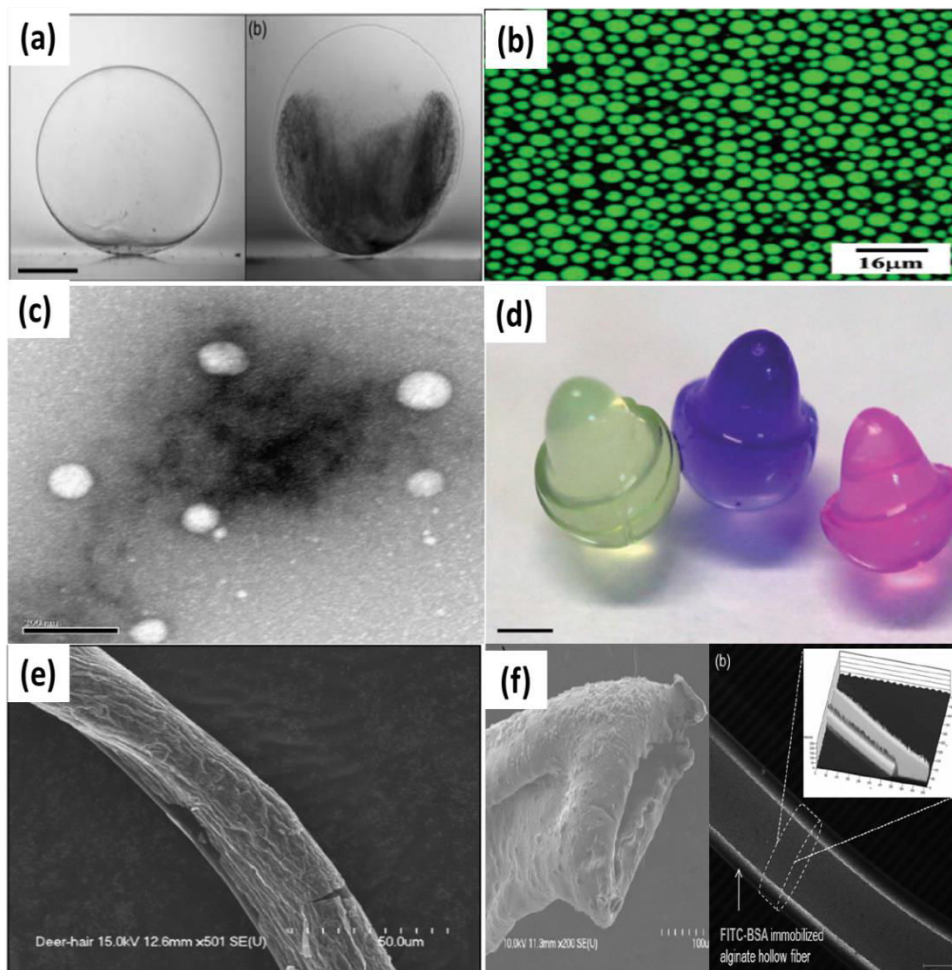


**Figure 8.** Exemples de biomatériaux développés à partir d'un hydrogel d'alginate. Capsules millimétriques à cœur liquide avec une fine membrane d'alginate(a), microsphères d'alginate

*obtenues par émulsification (b), nanocapsules d'alginate (c), photo de capsules anisotrope en forme de champignon (d), microfibre pleine (e) et microfibre creuse (f). Adaptée de (Bremond, Santanach-Carreras, Chu, & Bibette, 2010)(H. Zhu, Srivastava, Brown, & McShane, 2005)(Lertsutthiwong, Noomun, Jongaroonngamsang, Rojsitthisak, & Nimmannit, 2008)(Mele et al., 2013)(Shin et al., 2007)(K. H. Lee et al., 2009)*

Comme détaillé dans la section (2.5) l'alginate présente de nombreuses caractéristiques favorables pour des applications d'encapsulation, comme une bonne biocompatibilité, une grande disponibilité, un faible coût, et une procédure de gélification simple dans des conditions relativement douces (Pawar & Edgar, 2012).

## **2.8. Techniques d'encapsulation avec de l'alginate**

Plusieurs techniques d'encapsulation en utilisant l'alginate ont été développées permettant d'obtenir des particules avec une large gamme de taille. En effet, le diamètre de particules d'alginate peut être  $> 1000 \mu\text{m}$  (macro), de  $0,2$  à  $1000 \mu\text{m}$  (micro) ou  $<0,2 \mu\text{m}$  (nanoparticules). Le tableau 2 résume les techniques d'encapsulation utilisant l'alginate, la taille des particules obtenue ainsi que les applications potentielles des différents systèmes (Ching, Bansal, & Bhandari, 2015).

**Tableau 2.** Synthèse des méthodes actuelles de production de particules à base d'hydrogel d'alginate (Ching, Bansal, et al., 2015).

Techniques	Taille des particules	Applications
Simple extrusion	1000-2000 $\mu\text{m}$	Encapsulation des probiotiques, des levures, huile de poisson, des médicaments, des protéines, des enzymes, des extraits de plantes et saveurs
Potentiel électrostatique	0.9-1.5 $\mu\text{m}$ 50-350 $\mu\text{m}$	Encapsulation de nanoparticules lipidiques, des probiotiques, des tissus animaux et humains et des enzymes.
Buse vibrante	<20 $\mu\text{m}$ 200-5000 $\mu\text{m}$	Encapsulation de cellules et de protéines
Jet rompu	200- 5000 $\mu\text{m}$	Encapsulation de cellules et de protéines
Disque tournant	300-600 $\mu\text{m}$	Encapsulation des bactéries, de la levure et les protéines
Buse tournante	270-2000 $\mu\text{m}$	Encapsulation de cellules et de protéines
Buse de pulvérisation	80-130 $\mu\text{m}$	Encapsulation de nanoparticules lipidiques, vaccin BCG, des antigènes, des protéines et des bactéries.
Atomisation (à contre-courant) « Impinging aerosol »	11-47 $\mu\text{m}$	Encapsulation de l'huile de poisson, le lysozyme, l'ibuprofène, le chlorhydrate de propranolol, les probiotiques, l'insuline
Emulsification	100- 1000 $\mu\text{m}$	Encapsulation de l'insuline
Microfluidique	50 - 70 $\mu\text{m}$	Encapsulation de cellules (probiotiques, mammifères)
Micro- nano-moulage	120 – 200 nm	Encapsulation de protéines (BSA)
Microgels hybrides	250-600 nm	Encapsulation de médicaments (doxorubicine), cellules (hémoglobine), l'insuline et herbicides

## **2.9. Capsules d'alginate à cœur liquide**

Nous présentons dans cette partie les procédés relativement récents de préparation de capsules d'alginate à cœur liquide à différentes échelles (de l'échelle nano- à millimétrique).

### **2.9.1. Nano-capsules d'alginate**

Une des méthodes les plus couramment utilisées pour la formation des nanocapsules est le dépôt de polymère à l'interface d'une goutte d'émulsion suivi de l'élimination du solvant. Une fois la couche de polymère déposée à l'interface, la membrane est stabilisée par réticulation intermoléculaire covalente ou physique (Paques, van der Linden, van Rijn, & Sagis, 2014).

Des nanocapsules d'alginate préparées par cette méthode ont été utilisées avec succès pour encapsuler différents principes actifs tels que la testostérone, des dérivés d'acyl ayant une activité anti-tumorale ainsi que de l'huile essentielle.

La préparation de ce type de système est schématisée dans la figure 9. Tout d'abord, le principe actif est solubilisé ou dispersé dans un solvant organique. Le mélange est ensuite lentement ajouté dans une solution aqueuse d'alginate contenant un agent tensio-actif (Tween-80). Par la suite, une émulsion huile-dans-eau (H/E) est réalisée par sonication (Fig. 9b). Du chlorure de calcium est ensuite ajouté lentement à l'émulsion pour former et stabiliser la membrane de nanoparticules (Fig. 9c). Enfin, la suspension aqueuse de nanocapsules est laissée au repos pendant un certain temps avant l'élimination du solvant (Fig. 9d) (Paques et al., 2014).

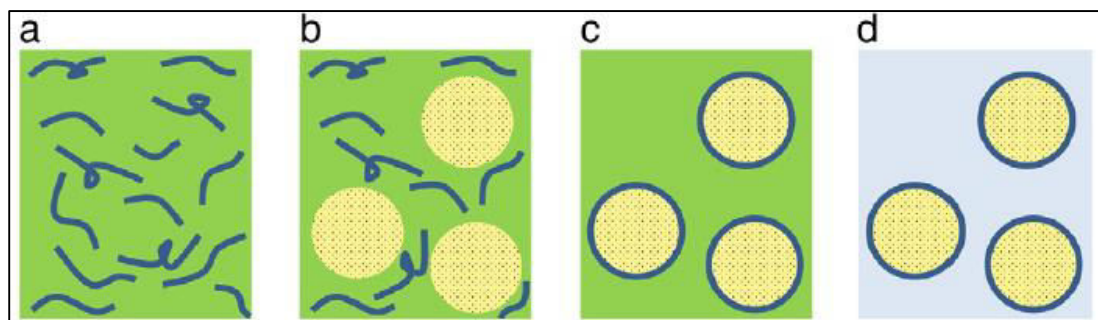


**Figure 9.** Représentation schématique de la formation de nanocapsules d'alginate. Solution d'alginate (a). Incorporation de la phase d'huile contenant le principe actif dissout dans la solution d'alginate (b). Addition de  $\text{CaCl}_2$  et formation de la membrane d'alginate à l'interface des gouttelettes d'huile (c). Elimination du solvant, lavage et dispersion des nanocapsules (d) (Paques et al., 2014).

## 2.9.2. Microcapsules d'alginate

### 2.9.2.1. La polymérisation multicouches (LbL assembly)

La technique de polymérisation multicouches par le dépôt séquentiel de polymères de charges opposées pour fabriquer des films a été rapportée la première fois par Iler, il y a presque 50 ans (Iler, 1966). A partir des années 90, cette technique s'est largement développée grâce aux travaux pionniers de Decher et Hong (Gero Decher & Hong, 1991)(G. Decher & Hong, 1991)(GHJD Decher, Hong, & Schmitt, 1992) (Hong, Lowack, Schmitt, & Decher, 1993). Cette approche a été par la suite appliquée pour la préparation de microcapsules notamment grâce aux travaux de Möhwald et Caruso (Caruso, Caruso, & Möhwald, 1998) (Caruso, Caruso, & Möhwald, 1999) (Donath, Sukhorukov, Caruso, Davis, & Möhwald, 1998).

Les microcapsules obtenues par polymérisation multicouches sont préparées par dépositions consécutives de polymères "complémentaires" à la surface d'une particule colloïdale sacrificielle (par exemple:  $\text{CaCO}_3$ ) par des interactions électrostatiques, liaisons hydrogènes,



interactions hydrophobes..., puis par dissolution de la matrice colloïdale (cœur de la capsules) afin de former une capsules à cœur liquide (Figure 10).

L'alginate a été utilisé en tant que polymère anionique lors de la préparation des microcapsules à cœur liquide par polymérisation multicouches en l'alternant avec des polymères cationiques d'origine naturelle (chitosane) ou synthétique (poly-L-lysine, polyornithine...) (Sukhorukov et al., 2004).

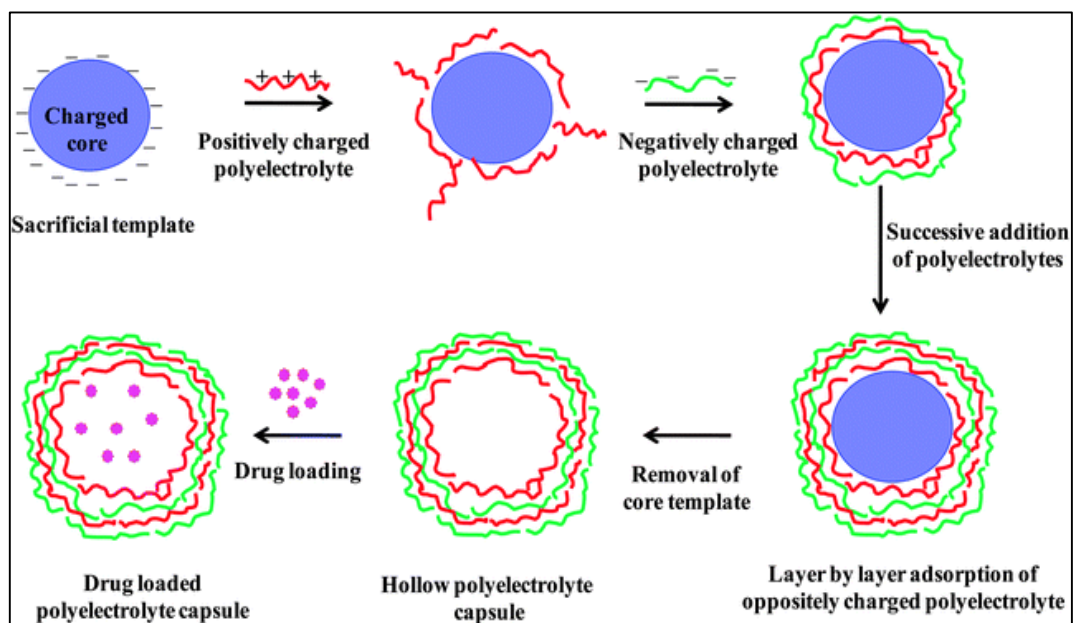


**Figure 10.** Schéma de la formation de capsule par polymérisation multicouches. Des couches successives sont déposées à la surface d'un colloïde exposé alternativement à des polymères de charges opposées. La matrice du colloïde est ensuite dissoute pour former une capsule à cœur liquide (Verma & Hassan, 2013).

Même si cette technique est généralement associée à la formation de microcapsules, elle a été également appliquée pour la formation de nanocapsules multicouches composées d'alginate/chitosane sur des nanoparticules de polystyrène (180 nm) utilisées comme colloïde sacrificiel (Ye, Wang, Liu, & Tong, 2005).

### **2.9.2.2. La microfluidique de gouttes**

D'une manière générale, la microfluidique est définie comme la science qui manipule de petits volumes de fluides en utilisant des canaux de la dimension de quelques dizaines de micromètres et portant sur les écoulements de fluides simples ou complexes dans des microsystèmes artificiels (Whitesides, 2006).

La microfluidique de gouttes constitue une branche importante de la microfluidique dont l'objectif principal est de générer et de manipuler la formation de gouttelettes à partir d'un fluide. Ces gouttelettes peuvent ensuite être utilisées pour la synthèse et la fabrication de microcapsules polymériques monodisperses (Kim, Utada, Fernández-Nieves, Hu, & Weitz, 2007) (Shah, Kim, Agresti, Weitz, & Chu, 2008)(Tumarkin & Kumacheva, 2009).

Cette application a offert donc la possibilité de fabriquer des structures de type cœur-membrane à base d'alginate par émulsification double (Figure 11). Le fluide interne contenant les composés à encapsuler est émulsifié dans un fluide intermédiaire, et cette première émulsion est à nouveau émulsifiée dans un troisième fluide (la phase continue) à cœur huileux (Ren, Ju, Xie, & Chu, 2010).

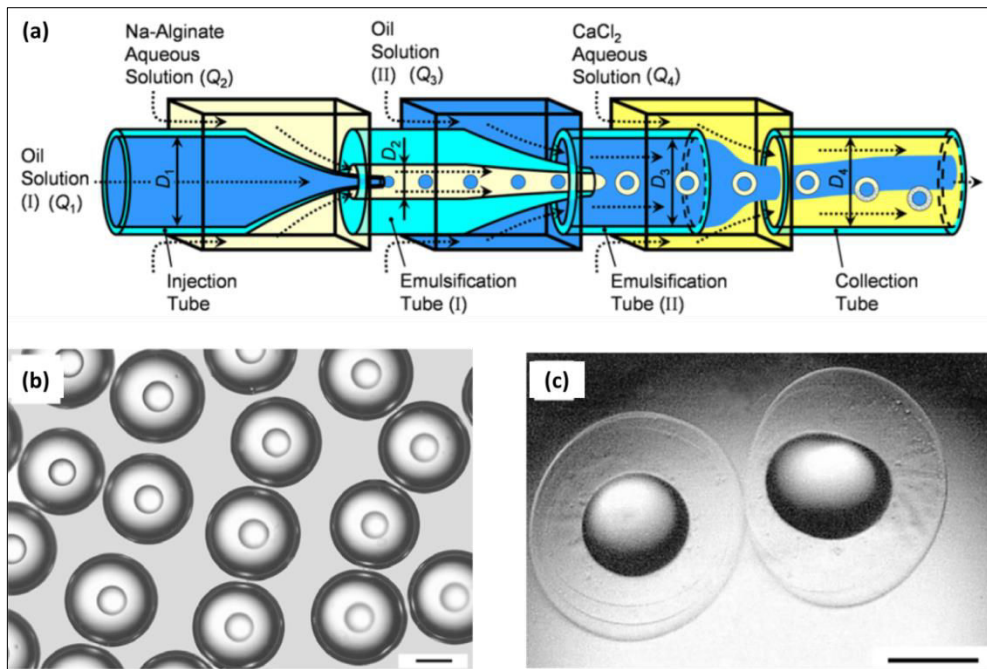


**Figure 11.** Préparation de microcapsules par microfluidique. Illustration schématique du dispositif microfluidique capillaire (a), photo de la double émulsion H/E/H (b) et structure des capsules à cœur d'huile (Ren et al., 2010).

### 2.9.2.3. Emulsification stabilisée par des nanoparticules-gélification «pickering emulsion-gelation»

Une méthode originale basée sur la gélification à l'interface d'une émulsion stabilisée par des nanoparticules solide de  $\text{CaCO}_3$  (Pickering emulsion) a été récemment développée. L'intérêt de cette méthode est l'absence d'utilisation d'équipement spécifique pour la formation des microcapsules (Leong, Tey, Tan, & Chan, 2015).

Les étapes de préparation sont schématisées dans la figure 12. Tout d'abord, la phase huileuse est émulsionnée dans une solution aqueuse contenant une dispersion de nanoparticules de  $\text{CaCO}_3$  (a), les nanoparticules sont ensuite absorbées à l'interface, puis l'alginate est introduit dans la phase aqueuse avant que les nanoparticules de  $\text{CaCO}_3$  ne soient dissoutes à l'interface

par diminution du pH pour libérer les cations  $\text{Ca}^{2+}$  (c), et permettre donc la gélification de l'alginate à l'interface H / E et la formation des microcapsules à cœur d'huile.

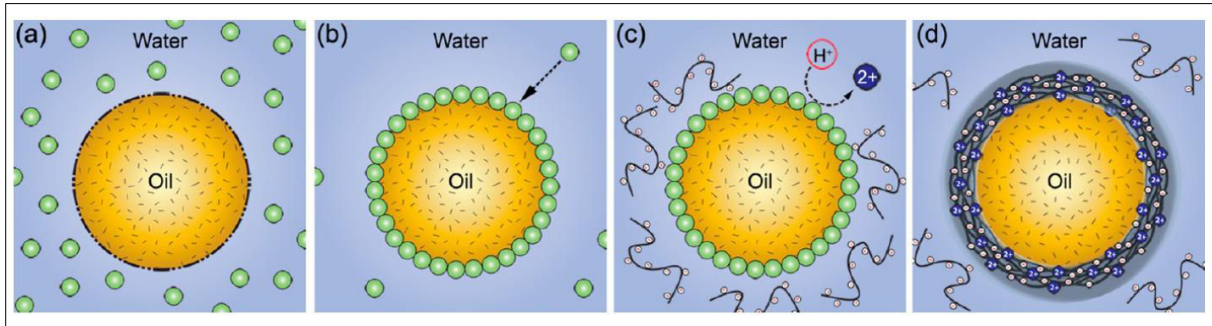


*Figure 12. Etapes de préparation de microcapsules d'alginate par émulsification et gélification à l'interface (Leong et al., 2015).*

#### **2.9.2.4. Association : Buse vibrante-potentiel électrostatique**

La technologie de buse vibrante est basée sur le principe selon lequel un écoulement laminaire à jet de liquide est coupé en gouttelettes de taille égale par une vibration superposée. La fréquence de vibration détermine la quantité produite de gouttelettes. En association avec un potentiel électrostatique à la sortie de la buse, le jet est dispersé. L'utilisation d'une buse coaxiale (concentrique) permet donc la co-extrusion et la stabilisation physique des gouttes alginate /cœur avant la gélification une fois que les billes entrent dans le bain de  $\text{CaCl}_2$ . Des équipements industriels ont été conçus en combinant buse vibrante – potentiel électrostatique. Au cours de cette thèse une partie des travaux a été menée en utilisant un encapsulator Buchi B-395 Pro (Figure.13).

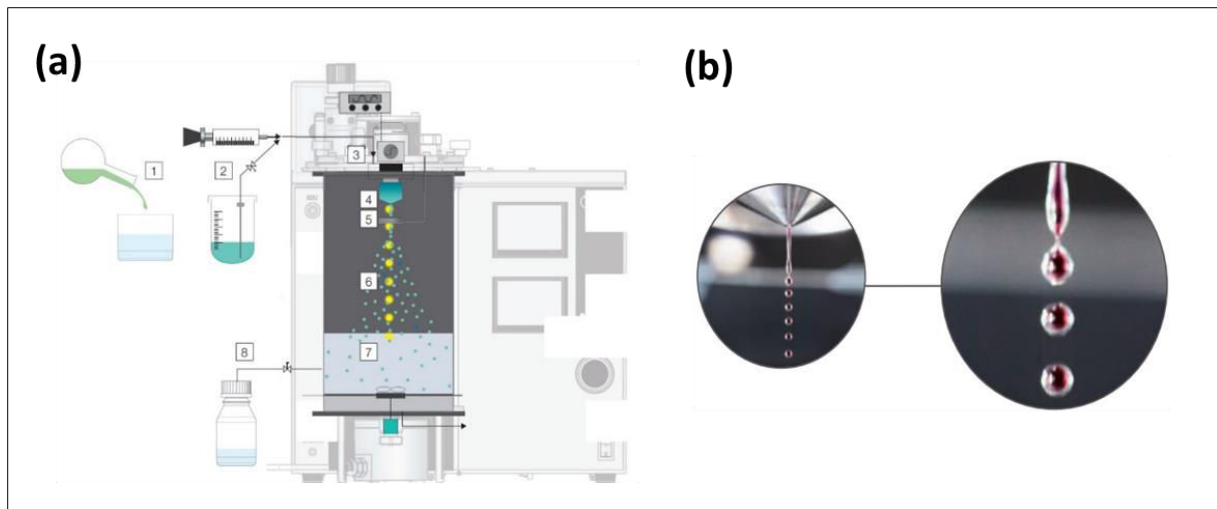


**Figure 13.** Principe de l'encapsulador BUCHI B-395 Pro(a) et photo du Jet à la sortie de la buse coaxiale.

### 2.9.3. Capsules millimétriques d'alginate

Les capsules millimétriques à cœur liquide présentant une membrane d'hydrogel d'alginate de calcium ont un large éventail d'applications allant de la biotechnologie à la gastronomie moléculaire (Alessandri et al., 2013) (Fu et al., 2014).

En ce qui concerne le procédé de fabrication, il existe trois principales approches qui sont la coextrusion et electro-coextrusion, la polymérisation multicouches et la sphérification inverse qui est le procédé utilisé au cours de cette thèse et procédé de base dans la fabrication des perles gastronomiques 'Cookal'.

#### 2.9.3.1. Coextrusion et electro-coextrusion

La première est basée sur des dispositifs de millifluidique ou minifluidique, par co-extrusion ou par électro co-extrusion du cœur de la capsules (mélange interne) et de la solution d'alginate (solution périphérique) dans un bain de  $\text{CaCl}_2$  pour former les capsules d'alginate (Figure 14) (Bremond et al., 2010) (Phawaphuthanon, Behnam, Koo, Pan, & Chung, 2014) (Rolland et al., 2014).

L'épaisseur de la membrane est contrôlée en changeant le rapport entre les débits des solutions interne et périphérique (Bremond et al., 2010).

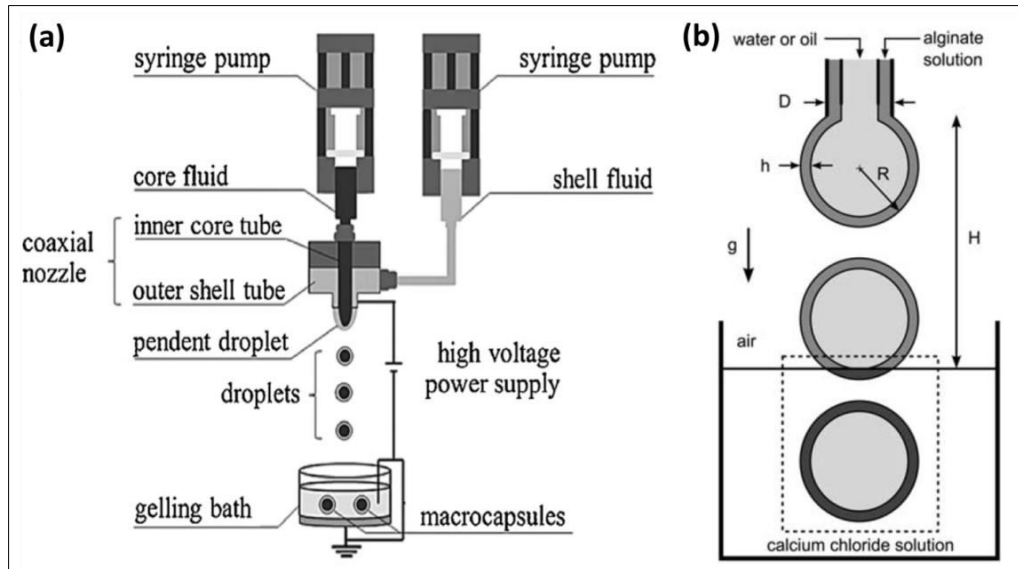


**Figure 14.** Principe de l'électro-coextrusion (a) et de la coextrusion (b). Adaptée de (Bremond et al., 2010) (Phawaphuthanon et al., 2014).

### 2.9.3.2. Polymérisation multicouches

La seconde méthode est basée sur la formation de billes d'alginate par simple extrusion goutte à goutte d'une solution d'alginate dans un bain de  $\text{CaCl}_2$ . Les hydrogels sphériques d'alginate sont ensuite enrobés par l'ajout d'une couche de polymère cationique ou de plusieurs couches de revêtement en alternant l'alginate avec un polymère de charge opposée de type chitosane ou Poly-L-lysine. L'opération d'enrobage peut être répétée jusqu'à l'obtention du nombre de couches souhaité (Breguet, Gugerli, Perneti, von Stockar, & Marison, 2005) (Correia, Sher, Reis, & Mano, 2013).

Enfin, le cœur d'alginate est dissout par incubation des capsules dans une solution d'agent chélatant (citrate de sodium, EDTA). La figure 15 illustre les différentes étapes de fabrication de capsule d'alginate à cœur liquide par polymérisation multicouches.

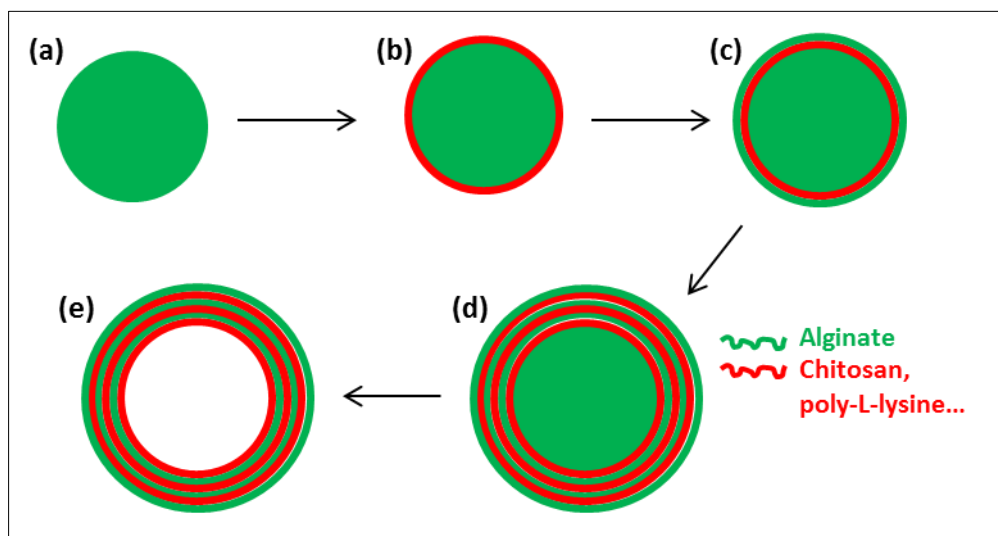


*Figure 15. Etapes de préparation de capsules d'alginate à cœur liquide par polymérisation multicouches.*

### 2.9.3.3. Gélification inverse

Pour la dernière approche, les gouttelettes de  $\text{CaCl}_2$  contenant la molécule active sont injectées goutte à goutte dans un bain d'alginate de sodium, une membrane d'alginate se forme instantanément lorsque les deux solutions entrent en contact, après un certain temps de séjour, les capsules partiellement gélifiées sont transférées dans une solution de  $\text{CaCl}_2$  pour terminer le processus de réticulation (Figure 16).

L'épaisseur de la membrane dépend de la concentration en alginate de sodium et du temps de séjour dans la solution de polymère. A la sortie du bain de gélification, les capsules doivent être rincées afin d'éviter l'agrégation des capsules par gélification externe (Blandino, Macías, & Cantero, 1999).

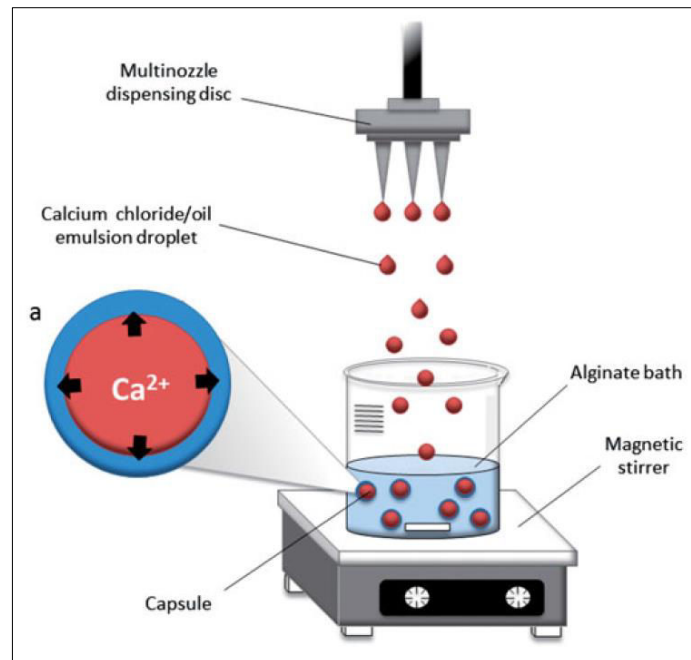


**Figure 16.** Principe de l'encapsulation par sphérification inverse (Martins, Renard, Davy, Marquis, & Poncelet, 2015).

Dans ce procédé, généralement un agent épaississant doit être ajouté à la solution de  $\text{CaCl}_2$  afin d'assurer la forme sphérique des capsules et éviter leur déformation par le cisaillement de la solution d'alginate (agitation) (Nigam, Tsao, Sakoda, & Wang, 1988) (Ana Blandino et al., 1999) (J. K. Park & Chang, 2000).

Cette technique d'encapsulation a été employée au cours de cette thèse pour la préparation des perles gastronomiques 'Cookal' (Figure 17).





*Figure 17. Exemple de perles gastronomiques Cookal à base de vinaigre balsamique.*

### **3. Capsules millimétriques intelligentes à base d'alginate**

Les fonctions principales des capsules sont l'encapsulation, le transport et la libération contrôlée du contenu de la capsule dans l'environnement externe (Hu, Tsai, Liao, Liu, & Chen, 2008a).

La fonctionnalité des capsules d'alginate dépend considérablement de leur perméabilité et stabilité mécanique et chimique (Chang, 2005).

Différents types de capsules intelligentes à cœur liquide avec une membrane d'alginate associé à d'autres types de polymères ont été développées.

Des capsules pH-sensibles ont été préparées après un enrobage des capsules d'alginate à cœur liquide avec une couche de silice et greffage d'acide polyméthacrylique à la surface des capsules. Lorsque le pH de l'environnement est inférieur à la valeur de pKa du PMAA, les groupements PMAA greffés se contractent à la surface de la membrane ce qui réduit sa perméabilité. En revanche, lorsque le pH est supérieur au pKa du PMAA, les groupements greffés gonflent ce qui augmente la perméabilité de la membrane (Mei, Xie, Yang, Ju, Wang, Wang, et al., 2013)(Mei, Xie, Yang, Ju, Wang, Zhang, et al., 2013).

Des capsules thermosensibles ont également été développées par incorporation de microgels de poly(N-isopropylacrylamide) (PNIPAAm) au niveau de la membrane des capsules préparées par un procédé de coextrusion millifluidique. Le PNIPAAm est le polymère thermosensible le plus utilisé puisqu'il présente une transition de phase dans l'eau à 34°C, proche de la température corporelle. La thermo-sensibilité des capsules dépend de la quantité incorporée de microgels de PNIPAAm et de la masse moléculaire de la molécule encapsulée (Wang et al., 2011).

Des capsules d'alginate avec des propriétés magnétiques ont été développées en incorporant des nanoparticules magnétiques au niveau du cœur liquide ou dans la membrane des capsules. Ces systèmes magnéto-sensibles ont une large gamme d'applications potentielles, y compris comme commutateurs ou capteurs, ou pour des applications nécessitant une libération contrôlée de leur contenu (délivrance de médicaments) (Degen, Zwar, Schulz, & Rehage, 2015).

#### **4. Conclusion**

Dans ce chapitre les techniques d'encapsulation et des exemples de microcapsules 'intelligentes' répondant à différents types de stimuli chimiques, physiques ou biologiques sont présentés. Suivi d'une présentation détaillée de la structure chimique, des propriétés et des mécanismes de gélification de l'alginate qui est le polymère utilisé dans les différents travaux d'encapsulation au cours de cette thèse. Enfin, les différentes techniques de préparation des capsules d'alginate à cœur liquide à différentes échelles ont été détaillées.



## ***Chapitre II:***

### ***Influence de l'agent épaississant sur les propriétés physicochimiques des capsules d'alginate à cœur liquide***

G. Ben Messaoud, L. Sánchez-González, L. Probst, S. Desobry. Influence of internal composition on physicochemical properties of alginate aqueous-core capsules. *Journal of Colloid and Interface Science*



Comme détaillé dans le premier chapitre, les capsules millimétriques d'hydrogel d'alginate à cœur liquide peuvent être préparées par trois méthodes différentes (sphérification inverse, co-extrusion et polymérisation multicouches). Dans ce travail les capsules sont préparées par sphérification inverse qui consiste en une extrusion goutte à goutte d'un mélange contenant du chlorure de calcium dans un bain de gélification à base d'alginate. Généralement un agent épaississant doit être ajouté à la solution de  $\text{CaCl}_2$  afin de garantir la formation de capsules sphériques et de limiter leur déformation par le cisaillement dans le bain de gélification.

Dans des études antérieures, plusieurs polymères ont été utilisés pour ajuster la viscosité de la solution de chlorure de calcium. Cependant le choix de l'agent épaississant utilisé pour moduler la viscosité de la solution de  $\text{CaCl}_2$  a rarement été discuté.

Dans ce chapitre, on s'est donc naturellement intéressé à l'étude de l'impact de la composition du cœur liquide et plus précisément du polymère utilisé pour ajuster la viscosité de la solution de  $\text{CaCl}_2$  sur la perméabilité et la stabilité mécanique de la membrane d'alginate. Pour faciliter l'étude, on a sélectionné trois polymères de charges différentes (anionique, cationique et neutre). Les propriétés mécaniques des capsules et plus précisément de la membrane (module de Young surfacique) ont été évaluées par compression et ont été corrélées avec les propriétés viscoélastiques d'hydrogels plans d'alginate obtenues par rhéologie oscillatoire aux faibles amplitudes. Puisque la sphérification inverse est une gélification très rapide par diffusion des ions calcium de la goutte vers la solution d'alginate au contact des deux solutions, il est donc difficile de simuler la formation d'hydrogels plans dans les mêmes conditions de gélification que les capsules. Trois méthodes de gélification ont été testées et les hydrogels obtenus ont été caractérisés et comparés aux membranes des capsules d'alginate. La perméabilité de la membrane a été évaluée par suivi de la diffusion de la rouge cochenille, riboflavine et albumine sérique bovine (BSA) du cœur des capsules vers le milieu externe.



## **Influence of internal composition on physicochemical properties of alginate aqueous-core capsules**

Ghazi Ben Messaoud <sup>a\*</sup>, Laura Sánchez-González <sup>a\*</sup>, Laurent Probst <sup>b</sup>, Stéphane Desobry <sup>a</sup>

<sup>a</sup> Université de Lorraine. LIBio. ENSAIA. 2 avenue de la Forêt de Haye, TSA 40602, F-54505 Vandœuvre-lès-Nancy, France.

<sup>b</sup> Cookal Company, 21 avenue de la Meurthe, 54320 Maxéville, France.

(\* ) Contact information for corresponding author

Tel.: +33 (0)3 83 59 58 77

Fax: +33 (0)3 83 59 58 04

G. Ben Messaoud: [ghazi.ben-messaoud@univ-lorraine.fr](mailto:ghazi.ben-messaoud@univ-lorraine.fr)

L. Sánchez-González: [laura.sanchez-gonzalez@univ-lorraine.fr](mailto:laura.sanchez-gonzalez@univ-lorraine.fr)

### **Abstract**

#### *Hypothesis*

To enhance physicochemical properties of alginate aqueous-core capsules, conventional strategies were focused in literature on designing composite and coated capsules. In the present study, own effect of liquid-core composition on mechanical and release properties was investigated.

#### *Experiments*

Capsules were prepared by dripping a CaCl<sub>2</sub> solution into an alginate gelling solution. Viscosity of CaCl<sub>2</sub> solution was adjusted by adding cationic, anionic and non-ionic naturally derived polymers, respectively chitosan, xanthan gum and guar gum. In parallel, uniform alginate hydrogels were prepared by different methods (pouring, in situ forming and mixing). Mechanical stability of capsules and plane hydrogels were respectively evaluated by compression experiments and small amplitude oscillatory shear rheology and then correlated.



Capsules permeability was evaluated by monitoring diffusion of encapsulated cochineal dye, riboflavin and BSA. The core-shell interactions were investigated by ATR-FTIR.

### *Findings*

Results showed that inner polymer had an impact on membrane stability and could act as an internal coating or provide mechanical reinforcement. Mechanical properties of alginate capsules were in a good agreement with rheological behavior of plane hydrogels. Release behavior of the entrapped molecules changed considerably.

This study demonstrated the importance of aqueous-core composition, and gave new insights for possible adjusting of microcapsules physicochemical properties by modulating core-shell interactions.

**Keywords:** *Chitosan; Xanthan gum; Guar gum; Mechanical stability; Rheological characterization; Release behavior.*

## **1. Introduction**

Polysaccharide-based capsules are of widespread importance in the encapsulation field (Kosaraju, 2005) (Madene, Jacquot, Scher, & Desobry, 2006). Their main functions are the successful encapsulation, transportation and controlled release of the capsule content to the external environment (Hu, Tsai, Liao, Liu, & Chen, 2008).

Among natural polysaccharides, sodium alginate is widely used. It is a water soluble anionic polysaccharide, mainly found in the cell walls of brown algae and can be isolated from the bacteria *Pseudomonas* and *Azotobacter* (Sabra, Zeng, & Deckwer, 2001). This natural polymer possesses several attractive properties such as good biocompatibility, wide availability, low cost, and simple gelling procedure under mild conditions (Shilpa, Agrawal, & Ray, 2003). Alginate is a co-polymer which consists of alternating  $\beta$ -D mannuronic acid (M) and  $\alpha$ -L guluronic acid (G) linked in (1-4). These uronic acids units are distributed along the alginate

chain in a pattern of blocks: homopolymeric sequences containing only mannuronic acid units (M Blocks) and guluronic (G blocks) and heteropolymeric blocks containing both mannuronic and guluronic units (MG blocks) (Shilpa et al., 2003). Physical properties of sodium alginate are dependent of M/G ratio, sequence and molecular weight (Pawar & Edgar, 2012). The gelation mechanism is driven by the interactions between G-blocks which associate to form firmly held junctions due to divalent cations. In addition to G-blocks, MG blocks also participate, forming weaker junctions (Pawar & Edgar, 2012). The alginate hydrogel's cross-links involve electrostatic, hydrogen interactions van der Waals forces (Braccini & Pérez, 2001).

The millimeter-scale alginate liquid aqueous-core capsules are widely used for a large range of applications from biotechnology to molecular gastronomy (Alessandri et al., 2013) (Fu et al., 2014) (Smidsrød & Skjåk-Braek, 1990).

Concerning the manufacturing process, there are three main approaches for preparation of alginate liquid-core capsules of millimeter-scale size. The first one is based on milli-fluidic devices, by co-extrusion and electro co-extrusion of the inner core and Na-alginate drops into a  $\text{CaCl}_2$  bath to form the alginate capsules, of which the membrane thicknesses is regulated by changing the ratio between the flow rates of the inner and outer solutions (Bremond, Santanach-Carreras, Chu, & Bibette, 2010) (Rolland, Santanach-Carreras, Delmas, Bibette, & Bremond, 2014) (Phawaphuthanon, Behnam, Koo, Pan, & Chung, 2014). The second method is based on the formation of alginate beads hydrogel followed by coating with oppositely charged polymers and finally by alginate core removal using a chelating agent (Sato, Hoshina, & Anzai, 2011) (Correia, Sher, Reis, & Mano, 2013) (Taqieddin & Amiji, 2004). For the last approach, the  $\text{CaCl}_2$  droplets containing the active molecule is dropped into a sodium alginate bath to form the inner side of the membrane, and then the partially gelled capsules are transferred into a  $\text{CaCl}_2$  solution to complete the reticulation process (Blandino, Macías, & Cantero, 1999).

In this method, generally a thickening agent must be added to the CaCl<sub>2</sub> solution in order to ensure the spherical shape and to prevent capsule shear deformation (Blandino et al., 1999). In previous studies, capsules with various core saccharides like sucrose (Nussinovitch, Gershon, & Nussinovitch, 1996) (Zhang & Salsac, 2012), xanthan gum (Cheong, Park, Kim, & Chang, 1993), dextran (Nigam, Tsao, Sakoda, & Wang, 1988), carboxymethyl cellulose (Blandino et al., 1999) (Nussinovitch et al., 1996) (Patel, Pusch, Mix-Wagner, & Vorlop, 2000), guar gum (Nussinovitch et al., 1996), polyethylene glycol (Koyama & Seki, 2004a) and glycerol (Ben Messaoud, Sánchez-González, Jacquot, Probst, & Desobry, 2015) (Leick, Kemper, & Rehage, 2011) were developed.

In the present work three thickening agents (anionic, cationic, and neutral biopolymers, respectively) were chosen: xanthan gum (XG), chitosan (CS) and guar gum (GG). XG is an extracellular anionic polysaccharide secreted by the microorganism *Xanthomonas campestris*. It is a complex polysaccharide consisting of a primary chain of  $\beta$ -D-(1,4)-glucose backbone, which has a branching trisaccharide side chain comprised of  $\beta$ -D-(1,2)-mannose, attached to  $\beta$ -D-(1,4)-glucuronic acid, and terminates in a  $\beta$ -D-mannose (Elçin, 1995).

CS is a cationic polysaccharide composed essentially by  $\beta$ -(1–4) linked glucosamine units together with some proportion of N-acetyl glucosamine units. It is obtained by extensive deacetylation of chitin; a polysaccharide widely spread in nature (Pillai, Paul, & Sharma, 2009). GG is derived from the ground endosperm of guar seeds (*Cyamopsis tetragonoloba*). This non-ionic polysaccharide has a backbone built up by D-mannopyranosyl residues linked  $\beta$ -(1–4) and usually bearing, in different extent, side chains of single galactopyranosyl units linked  $\alpha$ -(1–6) (Heyman, De Vos, Van der Meeren, & Dewettinck, 2014).

For core-shell structures, the core composition could play an important role on the final physicochemical properties of capsules, for example mechanical stability could be affected by

core swelling [12]. Guest molecules could be also incorporated in capsules core to interact with the encapsulated active molecule and to control its loading or release (Shen et al., 2013). At the nanoscale, core composition could impact significantly the mechanical properties of core-shell spheres (Still et al., 2008).

In the best of our knowledge, there is no information about the influence of aqueous-core composition on final physicochemical properties of the alginate liquid-core capsules. Studies, in which the thickening agent choice was justified, focused on the thickener diffusion after capsules preparation (Koyama & Seki, 2004b) or on control of capsule content viscosity to obtain a low viscous core (Zhang & Salsac, 2012) or to facilitate microorganisms' proliferation (Koyama & Seki, 2004a).

The aim of this work was to study the influence of the thickening agent on the physicochemical properties of alginate liquid-core capsules and to correlate them to plane hydrogels prepared by three gelation approaches. The density of alginate capsules were modulated by anionic XG, non-ionic GG and cationic CS. The mechanical properties of capsules membrane as well as permeability to three model molecules were studied.

## **2. Materials and methods**

### **2.1. Materials**

Sodium alginate (SA) from brown algae with a typical M/G ratio around 1.6 was purchased from Sigma Aldrich (Chemie, Steinheim, Germany). The average viscosity molecular weight of alginate was calculated using the Mark–Houwink–Sakurada correlation:  $[\eta] = KM_v^a$ . By measuring the zero-shear viscosity using a rotational rheometer (kinexus pro, Malvern Instruments, Orsay, France) equipped with a cone-and-plate (50 mm, 2°) geometry. The specific viscosity and subsequently the intrinsic viscosity  $[\eta]$  can be achieved. The calculated intrinsic

viscosity found a value of 4.73 dL / g and thus an average molecular weight  $M_v$  of  $1.69 \cdot 10^5$  was obtained (Thu et al., 1996).

Chitosan (CS) from shrimp shells (viscosity 0.02-0.3 Pa.s, 1 % wt in acetic acid at 20 °C, Deacetylation  $\geq 75$  %), xanthan gum (XG) from *Xanthomonas campestris*, guar gum (GG), Albumin from Bovine Serum BSA ( $M_w \approx 66$  KDa), new cochineal red dye ( $M_w = 604.46$  g / mol), riboflavin ( $M_w = 376.36$  g/mol) and D-(+)-Gluconic acid  $\delta$ -lactone (GDL) were purchased from Sigma Aldrich (Chemie, Steinheim, Germany). Calcium chloride dihydrate and calcium carbonate were obtained from VWR (International, Leuven, Belgium), acetic acid 99-100 % from Chem-lab NV (Zedelgem, Belgium) and tri-sodium citrate from Fisher scientific (Leicestershire, United Kingdom).

For alginate-FITC derivative synthesis, fluorescein isothiocyanate (FITC, isomer I), N-(3 dimethylaminopropyl)-N'-ethylcarbodiimidehydrochloride(EDC),N hydroxysulfosuccinimide sodium salt (NHSS) and 1, 6-diaminohexane were purchased from Sigma-Aldrich (Chemie, Steinheim, Germany).

## **2.2. Solutions preparation and characterization**

The cationic solution was prepared by dissolving 1 g of calcium chloride in 80 mL of 0.1 % vt acetic acid solution. Then XG, CS and GG powders were dispersed in stirred  $\text{CaCl}_2$  for modulating viscosity to ensure the spherical shape of capsules and prevent their deformation by shear stress resulting from the stirring of alginate solution. The final pH was adjusted to 5 by adding some NaOH droplet to prevent alginate precipitation during the subsequent encapsulation step. The final solution volume was adjusted to 100 mL and the final concentrations of XG, CS and GG were 0.35, 1.2 and 1 % wt, respectively.

These concentrations were selected in order to obtain the same viscosity during the extrusion step as detailed in supplementary information (Fig 1 and table 1).

The shear viscosity of the thickening agent solutions was studied with a dynamic rotational rheometer Malvern Kinexus (Malvern Instruments, Orsay, France) equipped with a cone-and-plate (50 mm, 2°) in the shear rate range from  $10^{-2}$  to  $10^3$  s<sup>-1</sup>. All measures were triplicated at 20 °C.

The used thickener solutions in this work are non-Newtonian fluids which could affect the droplet size during the encapsulation step. In fact, the shear rate encountered during extrusion through a syringe is related to the radius,  $r$ , of the needle's orifice and the volumetric flow rate,  $Q$ , by the following expression (eq.2):

$$\dot{\gamma} = n + \frac{4Q}{\pi r^3} \quad (2)$$

Where  $n$  is the power law index (eq.3)

$$\sigma = k \dot{\gamma}^n \quad (3)$$

Where  $\sigma$  is the shear stress,  $k$  is the consistency index,  $\dot{\gamma}$  is the shear rate, and  $n$  is the flow behavior index.

By measuring the volumetric flow rate and the internal radius of the orifice, the shear rate at the outlet of the syringe is approximately of 2 s<sup>-1</sup>.

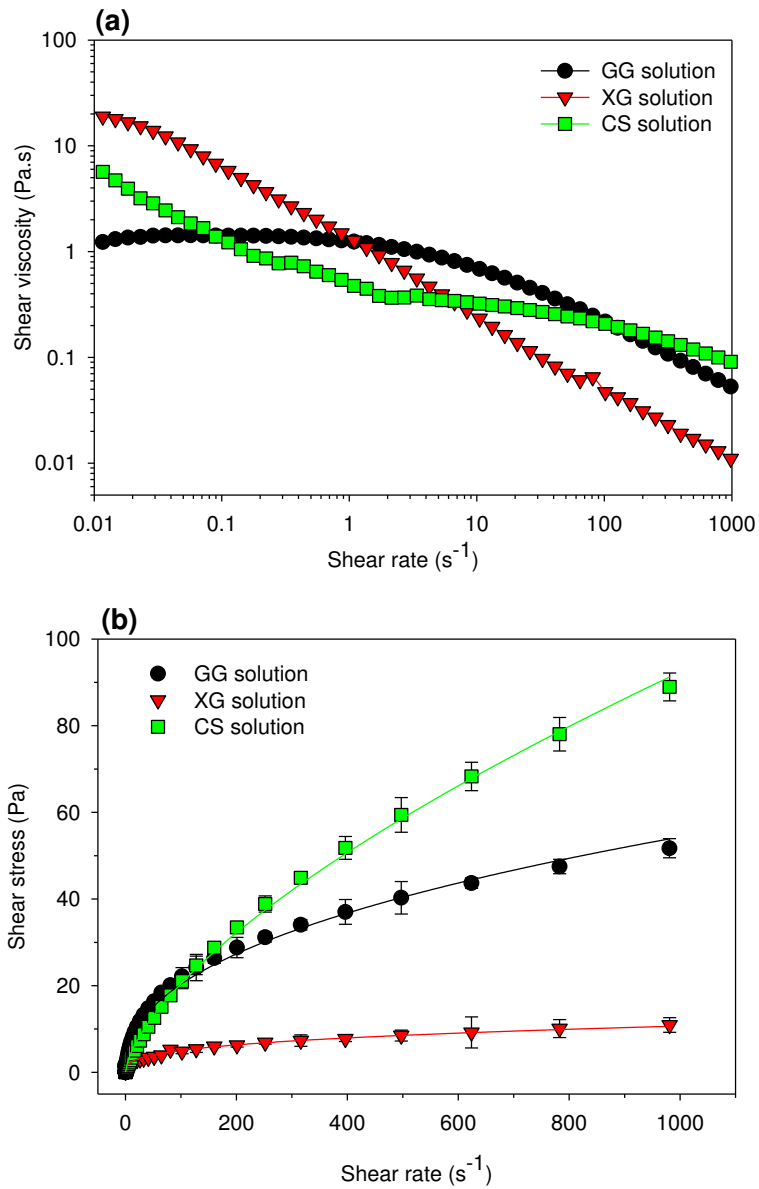


**Figure 1.** Flow curves of the thickening agent solutions. Shear viscosity evolution with shear rate (a) and shear rate vs shear stress. The solids lines are the fit to power law model (b).

The flow curves of the thickening agent solutions are plotted in Figure.2b, the solid lines represents the fits to the power law model. Results of power law model fits are reported in Table 1. The n and k values ranged from 0.325 to 0.655 and from 1.14 to 2.8, respectively.

**Table 1.** Rheological properties of the different thickening agent solutions. Mean values and standard deviation

<b>Thickening agent</b>	<b>Consistency index K (Pa.s)</b>	<b>Flow behavior index n</b>	<b>Correlation factor R<sup>2</sup></b>
<b>GG</b>	2.85 ± 0.13 <sup>a</sup>	0.427 (0.007) <sup>a</sup>	0.994
<b>XG</b>	1.14 (0.03) <sup>b</sup>	0.325 (0.005) <sup>b</sup>	0.995
<b>CS</b>	1.00 (0.04) <sup>c</sup>	0.655 (0.006) <sup>c</sup>	0.999

<sup>a, b, c</sup> Different letters in the same column indicate significant differences among thickening agents (p<0.05)

## **2.3. Alginate systems preparation**

### **2.3.1. Capsules**

Alginate aqueous-core capsules were prepared according to Blandino et al. (1999) by extrusion, using a simple one-step process.

The CaCl<sub>2</sub> solutions were extruded dropwise through a syringe equipped with a needle (outer diameter, 0.9 mm) with a flow rate of 2 mL / min using a peristaltic pump into 200 mL SA solution (0.5 % wt SA) stirred at 300 rpm to prevent droplets sticking together and decrease external mass transfer resistance. A dropping height of 5 cm was used to ensure the formation of spherical capsules.

As a result, a calcium alginate (CA) membrane surrounds the droplets and liquid core capsules are formed as soon as the two liquids came into contact. After a gelation time of 10 minutes, the capsules were filtered and rinsed with distilled water to wash out excess SA around the capsules and avoid external gelation. Then capsules were transferred into 1 % wt CaCl<sub>2</sub> pH 5 solutions for 30 minutes to stabilize gel membranes and complete reticulation process.

### **2.3.2. Alginate hydrogels**

In order to investigate the influence of the thickening agent (CS, GG and XG) on physicochemical properties, plane calcium alginate gels were prepared using three different methods.

#### **Poured hydrogels**



The plane gels were formed by adding 5 mL of 0.5 % wt alginate solution into a plastic petri dish. For initiating the gelation, 6 mL of CaCl<sub>2</sub> 1 % wt with the desired thickening agent was carefully poured over alginate solution. Finally, the obtained hydrogels were stored in CaCl<sub>2</sub> solutions (pH 5, 1 % wt) to complete the reticulation process.

### **In situ hydrogels**

CaCO<sub>3</sub> powder was dispersed in the stirred alginate solutions (0.5 % wt) and then sonicated for 5 min to decrease the particle size at a nominal frequency of 40 kHz at 40% of full power (Sonicator Vibra cell 75115, 500 watt, Bioblock Scientific Co). An appropriate amount of GDL powder was added under gentle stirring and alginate solutions were poured into petri dishes and samples were allowed to stand, with gelation taking place over night. The molar ratio of CaCO<sub>3</sub>/GDL was maintained at 0.5 in order to obtain a final pH of 7 (Kuo & Ma, 2001). The plane hydrogels were then incubated in the different thickening agent solutions (pH 5) for one day and finally were washed several times with CaCl<sub>2</sub> (pH5, 1 % wt) before the rheological characterization.

### **Mixed hydrogels**

To prepare mixed hydrogels, SA solution (0.5 % wt) was mixed with the thickening agent solution CaCl<sub>2</sub> 1 % wt and vortexed during 1 min and then transferred in a petri dish. The obtained hydrogels were stored in CaCl<sub>2</sub> solution (pH 5, 1 % wt) to complete the reticulation process.

## **2.4. Capsules characterizations**

### **2.4.1. Measurements of capsule dimensions**

For capsules fluorescence imaging, alginate-FITC derivative was synthesized according to Zhu et al., (2005). Briefly, 120 mg of SA was mixed with EDC/NHSS (50 mg/30 mg) for the activation of carbonyl groups on alginate in pH 5.0 sodium acetic buffer for 30 min, followed by addition of 60 mg 1, 6-diaminohexane for another 4 h. The mixture was precipitated in 2-

propanol to remove unreacted diamine. The alginate-amine derivative was reacted with FITC (0.5 mg) in pH 8.5 sodium bicarbonate solution for 4 h and precipitated in acetone. Finally, the obtained alginate-FITC derivative was mixed with unlabeled SA solution (Zhu, Srivastava, & McShane, 2005).

The capsules dimensions were then performed under an optical microscope (Olympus AX70, Japan) equipped with fluorescence imaging and with a camera (Olympus DP70). The images were captured using Dp controller software (version 2.1.1). Fluorescence images were visualized using an FITC filter. Shell thickness and capsules diameter were hence calculated using image J software (National Institutes of Health, Bethesda, Maryland, USA). The data for one experimental condition were calculated from values taken from 20 capsules.

#### **2.4.2. Mechanical stability**

To investigate mechanical stability of calcium alginate capsules filled with different thickening agents, individual capsules were compressed between two parallel plates. A rotational rheometer Malvern Kinexus (Malvern Instruments, Orsay, France) with a plate-and-plate (20 mm) geometry was used. A force gap test was used to compress the capsules from 4 mm to 0.05 mm with a linear compression speed of 10  $\mu\text{m} / \text{s}$  (Leick, Kott, et al., 2011). The gap and the normal force being imposed were measured simultaneously at the upper plate. At least five replicates were considered for each type of capsule.

#### **2.4.3. Solutes release**

To investigate the permeability of the capsules, cochineal red dye, riboflavin and BSA were solubilized in the thickening agent solutions before the encapsulation step. The freshly prepared capsules were placed at 20 °C into 20 mL of water. At scheduled time intervals, the amount of released cochineal red, riboflavin and BSA was determined from solution absorbance at 500, 440 and 280 nm wavelength using a Uv-vis spectrophotometer Pharmacia Biotech Ultrospec 4000 (Richmond Scientific Ltd, Lancashire, U.K). To determine the total mass initially

encapsulated at the end of each experiment, 1 mL of tri-sodium citrate solution (1 M) was added to dissolve gel membrane by calcium chelation (Smidsrød & Skjåk-Braek, 1990).

#### **2.4.4. FTIR spectra**

Attenuated total reflectance Fourier transform infrared (ATR-FTIR) spectra of air dried CA capsules were acquired using a Tensor 27 mid-FTIR Bruker spectrometer (Bruker, Karlsruhe, Germany) equipped with an ATR accessory (128 scans, 4 cm<sup>-1</sup> resolution, wavenumber range : 4000 - 400 cm<sup>-1</sup>) and a DTGS detector. Spectral manipulations were performed using OPUS software (Bruker, Karlsruhe, Germany). Raw absorbance spectra were smoothed using a nine points smoothing function. Elastic baseline correction using 200 points and H<sub>2</sub>O/CO<sub>2</sub> correction were then applied. Then, spectra were centered and normalized.

#### **2.5. Hydrogels characterization**

The prepared gels were characterized by dynamic rheology measurements with a plate-and-plate geometry (20 mm) at 25 °C. First, an amplitude sweep was conducted by changing the shear strain from 0.001 to 100 % to determine the linear viscoelastic region. On the basis of this test, a value of 0.1 % strain within the linear regime was then used in the subsequent frequency sweep with the change of frequency between 0.02 and 10 Hz. Three replicates were considered for each type of hydrogel.

#### **2.6. Statistical analysis**

Results were analyzed by analysis of variance (ANOVA) with 95 % significance level using SigmaPlot software (SigmaPlot Version 11.0, Systat Software Inc., San Jose, CA, USA).

### **3. Results and Discussion**

#### **3.1. Capsules dimensions**

Microscopic observation led to determine the average diameter and membrane thickness of alginate capsules filled with the different polymers (Fig.2).

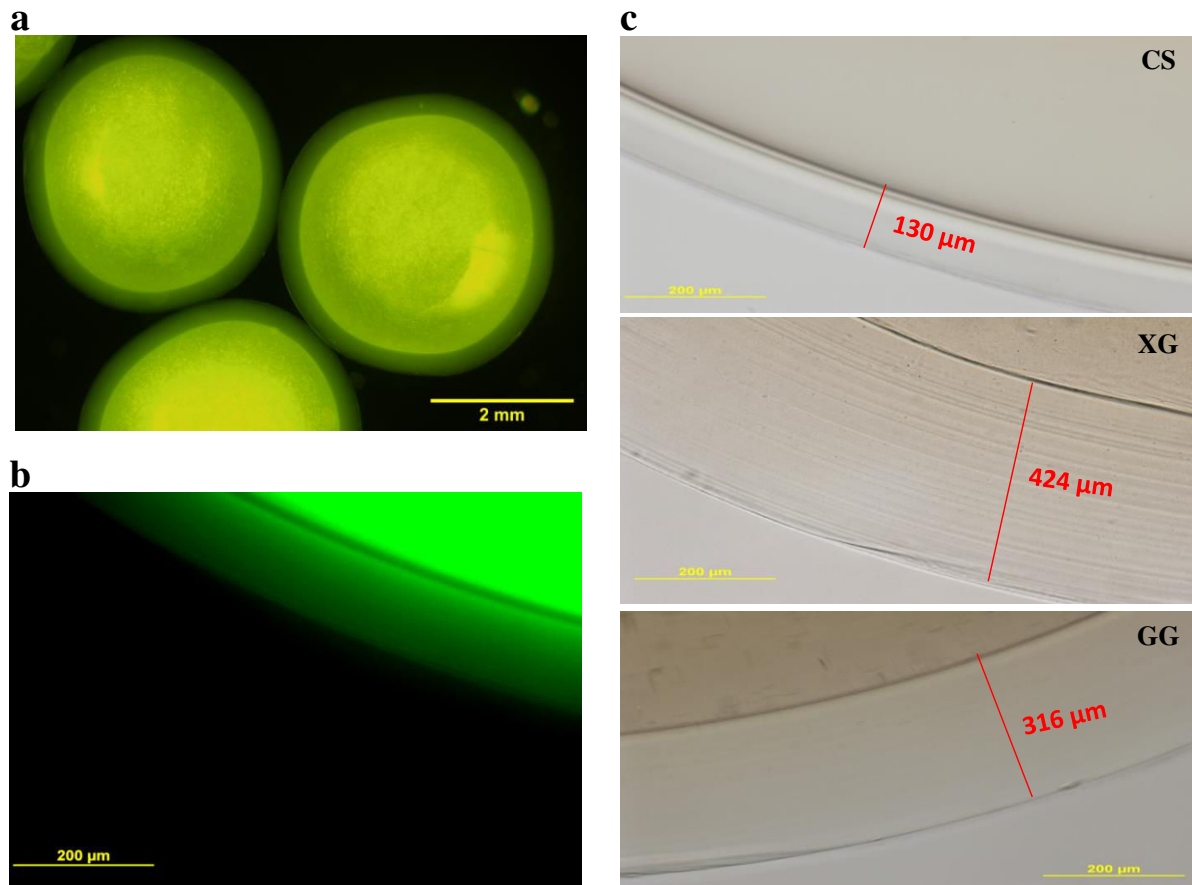


**Figure 2.** Microscopic images of alginate aqueous-core capsules. Fluorescence image of CA-GG capsules (a), fluorescence image of CA-CS membrane (b) and optical images of CA membrane obtained with the different thickening agents (c).

The average diameter of alginate capsules range from 3.6 to 3.9 mm and average thicknesses were 142, 327 and 434  $\mu\text{m}$  for CA-CS, CA-GG and CA-XG, respectively (Table 2).

**Table 2.** Diameter ( $d$ ) and membrane thickness ( $h$ ) of alginate capsules filled with the different thickening agents. Mean values and standard deviation

Thickening agent	Average diameter (mm)	Membrane thickness ( $\mu\text{m}$ )
GG	3.64 (0.1) <sup>a</sup>	327 (10) <sup>a</sup>
XG	3.57 (0.1) <sup>a</sup>	434 (21) <sup>b</sup>
CS	3.9 (0.1) <sup>b</sup>	142 (16) <sup>c</sup>

<sup>a, b, c</sup> Different letters in the same column indicate significant differences among thickening agents ( $p < 0.05$ )

The dimension of the capsules depends mainly on the droplet size before getting into contact with alginate solution. Generally, capsules size is predicted by the Tate's law, which estimates

the equilibrium between gravitational force pulling drop down and surface tension force holding drop outlet the needle tip at the moment of drop detachment (Chan, Lee, Ravindra, & Poncelet, 2009). In the other hand, the needle size is the most important factor (Ong, Lee, Radzi, Zakaria, & Chan, 2015).

No significant differences were observed in terms of CA-XG and CA-GG capsules diameters. However, it can be noted that the diameter of these capsules was significantly lower than CA-CS ones. In fact chitosan is a polycation and as soon as the two liquid entered into contact, a polyelectrolyte membrane is formed (Ong et al., 2015).

The membrane thickness measurements showed significant differences and suggested that alginate capsules membrane did not only depend only on crosslinking time, concentration of SA and calcium chloride but also on gelation kinetic influenced by core composition and diffusion behavior of calcium cations from the droplet through the alginate membrane during gelation.

### **3.2. Capsules mechanical stability**

Alginate capsules are sensitive to deformations that may lead to their rupture or to undesirable early release of their contents. Macrocapsules can be investigated in a dynamic rotational rheometer thanks to its sensitive vertical testing capabilities.

Typical results of such measurements are summarized in Fig.3a in terms of force–displacement curves. The Fig.3b shows the magnification of data used for linear regression and surface Young's modulus calculation.

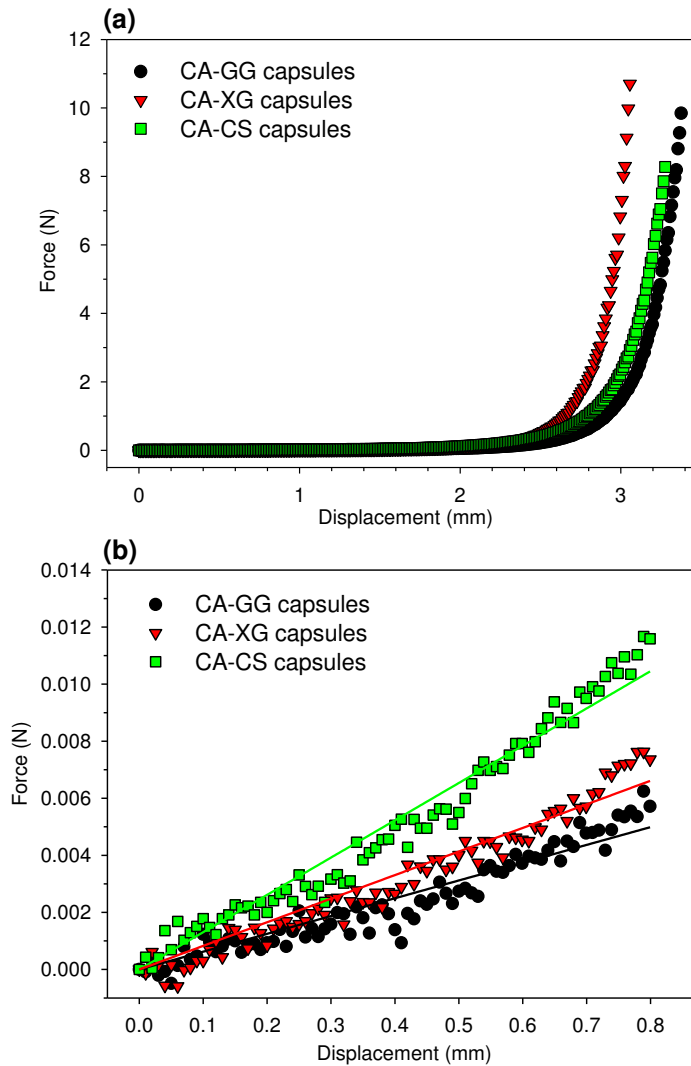


**Figure 3.** Typical force-displacement curves of alginate aqueous-core capsules filled with the different thickening agents (a) and magnification of data used for linear regression and surface Young's modulus calculation

The compression curves showed the same force-displacement behavior for all CA capsules types. The earlier increase of the compression curves of the CA-XG capsules can be related to the fact that these capsules are smaller in their diameter (3.57 mm) and therefore smaller displacements lead to higher deformations. The magnification of the data at small displacements showed that a higher external force was necessary to obtain the same compression for capsules filled with CS than capsules filled with XG and GG.

In fact, surface Young's modulus ( $E_s$ ), which is the measure of alginate capsule stiffness, is an interesting data to quantify mechanical stability.

$E_S$  was estimated by analyzing the force–displacement curves in the range of small deformations and using equation (1) (Leick, Kott, et al., 2011):

$$F = \frac{4E_S h}{r\sqrt{3(1 - \nu_S^2)}} d_D \quad (1)$$

Where  $d_D$  denotes capsule displacement,  $F$  is the measured force,  $h$  is the membrane thickness,  $r$  is the radius of the capsule and  $\nu_S$  the surface Poisson ratio for which a value of 1/3 was assumed for alginate hydrogel [24] (Leick, Henning, Degen, Suter, & Rehage, 2010).

This model is only valid for small deformations because the inner fluid leaks through the membrane pores during compression (Degen, Zwar, Schulz, & Rehage, 2015).

The surface Young's modulus of CA capsules is dependent on thickening agent nature. The highest value of Young's modulus was obtained with CS (45.1 N/m) which is approximately 3.7 and 5.5 times stronger than CA-XG and CA-GG capsules (12 and 8 N/m, respectively). The high stability of CA-CS capsules could be related to a high degree of cross-linking due to the reticulation of GG and MG blocks of alginate with  $\text{Ca}^{2+}$ , and formation of cooperative ionic bounds between M residues with the protonated amino groups of CS (Dupuy, Arien, & Minnot, 1994). In the other hand, CS could act as an internal membrane coating (Daly & Knorr, 1988). In fact, even in the absence of calcium salt, capsules could be formed by dripping a chitosan solution in an alginate gelling bath (Sankalia, Mashru, Sankalia, & Sutariya, 2007). The Young's modulus of the CA- XG was 1.5 times higher than CA-GG. The better resistance to compression of CA-XG could be related to the alginate shell thickness (Table 1), since a thicker membrane could lead to stiffer capsules (Rachik, Barthes-Biesel, Carin, & Edwards-Levy, 2006).

### 3.3. Solutes release measurements

Relative amounts of released cochineal red, riboflavin and BSA versus time elapsed after capsules preparation is plotted in Fig 4

For cochineal red dye, CA-CS capsules, cochineal red A dye cannot diffuse through the polyelectrolyte membrane. This could be explained by potential electrostatic interactions between the amino groups of the cationic CS and the sulfonates groups of the negatively charged cochineal red A in the aqueous core. CA-XG and SA-GG capsules, the amount of released cochineal red A increased rapidly in the first two hours and equilibrium state was nearly achieved in a time slot of 120 min.

For riboflavin, all Ca capsules showed the same release profile, where the amount of release vitamin increased rapidly in the first hour and equilibrium was achieved after 80 min. This relative lower equilibrium time compared to cochineal red release (120 min) is certainly due to lower molecular weight and therefore faster release from the alginate membrane.

For BSA, the diffusion equilibrium was not achieved for all CA-capsules after 7 hours. The relative slow BSA diffusion compared to riboflavin and cochineal red dye is related to its molecular weight. No variations were observed between CA-XG and CA-GG diffusion profile and released amount of BSA after 7 hours was not significantly different ( $75 \% \pm 3$  and  $71 \% \pm 3$ ), respectively.



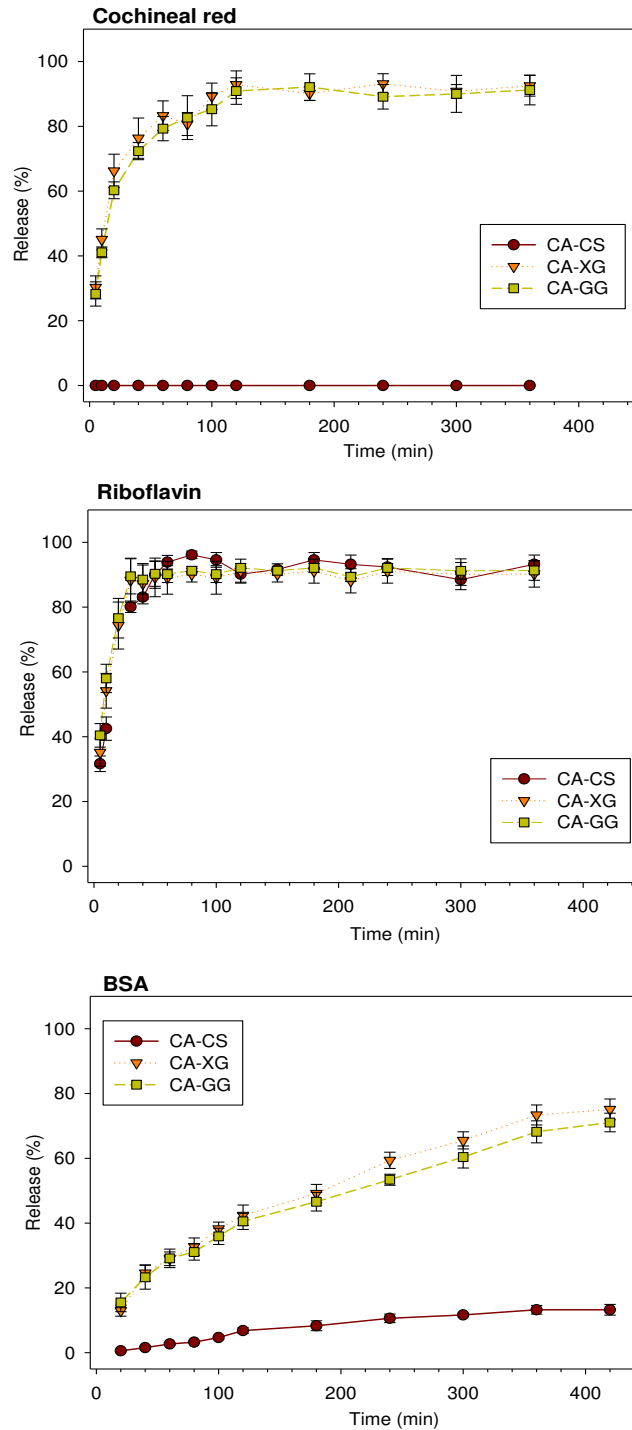


**Figure 4.** *Solutes release from alginate aqueous-core capsules. Mean values and standard deviation*

However, CA-CS capsules showed significant protein retention and the amount BSA released after 7 hours did not exceed 14 %. This suggested that a densely cross-linked membrane structure with very low chain mobility was formed. This retention behavior is explained by the

chemical stability of the polyelectrolyte complex between alginate hydrogel and the potential internal CS coating layer. Another possible explanation is the potential electrostatic interaction between the positively charged CS and negatively charged BSA which has an isoelectric point around pH 5 (Boeris, Farruggia, & Picó, 2010).

From the different release experiments, we can conclude that the diffusion profile of the encapsulated molecules could be controlled by the aqueous core composition and potential interaction between the active molecules with the guest polymer used to prepare the alginate core-shell capsules.

### **3.4. Rheology of plane hydrogels**

The membrane formation of alginate aqueous-core capsules during extrusion is a very fast microscopic gelation process. In fact, as soon as the two liquids (CaCl<sub>2</sub> droplet and alginate bath) entered into contact, both calcium ions and the thickening agent diffused from the thickening agent solution droplet to the external alginate solution. It's therefore difficult to prepare plane hydrogels which mimics exactly alginate membrane formation. Consequently, to study the influence of thickening agents on alginate shell layer, three type of hydrogels were prepared by pouring thickening agent mixture onto alginate solution, in situ calcium release followed by incubation in the thickening agent solutions or by mixing the two gelling solutions. Rheological frequency sweep tests were performed on three-dimensional alginate gel. The elastic ( $G'$ ) and viscous ( $G''$ ) moduli of CA hydrogels were investigated by dynamic mechanical analyses. The frequency dependence of these moduli was reported on Fig.5.

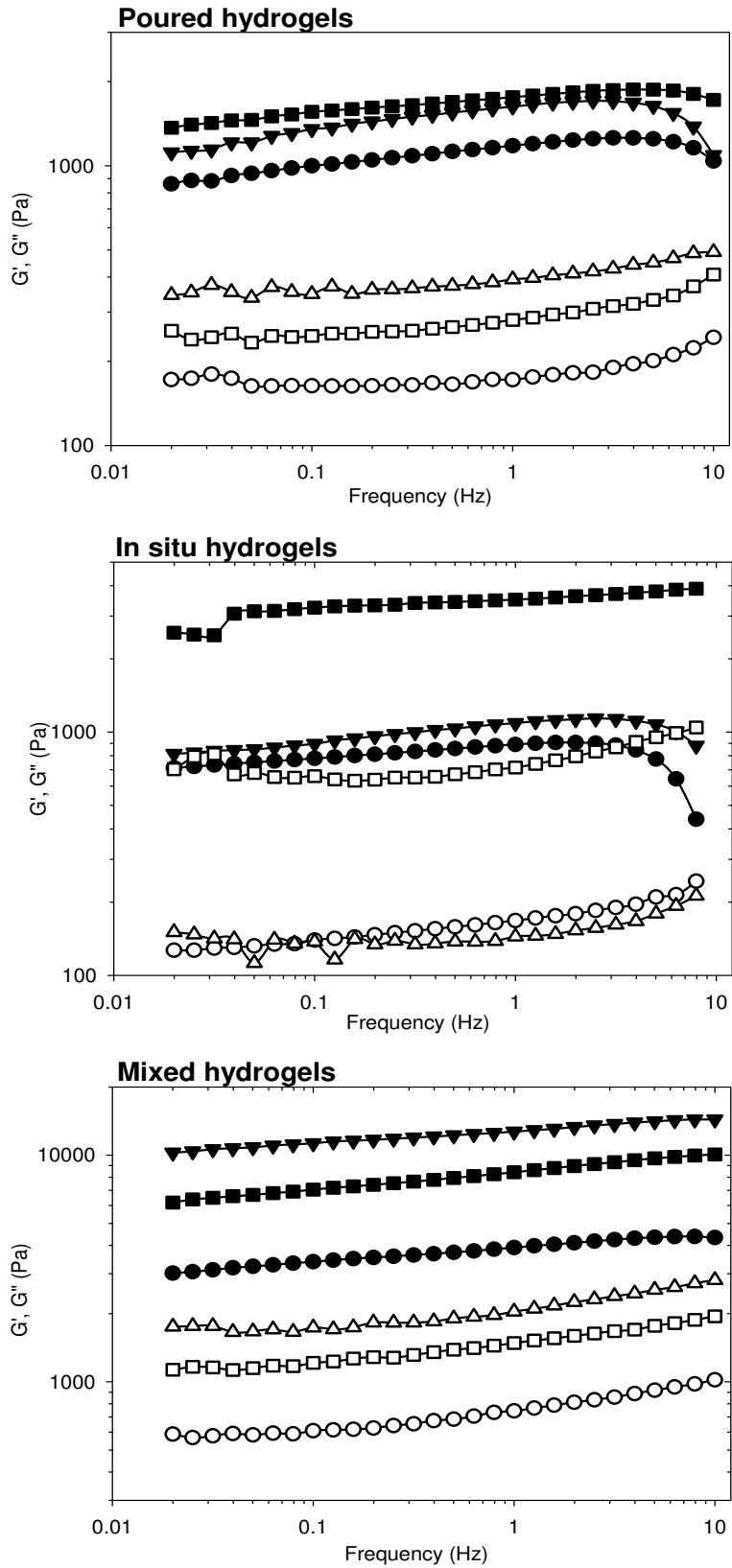


**Figure 5.** Frequency sweep data for the various prepared hydrogels. The legend for panel 'poured hydrogels' also applies to panels 'in situ and mixed hydrogels'.

As expected, all mechanical spectra showed that  $G'$  are higher than  $G''$ , confirming that the CA hydrogels have predominantly elastic rather than viscous character. This criterion distinguishes gels from viscous liquids and specifies that the deformation energy is recovered in the elastic stretching of chemical bonds (Stendahl, Rao, Guler, & Stupp, 2006).

For all hydrogels systems, we observed a frequency dependence evolution of  $G'$  and  $G''$ . In fact, slow increase of storage modulus with frequency indicated the existence of relaxation processes which could be induced by reversible entrapped entanglements release or intermolecular junctions opening (Leick, Kott, et al., 2011). These junctions resulted from coordination of  $Ca^{2+}$  cations to the alginate's inter-chain cavities made up of guluronate blocks, resulting in development of a so-called 'egg-box' (Grant, Morris, Rees, Smith, & Thom, 1973). For all systems,  $G'$  and  $G''$  depended strongly on the presence of CS, XG and GG. Concerning, poured and in situ hydrogels, highest  $G'$  and  $G''$  were obtained for CA-CS followed by CA-XG then CA-GG. However for the mixed gels, CA-XG showed greater stability than CA-CS and CA-GG. Thus, the influence of thickening agent is related to the approach used to prepare plane gel which plainly demonstrates the importance of gelation conditions on final hydrogel mechanical strength.

For poured and in situ hydrogels, CA-CS system showed the highest range of  $G'$  and  $G''$ . This behavior was certainly due to a high degree of cross-linking between  $Ca^{2+}$  and protonated amino groups of CS in one hand and CA carboxyl groups in the other hand. In general, the elastic modulus of an alginate gel depends on the number of cross-links, length and stiffness of the chains between cross-links (Stephen & Phillips, 2006). The CA-XG gel showed a higher  $G'$  and  $G''$  modulus range than CA-GG gel. The difference of stiffness between the two systems cannot be related to the number of cross-links because  $Ca^{2+}$  was used at the same concentration. So the affinity between the cross linker and the two polymers was the same.

For mixed hydrogels, semi-IPNs (inter-Penetrating Networks) are formed by mixing alginate and thickening agent solutions and final mechanical stability of the obtained hydrogels is modulated by several factors. Indeed, during this type of gelation, the mechanical properties of an alginate gel could be enhanced by potential molecular interactions between alginate and the thickening agent or alternatively decreased due to thickening agent spatial hindrance during the egg-box formation. Moreover, the final gel structure could be influenced by the molecular weight and chain stiffness of the thickening agent molecules. The higher stability of CA-XG could be explained by potential hydrogen bonding between alginate carboxyl groups and XG hydroxyl groups (Pongjanyakul & Puttipipatkachorn, 2007).

For CA-CS mixed gel, the mechanical properties could be affected by the competition between  $\text{Ca}^{2+}$  and  $\text{NH}_3^+$  CS amino groups to bind with  $\text{COO}^-$  alginate groups and consequently the decrease of calcium ions activity. In the other hand, ammonium groups are monovalent whereby the incorporated charge density is lower than for the divalent calcium ions (Leick, Kemper, et al., 2011).

For a better correlation of CA gels viscoelastic properties with the mechanical stability of CA aqueous-core capsules, the surface Young's moduli of the plane hydrogels were calculated according to Leick et al., 2011 (Leick, Kott, et al., 2011) (Eq.2):

$$E_s = 2\mu_s(1 + \nu_s) \quad (2)$$

Where  $E_s$  and  $\nu_s$  were defined in (Eq.3) and  $\mu_s$  is the two dimensional shear modulus which is the multiplication of storage moduli ( $G'$ ) with alginate hydrogel thickness (the used gap in rheological experiments).

The calculated  $E_s$  are reported in Fig.6 with the obtained from alginate compression experiments for comparison purpose.

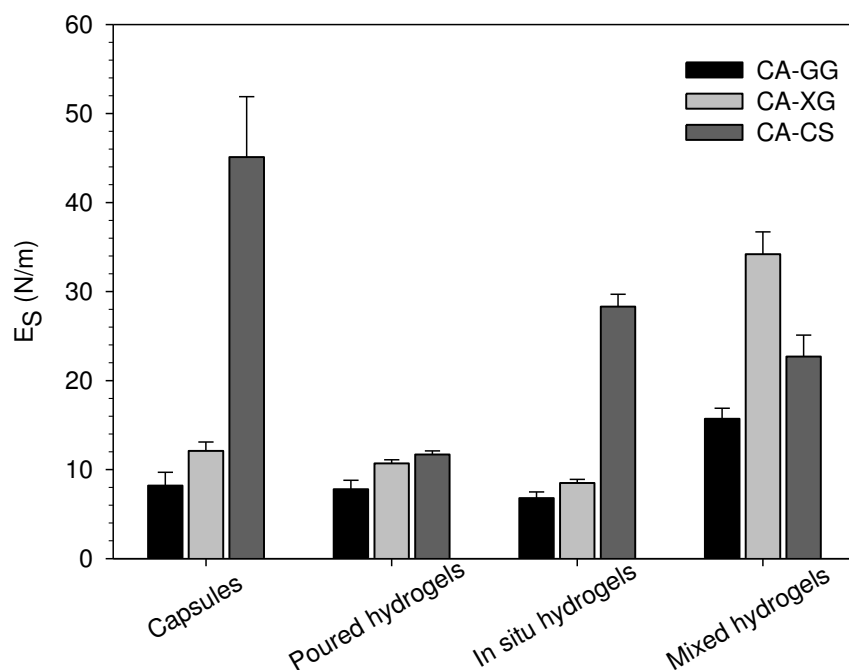


**Figure 6.** Calculated surface Young moduli  $E_s$  for the different hydrogels measured with capsule compression and frequency sweep rheology.

In general, the mechanical data obtained from frequency sweep test were in a good agreement with the surface Young's moduli calculated from compression. Even if, the  $E_s$  values were different from the data obtained by compression, however the data were in the same order of magnitude expected for CA mixed gel.

The greater surface Young's moduli of capsules compared to hydrogels systems could be explained by geometric effects, and shell densification. (Best et al., 2013)

From these observations, we can conclude that hydrogels prepared by *in situ* gelation followed by incubation in the polymer solutions showed mechanical similitudes with the aqueous core capsules, and could therefore simulate accurately the gelation condition of the capsules.

### 3.5. FTIR spectroscopy

The FTIR spectra of air dried CA-GG, CA-XG and CA-CS membranes are shown in Fig.7a. The Fig.7b showed the magnification of data in the wavenumber range ( $1700-1300\text{ cm}^{-1}$ ).

All spectra displayed two peaks due to the carboxylate group ( $\text{COO}^-$ ); an antisymmetric stretch at  $1594\text{ cm}^{-1}$  and a symmetric stretch at  $1413\text{ cm}^{-1}$  (Sartori, Finch, Ralph, & Gilding, 1997). A band between  $3000$  and  $3700\text{ cm}^{-1}$  (OH stretching) is followed by a small band ( $3000$ - $2850$ ) due to CH stretching. The band at  $1023\text{ cm}^{-1}$  is an antisymmetric stretch (C-O-C) given by the guluronics units (Pereira, Sousa, Coelho, Amado, & Ribeiro-Claro, 2003).

No significant differences were observed between the different CA dried membranes or films, were the same band were observed. However from the inset graph, where the FTIR spectra are presented with the same baseline, we could observe that CA-CS membrane showed greater peaks intensity of the two carbonyl vibrations with no significant change in band position. The higher intensity was assigned to the reaction between the carboxylate groups with calcium cations and with chitosan amino-groups (Lawrie et al., 2007).

CA-XG spectra showed a decrease of peak intensity compared to CA-GG and small shifts of the carboxylate bands. This observation could be related to potential hydrogen bonding between alginate carboxylate groups and XG hydroxyls groups. Pongjanyakul, & Puttipipatkachorn (2007) showed more significant change after XG incorporation into alginate beads which can be explained by the difference of the preparation process. In their case, beads were produced by mixing XG with alginate before dropping into  $\text{CaCl}_2$  bath and hydrogen bonding formation occurred in dispersion before beads reticulation. However in the current study, alginate capsules were prepared by dropping XG- $\text{CaCl}_2$  into alginate solution and so,  $\text{Ca}^{2+}$  /alginate interactions predominated.

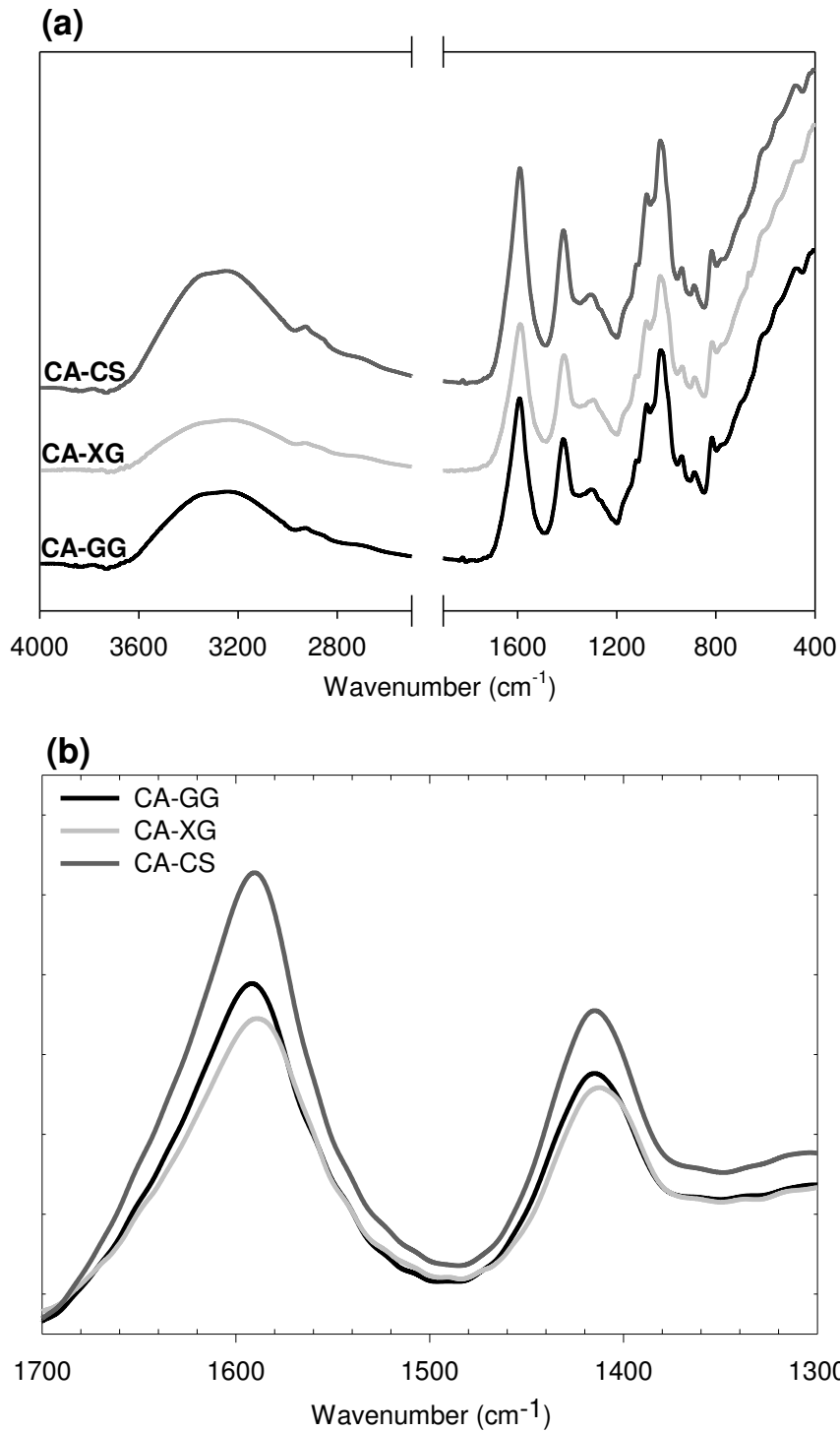


**Figure 7.** FTIR spectra of air dried CA-GG, CA-XG and CA-CS capsules membranes (a) and magnification of data in the wavenumber range 1700-1300 cm<sup>-1</sup> (b).

#### 4. Conclusion

The present study showed that the thickening agent used for alginate capsules preparation by extrusion modulated mechanical and release properties from soft membrane liquid-filled



alginate. Capsules mechanical stability was investigated by compression experiments and by measuring the resulting normal force. Separately, the mechanical properties of alginate hydrogels prepared using three different approaches were investigated by oscillatory shear rheology. From the frequency sweep data, the surface Young's moduli were determined and were in a good agreement with the mechanical study and the alginate capsules. The membrane permeability studied by monitoring BSA release changed considerably as function of thickening agent.

This study showed the importance of the aqueous-core composition, and gave new insights for the possible adjusting of physicochemical properties of macro and micro-capsules by modulating core-shell interactions.

### **Acknowledgments**

The authors acknowledge the financial support provided by COOKAL company and ANRT French Agency (project N° [312/2012](#)). The staff of Microscopy Service from the Faculty of Medicine (Lorraine University) is also acknowledged for their assistance in the use of fluorescence microscope.

## ***Chapitre III :***

### **Contrôle des propriétés physicochimiques des capsules d'alginate par incorporation de polymère dans la membrane pouvant interagir avec la molécule encapsulée**

G. Ben Messaoud, L. Sánchez-González, A. Jacquot, L. Probst, S. Desobry. Alginate/sodium caseinate aqueous-core capsules: a pH-responsive matrix. *Journal of Colloid and Interface Science* 440 (2015) 1-8.

G. Ben Messaoud, L. Sánchez-González, L. Probst, S. Desobry. Composite alginate/sodium caseinate microspheres for anionic dye removal. *En préparation*



Dans ce chapitre, l'objectif est de contrôler la diffusion de molécule encapsulée dans les capsules à base d'alginate par incorporation dans la membrane de polymère pouvant interagir avec la molécule encapsulée dans des conditions environnementales spécifiques (pH) et de limiter ainsi sa libération.

Les propriétés physicochimiques des capsules d'alginate ont été donc ajustées par incorporation du caséinate de sodium dans la membrane d'alginate. L'influence de la concentration en caséinate de sodium et du pH de préparation a été étudiée. Les capsules composites ont montré un renforcement des propriétés mécaniques qui peut être expliqué par des interactions entre les groupements carboxyliques du mélange protéique et les cations calcium, mais aussi par les interactions électrostatiques entre les groupements carboxyliques de l'alginate et les groupements amines du caséinate de sodium. La cinétique de diffusion de la rouge cochenille (utilisé comme molécule modèle dans cette étude) a montré un profil de libération pH-dépendant. Cette libération contrôlée est expliquée par une adsorption membranaire du colorant via des interactions électrostatiques entre les groupements sulfonates et amines du caséinate.

Comme perspective à cette étude, des microsphères (hydrogels sphériques) à base d'alginate et de caséinate de sodium ont été développées en utilisant un équipement basé sur une technologie de buse vibrante combinée à un potentiel électrostatique. Trois types de systèmes ont été synthétisés : microsphères simples (alginate), composites (alginate/caséinate de sodium) et composites enrobées avec une couche de caséinate de sodium. L'efficacité des microsphères pour l'élimination des colorants azoïques (Rouge cochenille et noir amido) a été évaluée. Ce type de système trouve des applications dans l'élimination de colorants à partir de rejets industriels (textile, plasturgie, etc...) par un mécanisme d'adsorption.



## **Alginate/sodium caseinate aqueous-core capsules: a pH-responsive matrix**

Ghazi Ben Messaoud<sup>a</sup>, Laura Sánchez-González<sup>a,\*</sup>, Adrien Jacquot<sup>a</sup>, Laurent Probst<sup>b</sup>,

Stéphane Desobry<sup>a</sup>

<sup>a</sup>Laboratoire d'Ingénierie des Biomolécules (LIBio). ENSAIA-*Université de Lorraine*. 2 avenue de la forêt de Haye, TSA 40602, 54518 Vandœuvre-lès-Nancy Cedex, France.

<sup>b</sup>Cookal company. 21 avenue de la Meurthe, 54320 Maxéville, France.

\* Corresponding author

Tel.: +33 (0)3 83 59 58 77

Fax: +33 (0)3 83 59 58 04.

E-mail address: [laura.sanchez-gonzalez@univ-lorraine.fr](mailto:laura.sanchez-gonzalez@univ-lorraine.fr)

### **Abstract**

*Hypothesis:* Alginate capsules have several applications. Their functionality depends considerably on their permeability, chemical and mechanical stability. Consequently, the creation of composite system by addition of further components is expected to control mechanical and release properties of alginate capsules.

*Experiments:* Alginate and alginate-sodium caseinate composite liquid-core capsules were prepared by a simple extrusion. The influence of the preparation pH and sodium caseinate concentration on capsules physico-chemical properties was investigated.

*Findings:* Results showed that sodium caseinate influenced significantly capsules properties. As regards to the membrane mechanical stability, composite capsules prepared at pH 2 exhibited the highest surface Young's modulus, increasing with sodium caseinate content, explained by potential electrostatic interactions between sodium caseinate amino-groups and alginate carboxylic group. The kinetic of cochineal red A release changed significantly for

composite capsules and showed a pH-responsive release. Sodium caseinate-dye mixture studied by absorbance and fluorescence spectroscopy confirmed complex formation at pH 2 by electrostatic interactions between sodium caseinate tryptophan residues and cochineal red sulfonate-groups. Consequently, the release mechanism was explained by membrane adsorption process.

This global approach is useful to control release mechanism from macro and micro-capsules by incorporating guest molecules which can interact with the entrapped molecule under specific conditions.

**Keywords:** *composite capsules; surface Young's modulus; pH-responsive release; electrostatic interactions; membrane adsorption.*

## **1. Introduction**

Alginate is a water soluble anionic polysaccharide, extracted from brown seaweed (Phaeophyceae), or produced by members of the genera *Azotobacter* and *Pseudomonas* [1]. The structure consists of alternating blocks of 1,4-linked  $\beta$ -D-mannuronic acid (M) and  $\alpha$ -L-guluronic acid (G) residues. These uronic acid units are distributed along the polymer chain in a pattern of blocks, consisting of homopolymeric blocks (G and M-blocks) and heteropolymeric blocks (alternating sequence of M and G residues or MG-blocks) [2]. Alginate has a number of favorable characteristics suitable for encapsulation applications, such as good biocompatibility, wide availability, low cost, and simple gelling procedure under mild conditions [2]. The Gelation process is driven by the interactions of G and MG blocks which associate in the presence of divalent cations to form strong and weak junctions, respectively [2].

The alginate capsules functionality depends considerably on their permeability, mechanical and chemical stability [3].

Due to their negative surface charge, alginate capsules were used as negatively charged templates for coating with positively charged polymers such as chitosan [4] or poly-L-lysine [5] and for polyelectrolyte layer-by-layer assembly by alternating oppositely charged polymers [6].

Nevertheless, fabrication of such systems requires multiple steps and extended production time [7]. Consequently, creation of composite systems by adding other components to a common system was considered like a simple method to enhance capsule properties [8]. In particular, composite vehicles containing both proteins and polysaccharides were a promising system and may advantageously use distinct functional characteristics of each compound [9].

Sodium caseinate is commonly used as an ingredient in a wide range of formulated food emulsions and in pharmaceutical products [10].

It is a multicomponent mixture of four major constituents:  $\alpha_{s1}$ ,  $\alpha_{s2}$ ,  $\beta$  and  $\kappa$ -casein. These proteins possess several attractive properties, such as high hydrophilicity, non-toxicity, good biocompatibility, and availability of reactive sites for chemical modification [11].

As a polymer used in bioencapsulation field, sodium caseinate exhibited excellent surface-activity, emulsification, stabilization and self-assembly properties; water and small molecules binding capacities [12].

Until now, there has been little information on casein incorporation into alginate gel membrane. Encapsulation studies concerning alginate/sodium caseinate association focused on alginate beads preparation for the controlled release of hydrophobic molecules and to increase molecule residence time in the stomach [13].

The aim of this work was to study the influence of both sodium caseinate incorporation in alginate matrix and environmental pH on release properties of capsules. Macro-capsules were produced by a simple extrusion step. The membrane elastic properties were studied by compression experiments. Release properties of cochineal red dye, used as a model molecule, were studied by UV-vis spectroscopy.



## **2. Materials and methods**

### **2.1. Materials**

Alginic acid sodium salt (NaAlg) from brown algae (viscosity  $\leq 0.02$  Pa.s for an aqueous solution of 1% wt at 20 °C), casein sodium salt from bovine milk (NaCas), glycerol ( $\geq 99.5\%$ ,  $M_w = 92.09$  g/mol) and cochineal Red A ( $M_w = 604.46$  g/mol) were purchased from Sigma Aldrich (Steinheim, Germany). Calcium chloride dihydrate ( $M_w = 147.02$  g/mol) was obtained from VWR International (Leuven, Belgium), tri-sodium citrate ( $M_w = 294.09$  g/mol) from Fisher scientific (Leicestershire, United Kingdom) and HCl (37%, AnalR NORMAPUR) from VWR International (Fontenay-sous-Bois, France). All reagents were used without further purification.

### **2.2. Capsule preparation**

To prepare the liquid-core solution, 1% wt  $\text{CaCl}_2$  was solubilized into 90% of glycerol ( $\eta = 0.22$  Pa.s, 20 °C) to modulate the viscosity of cross-linking solution and ensure capsules spherical shape [14]. To investigate the influence of pH, cross linking solutions with different pH values (pH 7, 4.8, 3 and 2) were prepared from the stock solution by adding some drops of HCl. In order to study the passive release of the capsules, cochineal red A food dye was solubilized in the cross-linking solutions.

To prepare gelling solutions, NaAlg 1.5 % wt was prepared by dispersion of NaAlg powder in distilled water under stirring until complete dissolution. Aqueous solution of NaCas 2% wt was prepared by adding slowly the powder into stirred distilled water at room temperature. Solutions of pure components were mixed together in the composition range 0.5% and 0.25–0.75%wt of NaAlg and NaCas, respectively. Concentrations were chosen taking into

account Na-alg/NaCas/water phase diagram to ensure a homogeneous monophasic system [15]. Sodium azide (0.01 % wt) was then added for sample preservation.

The CaCl<sub>2</sub> solution was then extruded dropwise through a needle (outer diameter, 0.9 mm) into stirred NaAlg and NaAlg-NaCas mixtures. A dropping height of 5 cm was used to ensure the formation of spherical capsules [16].

Four systems were obtained based on the NaAlg-NaCas ratio (1:0, 1:0.5, 1:1 and 1:1.5).

After a gelation time of 10 minutes, capsules were rinsed with distilled water to avoid external gelation [14]. Then capsules were transferred into a 0.5 % wt CaCl<sub>2</sub> solution (pH 7, 4.8, 3 and 2) to stabilize capsule membranes.

## **2.3. Characterization of solutions**

### **2.3.1. NaAlg-NaCas mixture**

To investigate the influence of NaCas incorporation on NaAlg solution properties, the zero shear viscosity of NaAlg-NaCas mixture was measured using a rotational rheometer Malvern Kinexus (Malvern Instruments, Orsay, France) with a cone-and-plate geometry (50 mm, 2°) and surface tension by using a Krüss K100 tensiometer (Krüss GmbH; Hamburg, Germany). All measures were triplicated at 20 °C.

### **2.3.2. Zeta potential of NaCas solution**

To investigate the influence of pH on casein micelles surface charge, electrophoretic mobility ( $\mu_E$ ) of diluted NaCas solution (0.1 % vt) was measured using Malvern Zetasizer Nano ZS (Malvern instrument, Worcestershire, UK) and the zeta potential  $\zeta$  was obtained using the Henry equation with the Smoluchowski approximation. Three readings were made per sample and each measurement was repeated three times.

### **2.3.3. Dye-NaCas interaction**

### Absorbance spectroscopy

UV–vis absorbance spectra were recorded on a Shimadzu Uv-4000 absorption spectrophotometer in the wavelength range of 400–650 nm. Experiments were performed by keeping the Cochineal Red A concentration constant at 30  $\mu\text{M}$ , and NaCas was varied from 0 to 10 g/l at pH2. In these experiments, NaCas solutions was centrifuged in order to remove insoluble particles which could affect spectra absorbance in the studied wavelength range and each cochineal red/NaCas mixture was measured against solvent blank reference containing the same NaCas concentration.

### Fluorescence spectroscopy

The interactions between NaCas and cochineal red at pH 2 were studied by fluorescence spectroscopy using a spectrofluorometer (Model Flx, Safas, Monaco). Fluorescence spectroscopy was carried out with an excitation wavelength of 280 nm and emission spectra were recorded from 300 to 500 nm. The quenching experiments were performed by keeping the concentrations of NaCas at 0.025 % wt and Cochineal Red A concentration was varied from 0 to 41.4  $\mu\text{M}$ .

## **2.4. Characterization of capsules**

### **2.4.1. Measurements of capsule size and membrane thickness**

The external diameter and membrane thickness of capsules were performed under an optical microscope (Olympus AX70, Japan) equipped with a camera (Olympus DP70). Dp controller software (version 2.1.1) was used for taking pictures (Fig.1). Shell thickness and capsules diameter were therefore calculated using imageJ software (National Institutes of Health, Bethesda, Maryland, USA). The data for one experimental condition were calculated from values taken from 10 capsules.

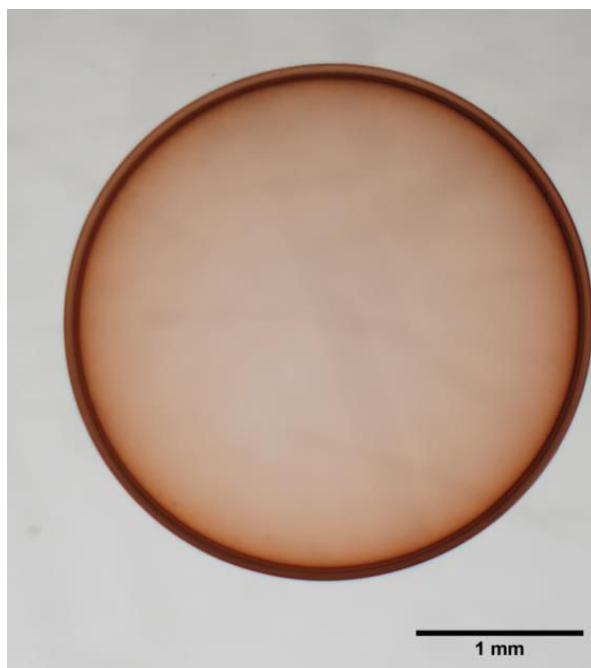


*Figure.1: Microscopic image of NaAlg-NaCas (1:0.5) capsule prepared at pH 2*

#### **2.4.2. Mechanical study**

To investigate mechanical stability, individual capsules were compressed between two parallel plates [17, 18]. A rotational rheometer Malvern Kinexus (Malvern Instruments, Orsay, France) with a plate-and-plate geometry was used. The upper plate had a diameter of 20 mm and the resulting normal force was measured in a range between 0.001 and 20 N.

A force gap test was used to compress the capsules from 4 mm to 0.05 mm with a linear compression speed of 10  $\mu\text{m} / \text{s}$ . The gap and the normal force being imposed were measured simultaneously at the upper plate. The surface Young's modulus can be calculated by a quantitative analysis of force-displacement curves at small deformations [18, 19].

Three replicates were considered for each type of capsule.

#### **2.4.3. Release properties**

Release of cochineal red dye was followed using a spectrophotometer (Uv - 4000 Shimadzu, Japan). Capsules were placed at 20 °C into 50 ml water at various pH-values (7, 4.8, 3 and 2). At scheduled time intervals, the amount of released dye was determined from solution absorbance at 500 nm wavelength.

To determine the total mass initially encapsulated at the end of each experiment, 1 ml of tri-sodium citrate solution (1M) was added to dissolve gel membrane by calcium chelation [20].

## **2.5. Statistical analysis**

The results are presented as mean  $\pm$  standard deviation. Comparisons between the various sets of data were carried by ANOVA test using Statgraphics® Plus 5.1. Multiple comparisons were performed through 95% LSD intervals.

## **3. Results and Discussion**

### **3.1. Capsules characterization**

Microscopic observation gave average diameter and membrane thickness of alginate and composite capsules (Fig.2).

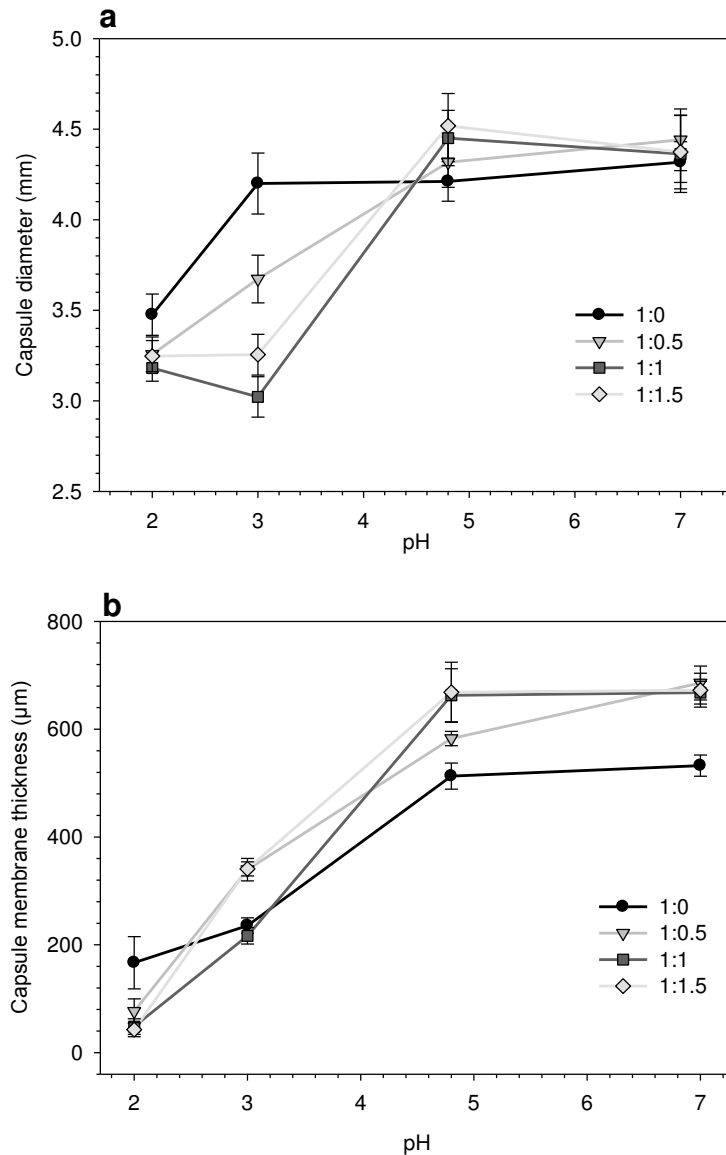


**Figure.2:** Diameter (a) and membrane thickness (b) evolution of NaAlg-NaCas capsules as function of pH.

The average diameter of alginate capsules ranged from 4.3 to 3.4 mm and from 3.25, 3.18 and 3.24 mm to 4.44, 4.45 and 4.51 mm for NaAlg-NaCas 1:0.5, 1:1 and 1:1.5, respectively (Fig.2a). Alginate capsules showed a size reduction from 4.3 to 3.4 mm at pH7 and 2, respectively. However, composite capsules exhibited the highest size at pH 4.8 and 7.

Generally, capsule size depends on droplet dimension before getting into contact with bath solutions [21]. In this study, cationic solutions were composed of 90 % glycerol and showed a

Newtonian flow; therefore droplet size was not only affected by the extrusion step. Consequently, size evolution of alginate and composite capsules was related to NaCas incorporation and to the preparation pH.

Membrane measurements (Fig.2b) showed a pH-dependent thickness of alginate capsules which decrease with pH diminution (from 532.4 to 166.8  $\mu\text{m}$  at pH 7 and 2, respectively), demonstrating alginate shrinkage in acidic conditions where the carboxylate groups are expected to exist in their protonated form [22].

However, membrane thickness decreased dramatically from pH 4.8 to pH 3 and 2, and this reduction could be explained by partial alginate precipitation during encapsulation step. In fact, the pKa values of both alginate monomers  $\beta$ -D-mannuronic acid (M) and  $\alpha$ -L-guluronic acid (G) residues are of 3.38 and 3.65, respectively [23].

From Fig.2b, we can therefore conclude that capsule diameter evolution depends strongly on capsule membrane thickness. The membrane thickness evolution of composite capsules with pH decrease was comparable to alginate capsules and the highest thickness was observed for pH 4.8 and 7.

We could expect that composite capsules would exhibit the thickest membrane at pH 4.8 by NaCas precipitation around isoelectric point (pI) ( $4.2 < \text{pI}_{\alpha\text{-s1}} < 4.7$ ,  $4.6 < \text{pI}_{\beta} < 5.1$  and  $4.1 < \text{pI}_{\kappa} < 5.8$  [15]). Nevertheless, alginate molecules could prevent sodium caseinate aggregation into a coherent network on the capsule membrane [24]. Microscopic characterization suggested NaCas existence in micellar state, which did not affect the membrane global volume.

It is interesting to note that all capsule's types exhibited a spherical shape, as a consequence of closer solutions viscosities before the encapsulation step [25] (Table 1).

**Table 1.** pH, zero shear viscosity and surface tension of NaAlg-NaCas mixture

NaAlg : NaCas	pH	$\eta_0$ (mPa.s)	ST (mN.m <sup>-1</sup> )
1 :0	6.72 (0.03) <sup>a</sup>	6.90 (0.05) <sup>a</sup>	68.21 (0.61) <sup>a</sup>
1 :0.5	6.65 (0.02) <sup>b</sup>	6.93 (0.03) <sup>a</sup>	50.38 (0.14) <sup>b</sup>
1 :1	6.63 (0.02) <sup>b</sup>	6.83 (0.12) <sup>a</sup>	48.79 (0.07) <sup>c</sup>
1 :1.5	6.62 (0.01) <sup>b</sup>	6.9 (0.07) <sup>a</sup>	48.93 (1.14) <sup>c</sup>

<sup>a, b, c</sup> Different letters in the same column indicate significant differences among NaAlg-NaCas mixture ( $p < 0.05$ ).

In fact, NaCas addition did not lead to viscosity changes. However, NaAlg - NaCas mixtures exhibited a significant surface tension decrease from 68.2 down to 48.9 for NaAlg 1:0 and NaAlg - NaCas 1:1.5, respectively due to interfacial and emulsifying properties of NaCas [26]. Thereby, drop impact on NaAlg - NaCas mixture surface was reduced by surface tension decrease and resulted on a spherical shape.

### 3.2. Mechanical stability

Alginate capsules are sensitive to deformations that may lead to their rupture or to undesirable early release of their contents. Thus, surface Young's modulus, which is the measure of alginate capsule stiffness, is an interesting data to quantify mechanical stability.

Surface Young's modulus was estimated by analyzing force–displacement curves in the range of small deformations and using equation (1) [8, 19]:

$$F = \frac{4E_s d}{a\sqrt{3(1 - \nu_s^2)}} d_D \quad (1)$$



Where  $d_D$  denotes capsule displacement,  $F$  is the measured force,  $E_S$  is the surface Young modulus,  $d$  is the membrane thickness,  $a$  is the radius of the capsule and  $\nu_S$  the surface Poisson ratio for which a value of  $\frac{1}{3}$  was assumed according to Leick et al, 2010 [16].

Table 2 summarized Young's moduli values of alginate and composite capsules, in function of preparation pH, calculated by linear regression from compression curves at small displacements.

**Table 2.** Calculated Surface Young's moduli (N / m) of alginate and composite capsules

pH	Capsule type			
	1 :0	1 :0.5	1 :1	1 :1.5
7	14.92 (0.54) <sup>a</sup>	14.8 (0.72) <sup>a</sup>	13.25 (1.71) <sup>a</sup>	11.98 (0.60) <sup>a</sup>
4.8	11.16 (0.32) <sup>b</sup>	18 (2.99) <sup>a,b</sup>	10.66 (1.62) <sup>a</sup>	13.17 (2.04) <sup>a</sup>
3	21.76 (4.89) <sup>a</sup>	18.82 (2.24) <sup>b</sup>	23.49 (0.67) <sup>b</sup>	19.50 (2.73) <sup>b</sup>
2	22.26 (2.86) <sup>a,c</sup>	63.46 (10.29) <sup>c</sup>	106.60 (25.38) <sup>c</sup>	165.89 (17.27) <sup>c</sup>

<sup>a, b, c</sup> Different letters in the same column indicate significant differences among pH preparation ( $p < 0.05$ ).

For alginate capsules, surface Young's modulus ranged from 14.9 to 22 N / m at pH 7 and pH 2, respectively indicating that a decrease in pH resulted in a stiffer alginate membrane.

The surface Young modulus increased significantly at pH 2 and 3 and can be explained by partial alginic acid precipitation at  $pH < pK_a$  of both alginate's monomers [23].

The membrane formation process could result from both ionic gelation and acid precipitation but accurate contribution of each mechanism cannot be clearly determined. In fact, membrane formation during extrusion was a very fast microscopic gelation process. As soon as the two

liquids (CaCl<sub>2</sub> droplet and gelation bath) entered into contact, both hydrogen and calcium ions diffused from the glycerol droplet to the external alginate solution and both mechanisms occurred simultaneously during membrane formation.

It was shown that, as in the case of ionic gels, homopolymeric blocks of L-guluronic acid residues had the strongest tendency towards junction formation in acid gels, but, in contrast to the ionic gel, the homopolymeric blocks of D-mannuronic acid resulted in stable junction zones and had a significant effect in supporting gel formation [23]. Heteropolymeric blocks alternating MG residues did not contribute to junctions under acidic conditions [27].

For composite capsules, the highest surface Young modulus was obtained at pH 2 for all NaAlg-NaCas ratios (63.5, 106.6 and 166 for 1:0.5, 1:1 and 1:1.5, respectively). In general, when pH decreased below the protein's isoelectric point, the net positive charge of the protein increased; the positively charged residues of NaCas could therefore interact with negatively charged alginate [28]. Thus, potential electrostatic interactions could occur between carboxylate alginate groups (COOH) and positively charged tertiary amine groups (-N(CH<sub>3</sub>)<sub>2</sub>) of caseinate into capsule membrane [29].

In fact, even if most alginate carboxylate groups are expected to be present under non-ionic carboxylic acid form at pH 3 and 2, some percentage would be in COO<sup>-</sup> state and could interact with NaCas amino-groups [30].

Alginic acid gel formation monitored with SAXS showed that alginate acid gelation start with an initial phase consisting of quasi-ordered junction zone composed of 3-4 laterally associated chains, followed by junction zones formation to produce random aggregates, finally leading to network formation [27]. Therefore, NaCas may interact with the random aggregate during gel formation.

### 3.3. Capsule release properties

Relative amounts of released cochineal red A versus time elapsed after capsules preparation were plotted for different pH and capsules composition (Fig. 3).

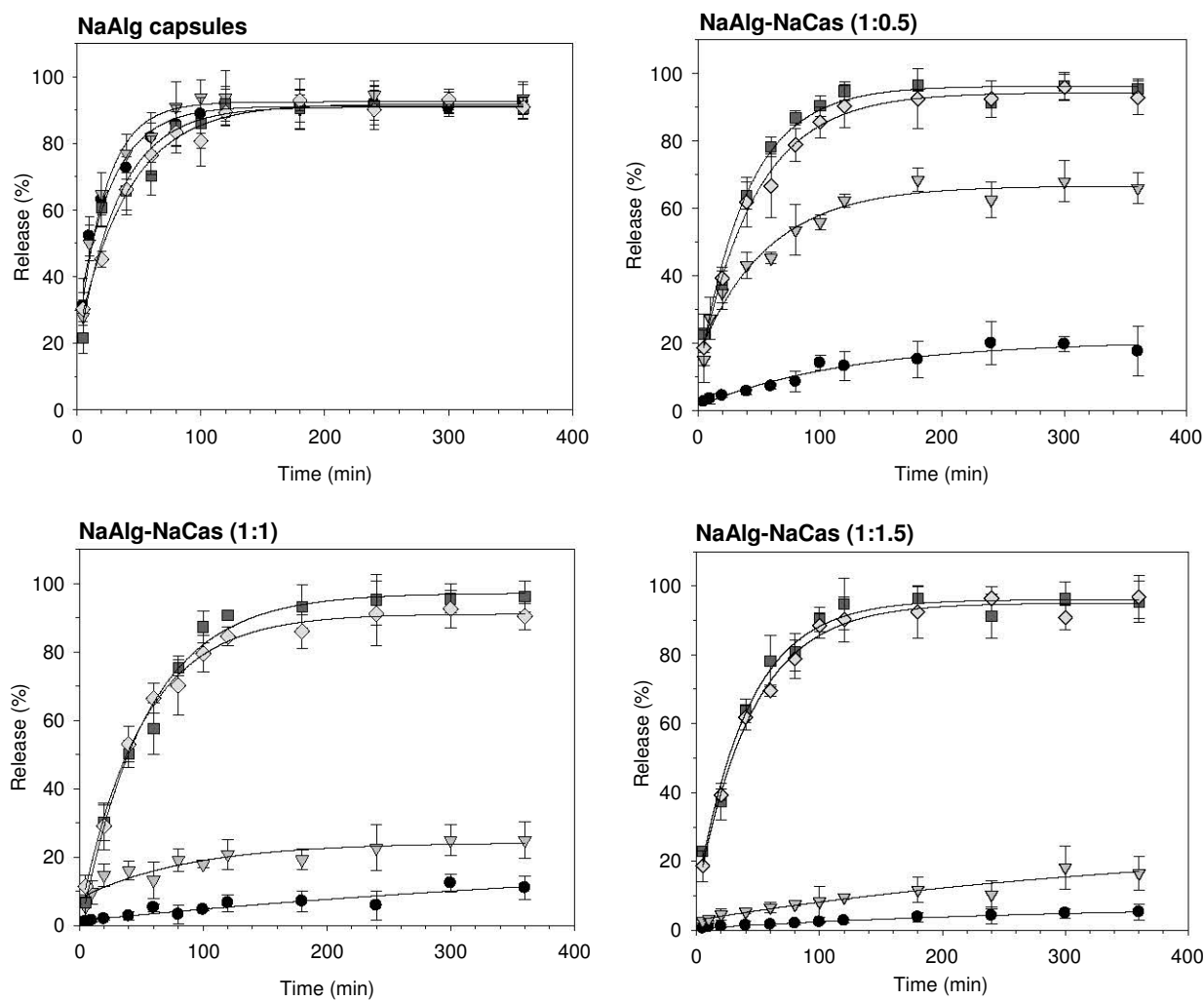


**Figure.3:** Cochineal red dye release for alginate and composite capsules at pH 2 (●), 3 (▼), 4.8 (■) and 7 (◆). The solid lines represent the results of fits of the experimental data to Equation (5).

Cochineal red release from alginate capsules (Fig. 3a) showed the same diffusion profile with a slightly slower dye release at neutral pH. Total amounts of released cochineal red A after 200 minutes were not significantly different in the range of the studied pH values. However, a

slower release was observed at pH 4.8 and pH 7, where the equilibrium state was nearly achieved after 180 minutes, versus 120 minutes at pH 2 and 3. Difference of dye release with pH-values was not significant but was related to alginate membrane thickness which could modify diffusive resistance. Compared to alginate capsules, composite capsules exhibited a strong pH-dependence on the total amount of dye released for the three NaAlg-NaCas mixtures studied (Fig. 3b, c and d). For pH 4.8 and pH 7, the total amount of cochineal red dye released as well as the rate of release were similar to that of alginate capsule without caseinate; so, pH-dependent release of cochineal red was not explained by the decrease of capsule membrane permeability.

The rate of the dye released as well as the total amount of released cochineal at equilibrium was significantly reduced at pH 3 and pH 2. Moreover, capsule dye retention increases with the amount of NaCas. In fact, at pH 2, the amount of released cochineal red dye after six hours reached 17.6, 10.9 and 5.2 % for NaAlg-NaCas 1:0.5, 1:1 and 1:1.5 composite capsules, respectively. Microscopic observations of composite capsules (1:0.5) stored one week with daily external acid (pH 2) media replacement, indicated intense red colored membrane which suggested that the entrapped dye was preferentially adsorbed in the composite membrane (Fig.1).

### 3.3.1. Kinetics of dye release

For a quantitative analysis of the dye release kinetics, experimental data can be analyzed with respect to equation (2), which describes solute diffusion out of a homogeneous sphere [31].

For a constant diffusion ( $D_m$ ), solute concentration ( $C$ ) in the volume outside the capsule of radius ( $r$ ) after a time  $t$  is [5]:

$$C(t) = C(\text{eq}). \left( 1 - \sum_{n=1}^{\infty} \frac{6\alpha(1 + \alpha)}{9 + 9\alpha + \alpha^2 q_n^2} \cdot \exp \left( -\frac{D_m q_n^2}{r^2} \cdot t \right) \right)$$

(2)

Where  $\alpha$  denotes the effective volume ratio.

$$\alpha = k_m \frac{V_b}{V_c} \quad (3)$$

$V_b$  is the bulk volume and  $V_c$  is the capsule volume. The partition coefficient  $K_m$  was the ratio of cochineal red concentration in the capsule and in the bulk, at equilibrium.

For  $\alpha \gg 1$ , the parameters  $q_n$  in equation (2) was simplified by:

$$q_n = n \cdot \pi \quad (4)$$

Leick et al., 2011 reported theoretical approach used for equation (2) solving to describe anthocyanin release from alginate and alginate poly-l-lysine capsules [5].

Experimental data were therefore fitted with the following exponential function (equation 5):

$$C(t) = C_{eq} (1 - k_1 \exp(-k_2 (t - t_0)))$$

$$k_1 = \frac{6\alpha(1+\alpha)}{9+9\alpha+\alpha^2\pi^2}; k_2 = \frac{D_m\pi^2}{r^2} \quad (5)$$

Fitting experimental data leads to the determination of diffusion constant  $D_m$  and equilibrium cochineal red concentration in the bulk solution  $C_{eq}$ . Results were summarized in Table 3.

**Table 3.** Diffusion parameters resulting from the fit of Cochineal red dye release from alginate and composite capsules: Equilibrium concentration ( $C_{eq}$ ) and average diffusion constants ( $D_m$ ).

		Capsule type							
		1 :0		1 :0.5		1 :1		1 :1.5	
pH	$C_{eq}$	$D_m$	$C_{eq}$	$D_m$	$C_{eq}$	$D_m$	$C_{eq}$	$D_m$	
	(%)	( $10^{-10} \text{ m}^2/\text{s}$ )	(%)	( $10^{-10} \text{ m}^2/\text{s}$ )	(%)	( $10^{-10} \text{ m}^2/\text{s}$ )	(%)	( $10^{-10} \text{ m}^2/\text{s}$ )	
2	91.1 (8.6)	1.84 (0.39)	20.8 (2.9)	0.34 (0.11)	17.0 (4.7)	0.17 (0.02)	7.6 (0.8)	0.14 (0.01)	
3	92.5 (10.6)	3.36 (0.75)	66.6 (6.2)	1.01 (0.23)	22.8 (3.7)	0.81 (0.08)	26.9 (14.0)	0.15 (0.01)	
4.8	90.9 (13.7)	2.25 (0.54)	96.2 (8.0)	1.98 (0.32)	97.1 (7.8)	1.58 (0.16)	96.0 (7.9)	2.07 (0.49)	
7	91.8 (5.9)	1.89 (0.26)	94.3 (5.3)	1.79 (0.49)	91.8 (3.1)	1.63 (0.04)	95.0 (5.6)	1.79 (0.48)	

The diffusion constant  $D_m$ , which combines the diffusion processes in the membrane and in the liquid core of the capsules, significantly decreased with the NaCas amount at pH 2 and pH 3 as described previously in the qualitative analysis.

### 3.3.2. pH-responsive release mechanism

In order to understand the mechanism of controlled release from composite capsules, zeta potential of NaCas was measured as a function of pH (Fig. 4a).

The zeta potential of NaCas changed from negative to positive as the pH was decreased from 7 to 2, and the net NaCas charge was close to zero between pH 4 and 4.8, which is close to the pI of the protein. Furthermore, below the isoelectric point, NaCas was charged positively and may interact with the oppositely charged cochineal Red A which possesses three negatively charged sulfonates (Fig. 4b) [32].

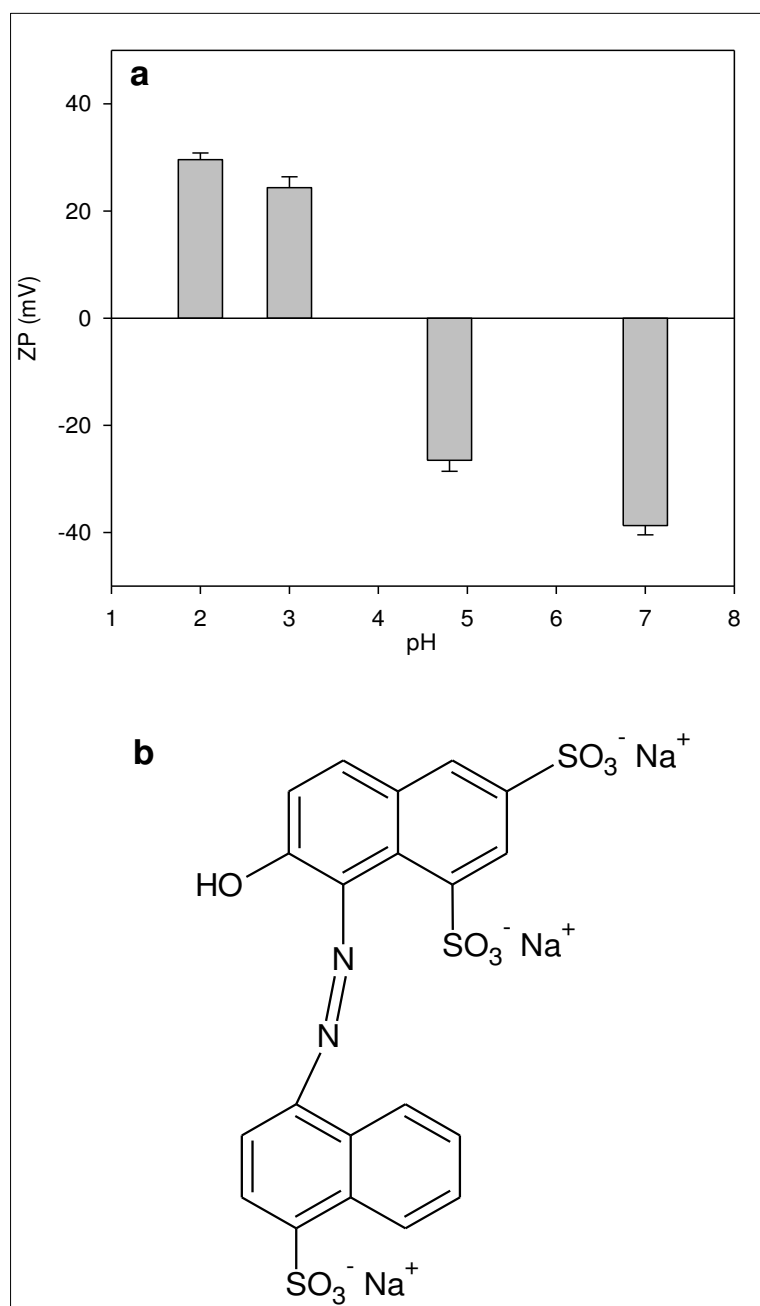


**Figure.4:** (a) Zeta potential evolution of NaCas with pH and (b) molecular structure of cochineal red A dye.

To confirm possible dye-protein complex formation, UV-vis spectra absorbance of cochineal red A at pH 2 with various NaCas concentrations was studied (Fig. 5).

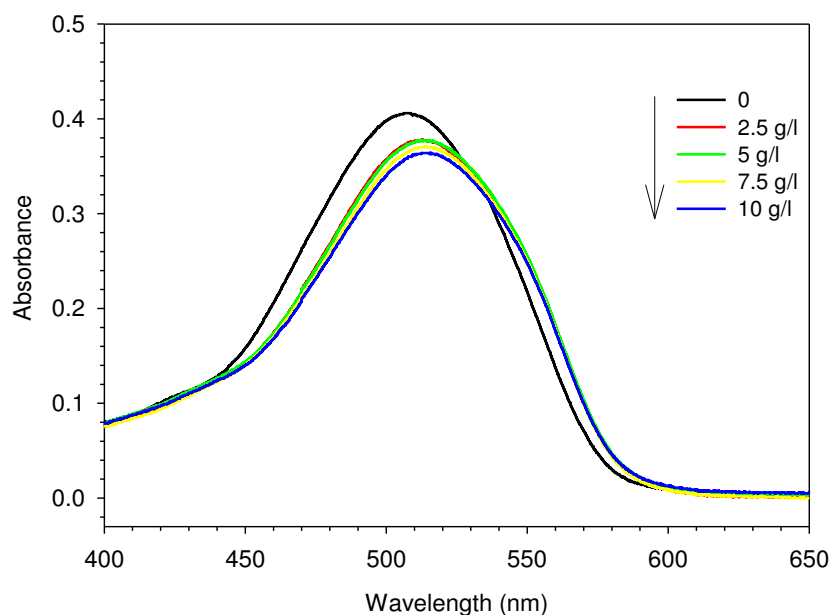


**Figure.5:** Absorption spectra of Cochineal Red A ( $30 \mu\text{M}$ ) at pH 2 with increasing NaCas concentration at  $20 \text{ }^\circ\text{C}$ .

In fact, this method is a simple but effective to detect aggregation [32].

Upon addition of NaCas, absorbance intensity of cochineal red A decreased with increasing NaCas concentration. This observation was explained by complex formation between cochineal red A and NaCas, and thereby reducing absorbance. Moreover,  $\lambda_{\text{max}}$  of cochineal red A was shifted from 507 nm to 512-513 nm in the presence of NaCas.

The binding mechanism between NaCas and cochineal red was studied by fluorescence spectroscopy (Fig.6).



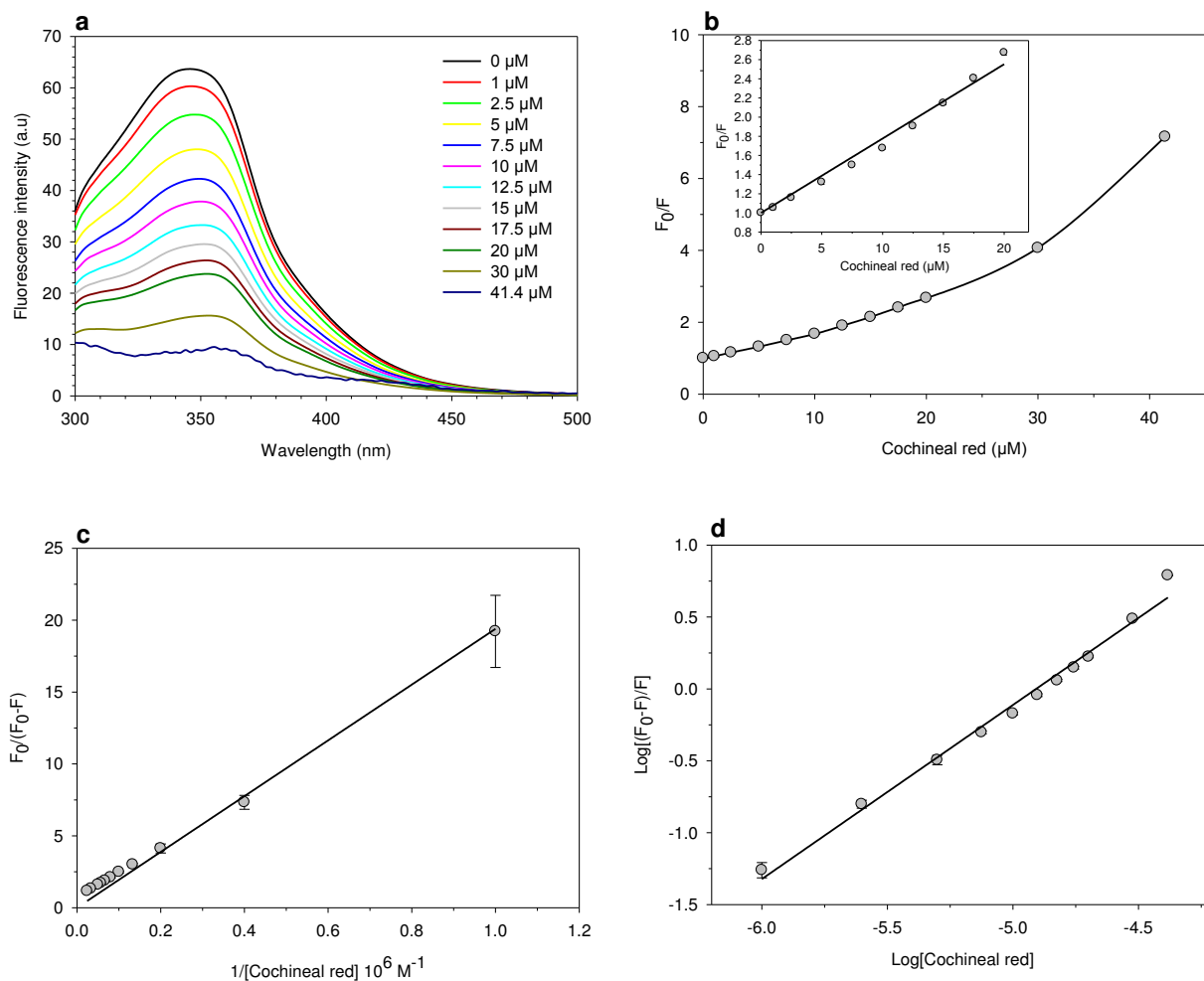


**Figure.6:** Quenching experiments of NaCas / Cochineal red A at pH 2. (a) Emission spectra of NaCas solution (0.025 wt %) at 20 °C at different concentrations of cochineal red A, (b) Stern-Volmer plot of  $F_0/F$  as function of the concentration of cochineal red A measured at 350 nm, (c) Modified Stern–Volmer plot based on Equation 7 and (d) Plot of  $\text{Log} [(F_0-F)/F]$  as a function of  $\text{log} [\text{cochineal red A}]$ .

The fluorescence spectra of NaCas without and with different concentrations of cochineal red are shown in Fig. 6a. NaCas showed an emission band around 350 nm. Upon addition of cochineal red, the intrinsic fluorescence intensity of NaCas emission band around 350 nm decreased with increasing Cochineal red A concentration. A gradual shift of the emission peak toward higher wavelength was also observed.

In general, fluorescence quenching leads to a decrease of fluorescence intensity of a fluorescent molecule as a result of diverse molecular interactions such as excited state reactions, energy transfer, ground-state complex formation, and collisional quenching [33].

Fig 6.b shows the plot of  $F_0/F$  as a function of the dye concentration. In this Stern–Volmer plot, an upward deviation from linearity at high cochineal red concentrations ( $> 20 \mu\text{M}$ ) was observed [33] and suggests that fluorescence quenching results from collision (dynamic quenching) and complex formation (static quenching) between NaCas and dye [33].

Analysis of quenching data (the initial linear portion) at low concentration ( $\leq 20 \mu\text{M}$ ) was done according to the Stern–Volmer equation:

$$\frac{F_0}{F} = 1 + k_q \tau_0 [Q] = 1 + k_{SV} [Q] \quad (6)$$

Where  $F_0$  and  $F$  are the fluorescence intensities before and after addition of the quencher, respectively  $k_q$  is the bimolecular quenching constant,  $\tau_0$  is the average lifetime of the fluorophore in absence of quencher,  $[Q]$  is the quencher concentration, and  $K_{SV}$  is the linear Stern–Volmer quenching constant.

For the determination of available binding sites ( $f$ )  $F_0/F$  could be related to  $[Q]$  by the modified form of the Stern–Volmer equation (Fig. 6c) [34].

$$\frac{F_0}{F_0 - F} = \frac{1}{f} + \frac{1}{f} \frac{1}{K_{SV}} \frac{1}{[Q]} \quad (7)$$

For dye–protein interaction, the binding constant ( $K$ ) was calculated from Fig. 6d by use of equation (8):

$$\log\left[\frac{F_0 - F}{F}\right] = \log K + n \log [Q] \quad (8)$$

Where  $n$  is the number of binding sites.

The quenching parameters obtained from equations (7) and (8) were reported in table 4.

The fraction of binding sites available for complexation ( $f$ ) is greater than 1 (1.68), which can be explained by contribution of both dynamic and static quenching or by possible presence of further binding sites due to NaCas composition (mixture of four main caseins which can differ by the number of tryptophan residues and their positions in respective molecules [35].

The large binding constant  $k$  ( $8.77 \cdot 10^5$ ) suggested that cochineal red A had a strong affinity for NaCas tryptophan residues.

Based on this information, we can conclude that the controlled release mechanism from composite capsules was related to membrane adsorption process at pH below NaCas isoelectric point, due to electrostatic interactions between entrapped dye and NaCas micelles confined into the alginate membrane (Fig.7). In fact, negative sulfonate groups of azo dyes are known to interact with basic side chains of amino acid residues from proteins through electrostatic forces [32, 36].

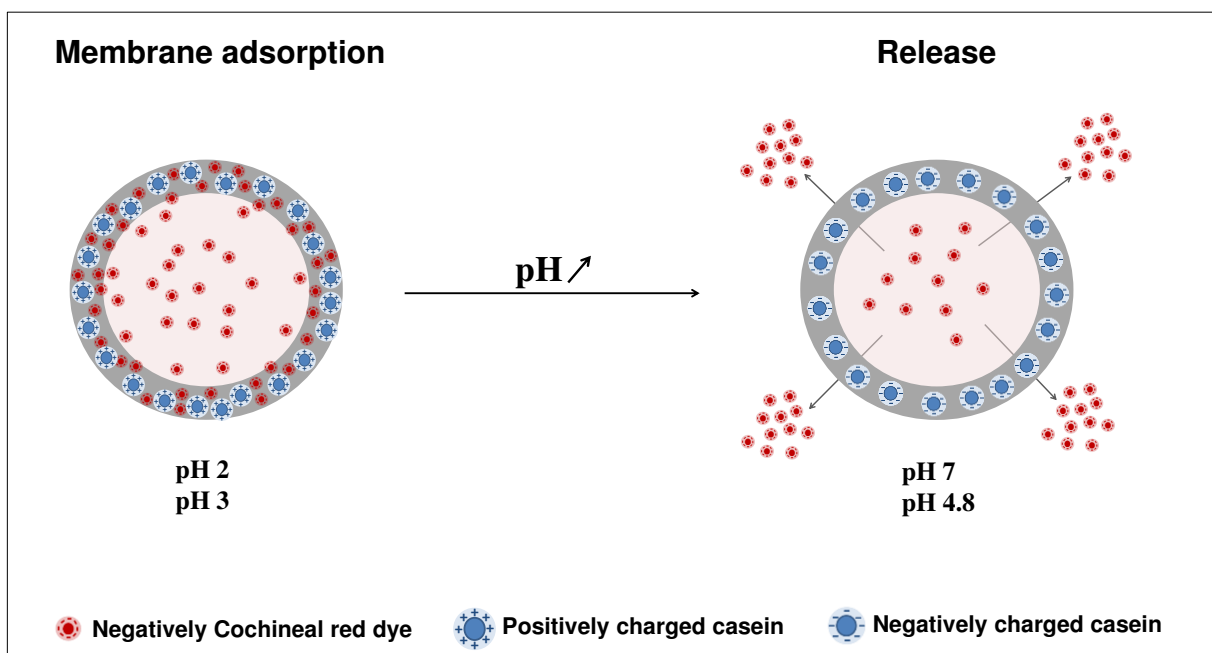


**Figure.7:** Schematic representation of the pH-responsive release mechanism of cochineal red A from NaAlg-NaCas capsules.

#### 4. Conclusion

In conclusion, we studied permeability, structure and deformability of NaAlg and NaAlg-NaCas composite capsules. In particular, pH and NaCas amount influences on these properties were investigated during encapsulation process. Capsules mechanical stability was investigated by compression experiments and by measuring the resulting normal force. With these experiments, incorporation of NaCas was shown to increase capsules stability at low pH, and was explained by electrostatic interactions between NaCas amino-groups and alginate carboxylate groups.

Composite capsules displayed a retarded release with high dye retention at pH 2 and 3 compared to NaAlg capsules. By adding NaCas into alginate membrane, the amount of dye released after 2h was reduced from  $\approx 95\%$  to  $\approx 7\%$  at pH 2. Absorbance and fluorescence spectroscopy indicated that the pH-responsive mechanism of composite capsules was explained by the interaction between NaCas and entrapped cochineal red dye through electrostatic interactions. The high affinity between these two molecules under acidic conditions could lead to several applications, such as effluents removal from water by designing NaAlg-NaCas beads, especially for azo dyes adsorption extensively used in food, cosmetic, textile, paper and printing industries [37].

The general strategy used in this study could be useful for developing new types of macro and micro-capsules with controlled release behavior. For example, the design of pH sensitive system for oral drug delivery applications [38], like the encapsulation of ionic drugs which target the intestines ( $\approx$  pH 7.4) to ensure their retention and avoid their undesirable early release during their passage through the stomach ( $\approx$  pH 1.2).

Lastly, the incorporation of guest molecules which can interact with entrapped molecules under specified conditions would be an easy method for targeted release applications.

## Acknowledgments

The authors are grateful to COOKAL and GYMNOKIDI companies and ANRT French Agency for their financial support (project N° 312/2012). Carole Perroud and Carole Jeandel are also acknowledged for their technical support.

## References

- [1] W. Sabra, A. P. Zeng and W. D. Deckwer, *Applied Microbiology and Biotechnology*, 2001, **56**, 315–325.
- [2] S. N. Pawar and K. J. Edgar, *Biomaterials*, 2012, **33**, 3279-3305.
- [3] T. M. S. Chang, *Artificial Cells*, Thomas, Springfield, III, 1972.
- [4] A. Bartkowiak and D. Hunkeler, *Chemistry of Materials*, 1999, **11**, 206-212.
- [5] S. Leick, A. Kemper and H. Rehage, *Soft Matter*, 2011, **7**, 6684-6694.
- [6] B. G. De Geest, S. De Koker, G. B. Sukhorukov, O. Kreft, W. J. Parak, A. G. Skirtach, J. Demeester, S. C. De Smedt and W. E. Hennink, *Soft Matter*, 2009, **5**, 282-291.
- [7] B. M. Wohl and J. F. J. Engbersen, *Journal of Controlled Release*, 2012, **158**, 2–14.
- [8] S. Leick, M. Kott, P. Degen, S. Henning, T. Pasler, D. Suter and H. Rehage. *Physical Chemistry Chemical Physics*, 2011, **13**, 2765–2773
- [9] L. Wei, C. Cai, J. Lin and T. Chen, *Biomaterials*, 2009, **30**, 2606-2613.
- [10] F. C. Millar and O. I. Corrigan, *Drug Development and Industrial Pharmacy*, 1991, **17**, 1593–1607.
- [11] A. O. Elzoghby, W. S. Abo El-Fotoh and N. A. Elgindy, *Journal of controlled release*, 2011, **153**, 206-216.
- [12] Y. D. Livney, *Current Opinion in Colloid and Interface Science*, 2010, **15**, 73–83.
- [13] S. K. Mishra, A.K. Philip and K. Pathak, *PDA Pharmaceutical Science and Technology today*, 2008, **62**, 421–428.
- [14] A. Blandino, M. Macias and D. Cantero, *Journal of Bioscience and Bioengineering*, 1999, **88**, 686–689.
- [15] Y. A. Antonov and P. Moldenaers, *Food Hydrocolloids*, 2011, **25**, 350-360.
- [16] S. Leick, S. Henning, P. Degen, D. Suter, H. Rehage, *Physical Chemistry Chemical Physics*, 2010, **12**, 2950-2958
- [17] M. Carin, D. Barthès-Biesel, F. Edwards-Lévy, C. Postel and D.C Andrei, *Biotechnology and bioengineering*, 2003, **82**, 207-212.

- [18] M. Rachik, D. Barthès-Biesel, M. Carin and F. Edwards-Lévy, *Journal of Colloid and Interface Science*, 2006, **301**, 217-226.
- [19] A. Fery and R. Weinkamer, *Polymer*, 2007, **48**, 7221-7235.
- [20] O. Gåserød and G. Skjåk-Bræk, *Trends in Biotechnology*, 1990, **8**, 71–78.
- [21] D. Poncelet, V. G. Babak, R. J. Neufeld, M. F. A. Goosen and B. Bugarski, *Advances in Colloid and Interface Science*, 1990, **79**, 213-228.
- [22] S.T Moe, G. Skjåk-Bræk, A. Elgsaeter and O. Smidsrød, *Macromolecules*, 1993, **26**, 3589–3597
- [23] K. I. Draget, G. Skjåk-Bræk and O. Smidsrød, *Carbohydrate Polymers*, 1994, **25**, 31-38.
- [24] L. Matia-Merino, K. Lau, E. Dickinson, *Food Hydrocolloids*, 2004, **18**, 271–281.
- [25] E. S. Chan, B. B. Lee, P. Ravindra and D. Poncelet, *Journal of Colloid and Interface Science*, 2009, **338**, 63–72.
- [26] C. C. Sánchez and J. M. Rodríguez Patino, *Food Hydrocolloids*, 2005, **19**, 407–416.
- [27] K. I. Draget, B. T. Stokke, Y. Yuguchi, H. Urakawa and K. Kajiwara. *Biomacromolecules*, 2003, **4**, 1661-1668.
- [28] E. Dickinson, *Trends in Food Science and Technology*, 1998, **9**, 347–354.
- [29] X. Huang, Y. Xiao and M. Lang, *Carbohydrate Polymers*, 2012, **87**, 790-798.
- [30] [S. H. Ching](#), [B. Bhandari](#), [R. Webb](#) and [N. Bansal](#), *Food Hydrocolloids*, 2014. DOI: 10.1016/j.foodhyd.2014.05.013
- [31] J. Crank, *The mathematics of diffusion*, Oxford, UK: Oxford University Press, 1979.
- [32] P. Bolel, N. Mahapatra, and M. Halder, *Journal of Agricultural and Food Chemistry*, 2012, **60**, 3727–3734
- [33] J. R. Lakowicz, *Principles of Fluorescence Spectroscopy*, 3rd ed.; Springer: New York, 2006.
- [34] D. P. Acharya, L. Sanguansri and M. A. Augustin, *Food Chemistry*, 2013, **141**, 1050–1054.
- [35] H. M. Farrell Jr., E.L. Malin, E.M. Brown and P.X. Qi, *Current Opinion in Colloid & Interface Science*, 2006, **11**, 135–147.
- [36] J. Sereikaite and V. A. Bumelis, *Central European Journal of Chemistry*, 2008, **6**, 509–512.
- [37] V. K. Gupta and Suhas, *Journal of Environmental Management*, 2009, **90**, 2313–2342.
- [38] Y. Qiu and K. Park, *Advanced Drug Delivery Reviews*, 2001, **53**, 21–339



## Composite alginate/sodium caseinate microspheres for anionic dye removal

Ghazi Ben Messaoud <sup>a</sup>, Laura Sánchez-González <sup>a,\*</sup>, Laurent Probst <sup>b</sup>, Stéphane Desobry <sup>a</sup>

<sup>a</sup> Laboratoire d'ingénierie des biomolécules (LIBio). ENSAIA-*Université de Lorraine*. 2 avenue de la forêt de Haye, TSA 40602, 54518 Vandœuvre-lès-Nancy Cedex, France.

<sup>b</sup> Cookal company. 21 avenue de la Meurthe, 54320 Maxéville, France.

\* Corresponding author

Tel.: +33 (0)3 83 59 58 77

Fax: +33 (0)3 83 59 58 04.

L. Sánchez-González: [laura.sanchez-gonzalez@univ-lorraine.fr](mailto:laura.sanchez-gonzalez@univ-lorraine.fr)

### Abstract

Various types of synthetic azo dyes appear in effluents of wastewater in some industries. Since a very small amount of dye in water is highly visible and can be toxic, the elimination of color from process or waste effluents is environmentally important. The adsorption using naturally derived polymers is an interesting alternative.

Alginate, alginate/caseinate composite and coated composite microspheres were prepared by dripping the polymers mixtures using an encapsulator based on a vibrating technology. The beads shape and size were examined. The efficiency of the prepared systems was studied against two anionic dyes: amido black 10B and new cocchine. The kinetic of dyes removal was studied at pH3 according to the pseudo first order and pseudo second order models. The influence of solution pH on the percentage of dye removal was studied. Results showed that the incorporation of caseinate didn't affect size distribution of microbeads. Concerning, the kinetic



of dyes adsorption at pH3, alginate beads showed only 7 and 34.6 % of dyes removal compared to composite microbeads 45 and 69.2 % for new coccine and amido black, respectively. The composite and coated systems showed higher dyes adsorption at  $\text{pH} \leq 4$ . Finally, Alg/Cas systems could be useful, since acetic acid is often used as a stimulator in the dyeing process, in which the pH of the dye solution is normally adjusted to 3-4.

## **1. Introduction**

Various industries like textile, dyestuffs, paper and plastics use dyes during their production process. As a result, considerable amounts of colored wastewater are generated. Dyes are the first contaminant to be recognized in wastewater (Banat, Nigam, Singh, & Marchant, 1996). In fact, the presence of very small amounts of dyes in water is highly visible (T. Robinson, Chandran, & Nigam, 2002). In addition to undesirable visible pollution, some dyes may present toxic or mutagenic properties (Hameed, Din, & Ahmad, 2007). Therefore, their elimination from industrial wastewater prior to their discharge is of great concerns on public health and ecological system.

To resolve this problem, numerous physical, chemical and biological techniques for dyes removal were developed (Tim Robinson, McMullan, Marchant, & Nigam, 2001).

Among physical techniques, adsorption is an effective method that have been successfully employed for color removal from wastewater (Chiou, Ho, & Li, 2004). This technique has several advantages in terms of flexibility, simplicity of design, ease of operation and relative low cost. Adsorption also does not result in the formation of harmful substances (Crini, 2006). There is also a growing interest in the use of biomaterials based on polymers obtained from renewable resources due to their availability and ease of employment.

Alginate is a water soluble anionic polysaccharide, extracted from brown seaweed (Phaeophyceae), or produced by members of the genera *Azotobacter* and *Pseudomonas*. The

structure consists of alternating blocks of 1,4-linked b-D-mannuronic acid (M) and a-l-guluronic acid (G) residues.

Due to its high affinity to divalent and trivalent cations, alginate has a capacity to remove toxic pollutants such as heavy metal ions (Davis, Volesky, & Mucci, 2003).

Thanks to its several advantages such as wide availability, low cost, and simple gelling procedure under mild conditions, alginate was successfully used as an adsorbent for pollutants removal, especially for heavy metals and cationic dyes adsorption thanks to its carboxylic groups. However the adsorption efficiency of anionic dyes is limited. (Rocher, Siaugue, Cabuil, & Bee, 2008)(Rocher, Bee, Siaugue, & Cabuil, 2010) (Liu et al., 2012)(Mahmoodi, 2011) (Aravindhana, Fathima, Rao, & Nair, 2007) (Perez-Ameneiro, Vecino, Barbosa-Pereira, Cruz, & Moldes, 2014) (Lu et al., 2015)(Vecino, Devesa-Rey, Cruz, & Moldes, 2015).

The preparation of composite system containing two or more polymers may advantageously use distinct functional characteristics of each compound.

Sodium caseinate is commonly used as an ingredient in a wide range of applications (Walstra, Jenness, & others, 1984).

Chemically, sodium caseinate is a multicomponent mixture of four major constituents:  $\alpha$ ,  $\beta$  and  $\kappa$ -casein. These proteins possess several attractive properties, such as high hydrophilicity, non-toxicity and availability of reactive sites for chemical modification (Elzoghby, El-Fotoh, & Elgindy, 2011).

Recently, we showed that the incorporation of certain amount of sodium caseinate into alginate hydrogel membrane of liquid-core capsules didn't affect the gelation of alginate and could even increase the mechanical stability of the system (Ben Messaoud, Sánchez-González, Jacquot, Probst, & Desobry, 2015).

The aim of this work was to study the influence of sodium caseinate incorporation into alginate hydrogel microspheres on removal efficiency of two anionic dyes: new cocine (NC), and

amido black 10B (AB). Three different microspheres systems were synthesized: simple alginate, composite alginate / caseinate and coated composite system by sodium caseinate adsorption at the microspheres surface. The prepared matrixes were characterized by microscopy and were assessed for dyes removal by studying the kinetic of adsorption at pH 3 by batch experiments and the influence of pH on the final dye removal between pH 3-10.

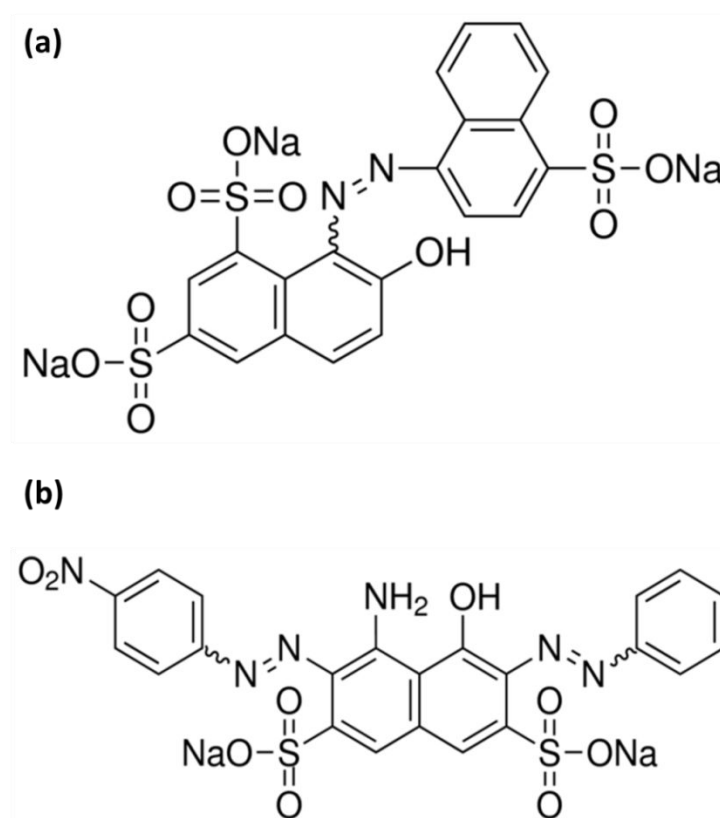


**Figure 1.** Chemical structures of new coccine (a) and amido black 10B (b).

## 2. Material and methods

### 2.1. Material

Alginic acid sodium salt (Alg) from brown algae (viscosity 0.02 Pa.s for an aqueous solution of 1% wt at 20 °C), casein sodium salt from bovine milk (Cas), New coccine NC ( $M_w = 604.46$  g / mol) and amido black AB 10B ( $M_w = 616.49$  g / mol) were purchased from Sigma Aldrich

(Steinheim, Germany). Calcium chloride dihydrate ( $M_w = 147.02$  g/mol) was obtained from VWR International (Leuven, Belgium). All reagents were used without further purification.

## **2.2. Microspheres preparation**

Aqueous Alg 2% (w/v) and Cas 8 % (m/v) were prepared by dispersion of the polymers powders into stirred distilled water at room temperature. After complete solubilization, the solutions of pure components were mixed together in the composition range 1% and 0 – 2% wt of Alg and Cas, respectively.

Then, the hydrogel microspheres were prepared with an Encapsulator B-395 Pro (BÜCHI Labortechnik, Flawil, Switzerland) based on a vibrating system. This technology is based on the principle that a laminar flowing liquid jet breaks up into equal sized droplets by a superimposed nozzle vibration. In this work, a 300  $\mu$ m nozzle was used for the preparation of Alg and Alg-Cas microspheres. The flow rate was adjusted to 9.2 ml / min and the vibration frequency which determined the quantity of droplets produced per second was set at 1530 Hz. The produced droplets were dripped in a  $\text{CaCl}_2$  solution 2 % (m / v) to allow microspheres formation. The beads were incubated in the gelling bath for 15 minutes to complete the reticulation process and then were filtered and washed to remove the excess of  $\text{CaCl}_2$ .

For the preparation of coated Alg/Cas composite beads, the capsules were transferred into a Cas solution 0.5% (m/v) at pH 3 in order to allow the adsorption of Cas layer on the surface of the hydrogel microspheres (Ching, Bhandari, Webb, & Bansal, 2015).

## **2.3. Capsules characterization**

### **2.3.1. Optical microscopy**

The morphology of microspheres were performed under an optical microscope (Olympus AX70, Japan) equipped with a camera (Olympus DP70). Dp controller software (dp controller, version 2.1.1) was used for taking photos.

### 2.3.2. Size

The particle size distribution was measured using laser diffraction instrument: Mastersizer 3000 with Hydro MV (Malvern Instrument, Worcester, UK). This instrument measures the angular variation in intensity of light scattered as a laser beam passes through a dispersed particulate sample. The angular scattering intensity data is then analyzed to calculate the size of particles responsible for creating a scattering pattern, using the Mie theory of light scattering. Particle size measurements are reported as a volume equivalent sphere diameter. The average of three readings per sample is represented.

## 2.4. Adsorption studies

### 2.4.1. Batch experiments

The adsorption equilibrium study for removal of various dyes was conducted at 20 °C and initial solution pH 3. Briefly, 5 g of wet microspheres were immersed in 50 mL of NC, MO and AB solutions (25 mg/ L) at room temperature.

At scheduled time intervals, the concentrations of the dye solutions were carried out using a Uv-vis spectrophotometer Pharmacia Biotech Ultrospec 4000 (Richmond Scientific Ltd, Lancashire, U.K) at the maximal wavelength of obtained after wavelength scans.

The adsorption capacity at equilibrium  $q_e$  (mmol/g) was calculated using the following equation:

$$q_e = \frac{(C_0 - C_e) \times V}{w} \quad (1)$$

Where  $C_0$  and  $C_e$  (mmol/L) are the concentrations of the dye solutions before and after the adsorption, respectively,  $V$  (L) is the volume of the solution and  $W$  (g) is the dried weight of microspheres.

### 2.4.2. Kinetic study

Kinetic studies were followed according to the method of batch equilibrium studies outlined in Section 2.5. The adsorption capacity  $q_t$  (mmol/g) at different contact time  $t$  (min) was determined using the following equation:

$$q_t = \frac{(C_0 - C_t) \times V}{w} \quad (2)$$

Where  $C_t$  (mmol/L) is the concentration of NC and AB at time  $t$  (min) in the solution.

### 2.4.3. Influence of initial pH

For the initial pH effect experiments, the pH of the dyes solutions was initially adjusted with aqueous solutions of acid or base (0.01 M HCl and 0.01 M NaOH) to reach pH values of 3–10. 5 g of the different system were placed in 50 ml of MO, AB and NC solutions at an initial concentration of 25 mg. L<sup>-1</sup>.

The percentage removal (%R) by the adsorbent was described by the following:

$$\% R = \frac{(C_0 - C_e)}{C_0} \times 100 \quad (3)$$

## 2.5. Data modeling

Adsorption kinetic modeling and data fitting was performed using SigmaPlot software (SigmaPlot Version 11.0, Systat Software Inc., San Jose, CA, USA).

## 3. Results and discussion

### 3.1. Physicochemical characterization of microspheres

In order to prepare different capsules architectures, solutions of pure Alg, mixture of Alg/Cas were dripped into a CaCl<sub>2</sub> solution using an encapsulator device. Then the Alg/Cas composite

capsules were coated into a Cas solution. The Fig.2 presents a scheme of the different microspheres type used as adsorbents in the current study.

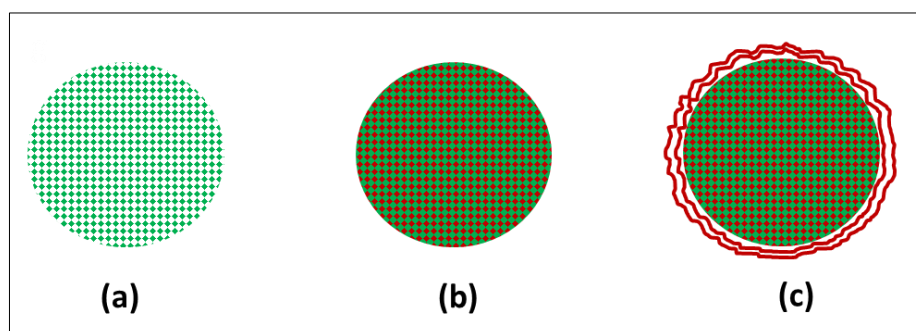


**Figure2.** Schematic representation of the adsorbent systems. Alg (a), Alg/Cas composite (b) and Cas coated Cas Alg/Cas composite microspheres (c).

Microscopic images of Alg and Alg/Cas microspheres are shown in Fig.3.

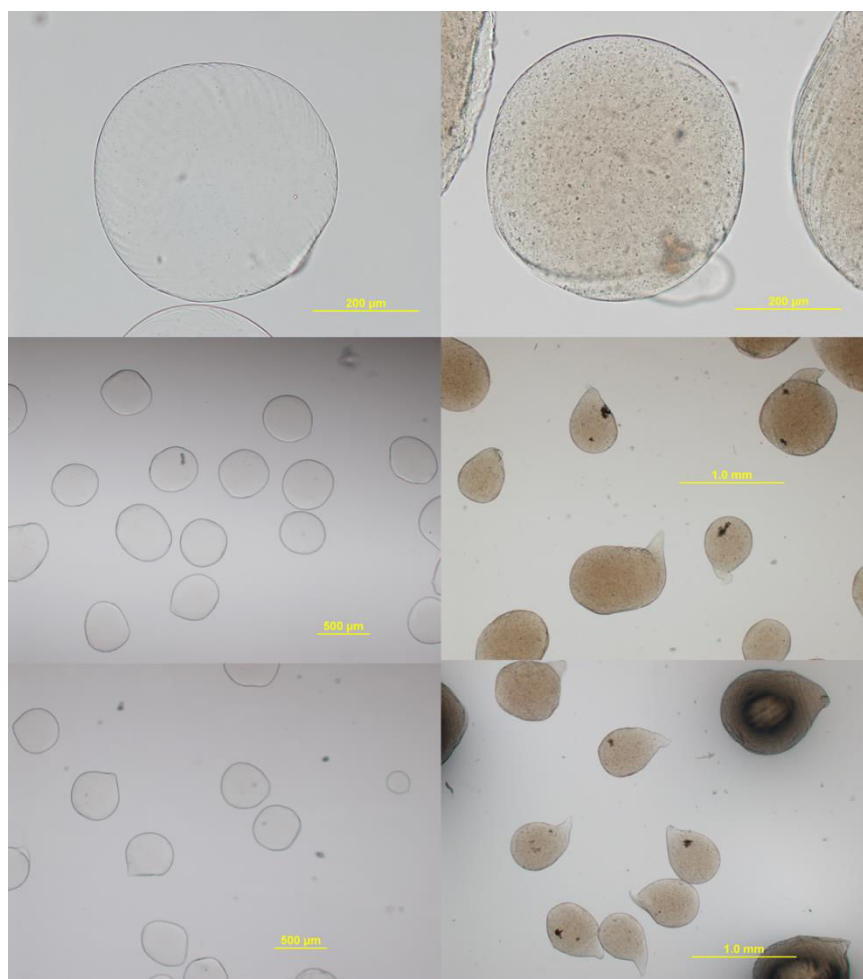


**Figure 3.** Microscopic images of Alg (left) and Alg/Cas composite microspheres (right).

Alg capsules were fairly spherical and transparent. The incorporation of Cas results in a relatively opaque system and globally decreases the roundness of the microspheres with the apparition of tails (Fig3). The modification of microspheres shape after Cas addition could be related to the increase of resistance to transforming into round droplets as they fall. In fact, the detached liquid droplets did not have sufficient time to transform into round droplets before contacting the gelling bath. In other words, the falling distance was insufficiently long for the accomplishment of the shape-transformation process (Voo et al., 2015).

Other parameters could be optimized during the encapsulation step, especially the frequency of the vibrating nozzle and the impact of the liquid droplets with the surface of the hardening bath which could be modulated by controlling the surface tension (Cellesi, Weber, Fussenegger, Hubbell, & Tirelli, 2004).

The size distributions of the prepared microspheres suspended in distilled water is presented in Fig.4. Typically the three types of microspheres systems showed the same size distributions, the average diameters of Alg, Alg/Cas and coated Alg/Cas microspheres were 550, 626 and 690  $\mu\text{m}$ , respectively. The Alg/Cas diameter is higher than pure Alg capsules, which could be related to potential swelling of both polymers at pH7 or to the mixture viscosity and therefore to larger droplets during the encapsulation step.

The coating process led to an increase of the average diameter, probably due to protein mixture adsorption at the surface of the composite capsules.



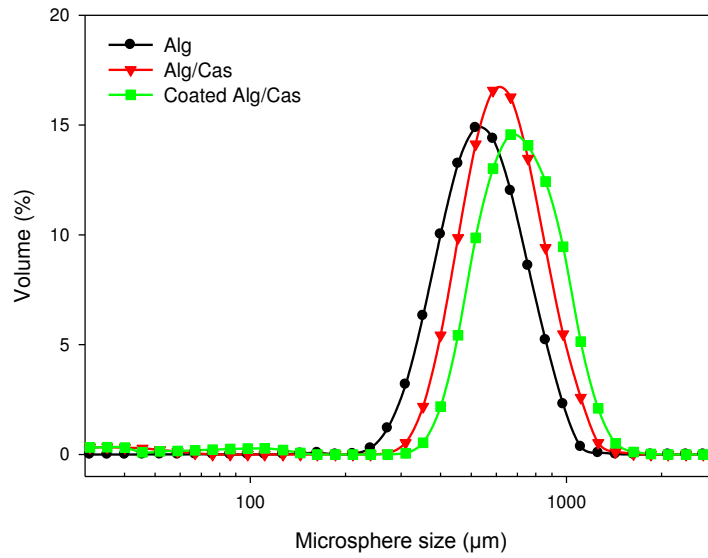


**Figure 4.** Size distribution of Alg, composite Alg/Cas and Cas coated Alg/composite capsules.

### 3.2. Adsorption kinetic study

Pseudo-first-order equation, pseudo-second-order equation were used as kinetic models to analyze the adsorption behaviors of the three anionic dyes for the different microspheres. The pseudo-first-order kinetic model fits with low solute concentration and reflects the adsorption rate (Lagergren,1898); while the pseudo-second-order kinetic model reflects the adsorbed amount at equilibrium and the adsorbed amount on the surface of the adsorbent (Ho & McKay, 1999).

The two models were expressed by the following Eqs. (4) – (5):

$$q_t = q_e(1 - \exp^{-k_1 t}) \tag{4}$$

$$q_t = \frac{q_e^2 k_2 t}{1 + q_e k_2 t} \tag{5}$$

Where  $q_e$  is the adsorption amount of the anionic dyes at equilibrium (mmol/g),  $q_t$  is the adsorbed amount at time  $t$  (mmol/g).  $k_1$  and  $k_2$  are the first order and second order rate constant, respectively.

Fig.5 presents the adsorption kinetics of AB and NC in the three types of microspheres systems.

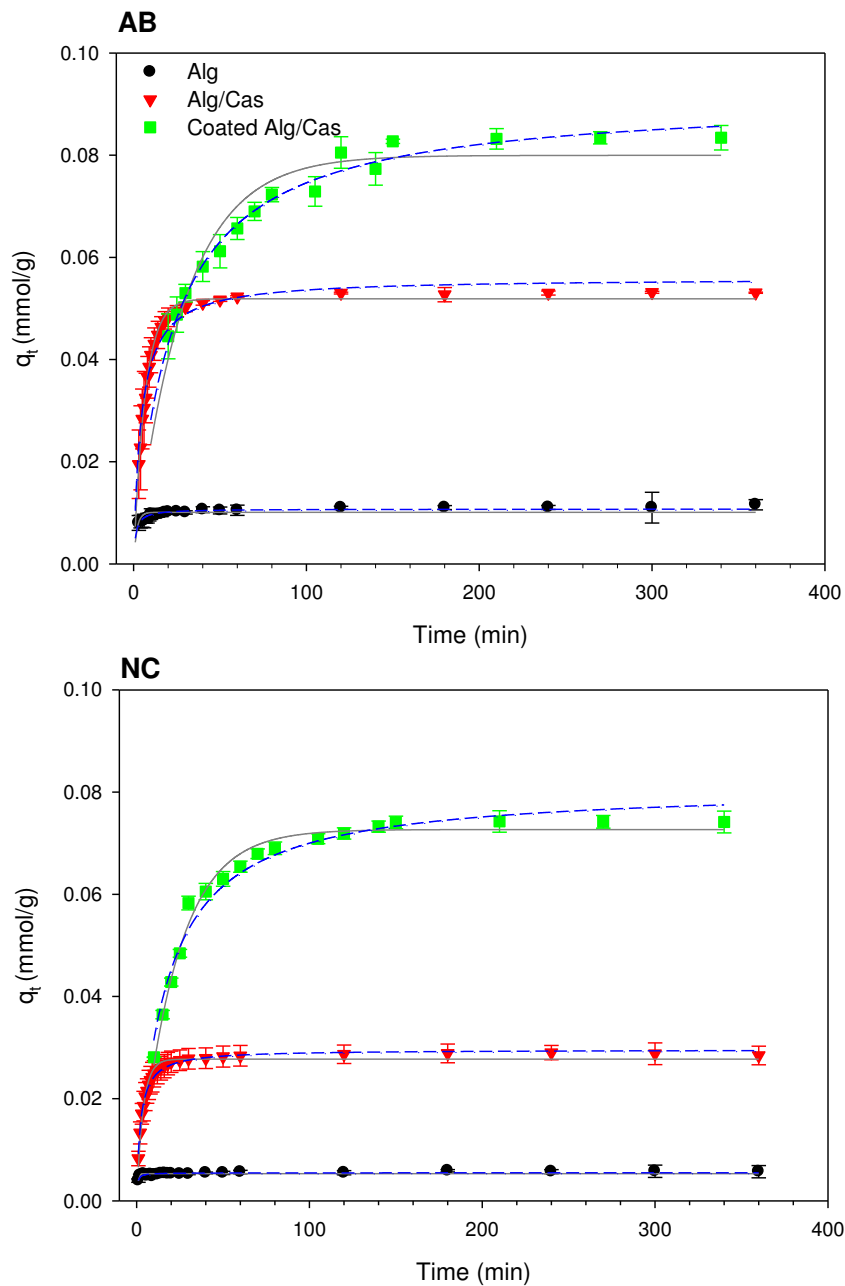


**Figure 5.** Kinetic modeling of AB and NC adsorption on Alg, Alg/Cas and coated Alg/Cas microspheres at pH3, pseudo first order model (solid) and pseudo second order (dash lines).

The adsorption kinetic of the NC and AB on the different microspheres showed the same profile with an exponential phase during which the amount of the adsorbed dye increased exponentially, followed by a stationary phase which corresponds to the achievement of the equilibrium phase. The coated microspheres showed the highest adsorption capacity followed by Alg/Cas and then by pure Alg microspheres, however this system showed the slowest dye adsorption kinetic.

The kinetic of dyes adsorption were fitted with Eqs. (4) and (5), The parameters of pseudo-first-order and pseudo-second-order kinetic models for the A A/C and CasAlgCas microbeads are summarized in Table 1.

**Table 1.** Kinetic models parameters for AB and NC for the three microspheres systems.

	$q_{exp}$ (mmol/g)	Pseudo first order			Pseudo second order		
		$k_1$	$q_{cal}$	$R^2$	$k_2$	$q_{cal}$	$R^2$
<b>AB</b>							
S1	0.011	0.541	0.010	0.628	80.725	0.011	0.909
S2	0.053	0.151	0.052	0.987	4.083	0.056	0.976
S3	0.083	0.035	0.080	0.959	0.485	0.092	0.983
<b>NC</b>							
S1	0.006	1.321	0.005	0.507	481.719	0.006	0.700
S2	0.029	0.271	0.028	0.965	15.307	0.029	0.992
S3	0.074	0.046	0.073	0.985	0.781	0.081	0.974

For Alg microspheres, the correlation coefficient ( $R^2$ ) of NC adsorption was too low for pseudo first and second order models (0.507 and 0.7, respectively).

For AB adsorption on Alg, the pseudo-second-order equation was higher than that of pseudo-first-order equation. In addition, the values of the calculated  $q_e$  from the pseudo-second-order model were much closer to the experimental values. It showed that the adsorption process fitted the pseudo-second-order equation well and it was mainly controlled by the chemical adsorption

mechanism which could be explained by hydrogen bonding and potential electrostatic interaction between the amino groups of AB and the carboxylic groups of Alg and hydrogen bonding.

For Alg/Cas composite and coated capsules the correlation coefficient ( $R^2$ ) of the pseudo-second-order equation was almost the same with that of the pseudo-first-order equation, which indicated that the adsorption process was suitable for both the pseudo-first-order equation and pseudo-second-order equation and was controlled by both physical and chemical adsorption mechanism.

### **3.3. Effect of pH**

The manner in which the pH of the environment affects the efficiency of adsorption of the dye from solution was also examined. The process was carried out in a pH range of 3-10, for initial dye concentration of 25 mg/ L. Adsorption tests were performed over 360 min.

Fig. 6 illustrates the percentage of NC and AB removal (%R) obtained with the different microspheres as function of pH at 20 °C.

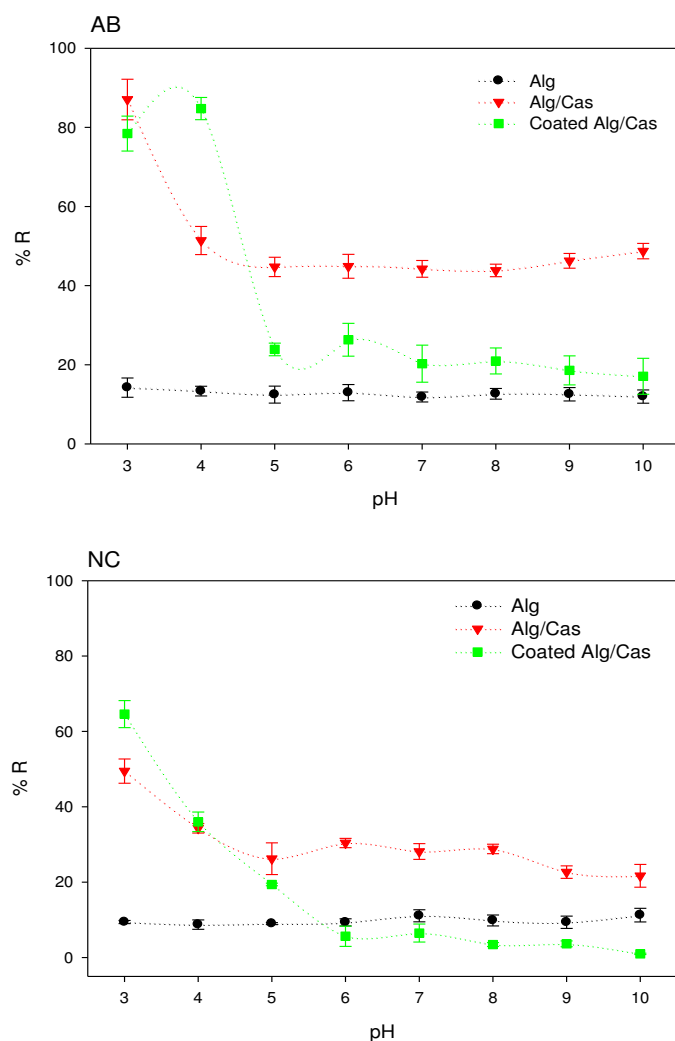


**Figure 6.** Effect of solution pH on AB and NC adsorption on Alg, Alg/Cas and coated Alg/Cas composite microspheres. Lines to guide the eyes

The efficiency of adsorption of NC and AB on Alg microspheres didn't show pH-dependency. However, it was observed that an increase in the acidity of the solution increases the efficiency of the adsorption of the two dyes on Alg/Cas composite and coated microspheres. The percentage of AB and NC removal from a 25 mg/L solution increases from 17.7 and 10 % at pH10 to 78.9 and 68 % at pH3, respectively. This pH adsorption behavior is related to the protonation of the amino groups of sodium caseinate in to form  $\text{-NH}^{3+}$  cationic groups. Under these conditions the process of adsorption of the dye occurs via electrostatic interactions between caseinate amino groups and AB or NC negatively sulfonates.

The low efficiency of the adsorption process in basic solution (pH8-10) is related to the deprotonation of the amino groups and therefore only hydrogen bonds are formed between the support and the dye, reducing the efficiency of adsorption.

#### **4. Conclusion**

In the current study, sodium caseinate was incorporated in alginate microspheres which are used conventionally to remove cationic dyes due to their carboxylic groups. The protein mixture was incorporated inside the microspheres or inside and on the microsphere surface.

The microbeads systems were prepared by a dripping method and the efficiency of the three capsules types was studied against two anionic dyes (new cocchine and amido black 10B).

The composite and coated systems showed higher dyes adsorption at  $\text{pH} \leq 4$ . The pH-dependent efficiency of the microspheres containing sodium caseinate indicated that the major adsorption site of the microspheres is an amine group,  $-\text{NH}_2$ , which is easily protonated to form  $\text{NH}_3^+$  in acidic solutions. The strong electrostatic interaction between the amino groups of the protein mixture and dye anions can be used to explain the high adsorption capacity of anionic dyes onto the composite and coated systems. A study of the influence of dye concentrations as well as system reusability could bring more insights on the possibility of system applications. To facilitate adsorbent separation from the treated solution, magnetic nanoparticles could be incorporated on the microspheres. Finally, Alg/Cas systems could be useful, since acetic acid is often used as a stimulator in the dyeing process, in which the pH of the dye solution is normally adjusted to 3-4.



## ***Chapitre IV:***

### ***Amélioration des propriétés barrières des capsules par incorporation d'un polymère pH-sensible***

G. Ben Messaoud, Laura Sánchez-González, L. Probst, C. Jeandel, E. Arab-Tehrany, S. Desobry. Physico-chemical properties of alginate/shellac aqueous-core capsules: influence of membrane architecture on riboflavin release. *Carbohydrate Polymers*





L'alginate est très utilisé dans le domaine de la biotechnologie pour l'encapsulation de cellules car il possède plusieurs avantages tels que son faible coût, sa disponibilité, sa biocompatibilité et sa gélification dans des conditions relativement douces. De plus, les hydrogels à base d'alginate possèdent une perméabilité relativement large mais sélective assurant l'immobilisation de cellules tout en permettant la diffusion des nutriments vers les capsules et la diffusion des composés sécrétés par les cellules vers l'extérieur des capsules.

Ce dernier avantage pourrait rapidement devenir un inconvénient pour les applications de libération contrôlée et en particulier dans le cas d'encapsulation de molécules de faibles masses moléculaires.

Dans ce dernier chapitre, un polymère pH-sensible: la gomme laque (E904) issue de la sécrétion d'une cochenille asiatique (*Kerria lacca*) a été associée à l'alginate dans le but de réduire la perméabilité des capsules à cœur liquide.

Pour cela, la gomme laque a été incorporée soit directement au niveau de la membrane des capsules (système composite) soit appliquée comme couche externe (système enrobé) et ces deux systèmes ont été comparés par rapport à un système alginate simple (témoin). L'influence du pH de préparation, de la concentration de la gomme laque ainsi que son mécanisme de préparation (précipitation acide ou réticulation avec les ions calcium) ont été étudiés. Les capsules produites ont été évaluées selon 2 critères : la cinétique de libération de la riboflavine utilisée comme molécule modèle et la structure de leur membrane observée par microscopie.



**Physico-chemical properties of alginate/shellac aqueous-core capsules:  
influence of membrane architecture.**

Ghazi Ben Messaoud<sup>a</sup>, Laura Sánchez-González<sup>a,\*</sup>, Laurent Probst<sup>b</sup>, Carole Jeandel<sup>a</sup>, Elmira Arab-Tehrany<sup>a</sup>, Stéphane Desobry<sup>a</sup>

<sup>a</sup> Laboratoire d'ingénierie des biomolécules (LIBio). ENSAIA-*Université de Lorraine*. 2 avenue de la forêt de Haye, TSA 40602, 54518 Vandœuvre-lès-Nancy Cedex, France.

<sup>b</sup> Cookal company. 21 avenue de la Meurthe, 54320 Maxéville, France.

\* Corresponding author

Tel: +33 (0)3 83 59 58 77

Fax: +33 (0)3 83 59 58 04.

E-mail address: [laura.sanchez-gonzalez@univ-lorraine.fr](mailto:laura.sanchez-gonzalez@univ-lorraine.fr)

**Abstract**

Alginate core-shell capsules are of widespread importance in the encapsulation field. However, alginate membrane capsule possesses a relative large permeability which leads to potential loss of their content, especially low molecular weight molecules.

To enhance the physicochemical properties of Alginate capsules, shellac was incorporated into the membrane (composite capsules) or as an additional external layer (coated capsules). The influence of preparation pH, coating time, shellac concentration and preparation mechanism (acid precipitation or calcium reticulation) were investigated. Results showed that shellac influenced significantly capsules properties. The feasibility of shellac incorporation was closely related to calcium and polymer concentrations as showed by ATR-FTIR. Optical, fluorescence

and SEM microscopy highlighted different capsules and membranes architectures. In contrast to simple and composite capsules, coated capsules showed a pH-dependent release of the entrapped vitamin, especially by shellac crosslinking with calcium. This global approach is useful to control release mechanism of low molecular weight molecules from macro and micro-capsules.

**Keywords:** *Core-shell capsules; physicochemical properties; riboflavin; permeability; pH-dependent release.*

## **1. Introduction**

Polysaccharide-based capsules are of a general importance in the encapsulation field (Madene, Jacquot, Scher, & Desobry, 2006). Their main functions are the successful encapsulation, transportation and controlled release of the capsule content to the external environment (Hu, Tsai, Liao, Liu, & Chen, 2008b).

Alginate is one of the most dominantly used naturally derived polymer thanks to its interesting properties such as good biocompatibility, wide availability, low cost and gelation under mild conditions (Pawar & Edgar, 2012). This anionic soluble polysaccharide can be extracted from brown algae such as *Macrocystis pyrifera*, *Ascophyllum nodosum*, *Laminaria hyperborean*, or isolated from bacterial species such as *Azotobacter* and *Pseudomonas* (Shilpa, Agrawal, & Ray, 2003).

Chemically, alginate is an unbranched binary polysaccharide constituted of 1,4-linked  $\beta$ -D-mannuronic (M) and  $\alpha$ -L-guluronic acid (G) (Shilpa et al., 2003). The uronic acid residues are distributed along the chain polysaccharide in a pattern of homopolymeric blocks (G and M-blocks) and heteropolymeric blocks (MG-blocks) (Pawar & Edgar, 2012).

Alginate capsules functionality depends considerably on their permeability and physicochemical stability. The final hydrogel possesses a relatively large permeability since

cells can be immobilized while nutrients or compound excreted by the cells can diffuse out (Lim & Sun, 1980).

This selective retention and release of alginate hydrogels makes them a good carrier for biotechnology applications however the relative high porosity is not suitable for release applications of low molecular weight drugs.

In order to control their physicochemical properties, several strategies were developed such as the creation of composite capsule by incorporation of further polymers (M.-L. Zhu, Li, Zhang, & Jiang, 2015)(Ben Messaoud, Sánchez-González, Jacquot, Probst, & Desobry, 2015) or nanoparticles (Degen, Zwar, Schulz, & Rehage, 2015) into alginate membrane or by coating with positively charged polymers such as chitosan (Bartkowiak & Hunkeler, 2000) and poly-L-lysine (Leick, Kemper, & Rehage, 2011) or by polyelectrolyte layer-by-layer deposition by alternating oppositely charged polymers (Ye, Wang, Liu, & Tong, 2005).

The combination of alginate with other naturally derived polymers could control physicochemical properties of the final matrix.

Shellac is a purified resinous secretion of lac insects (*Kerria lacca*), which are mostly cultivated in host trees from India and other parts of the Far East (Aulton, Cole, & Hogan, 1995). It is a complex mixture of polar and non-polar components consisting of polyhydroxy polycarboxylic esters, lactones and anhydrides with the main acid components being aleuritic and terpenic (Patel, Remijn, et al., 2013) (Figure 1).

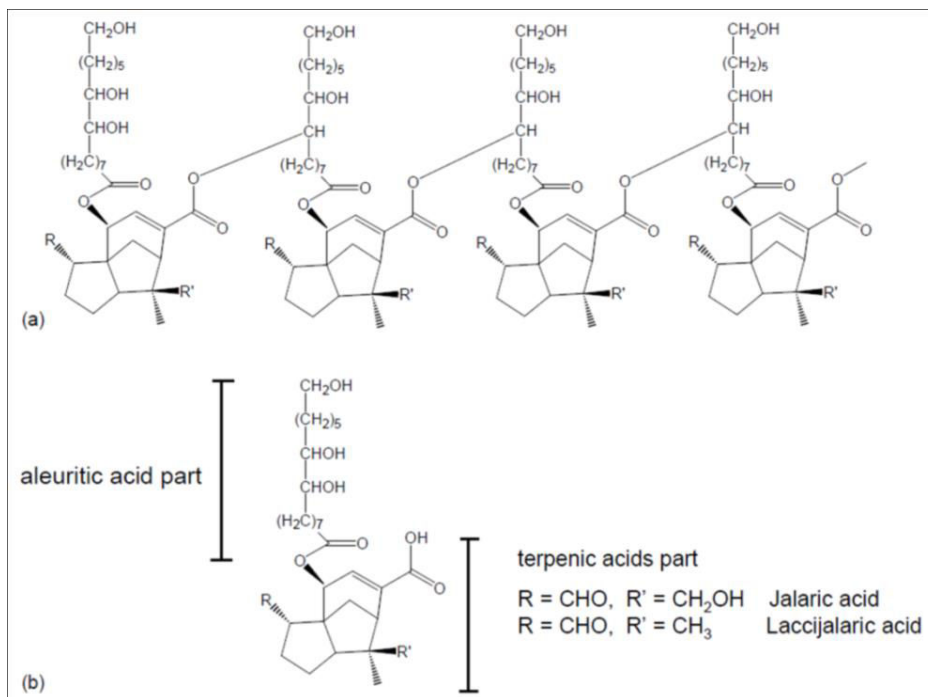


**Figure.1.** Chemical structures of shellac. Polyesters (a) and single esters (b). (Limmatvapirat et al., 2004)

Thanks to its excellent film forming and protective properties, nontoxicity and biodegradability, this natural polymer is widely used as adhesives, thermoplastics, sealants, insulating materials, and coating materials in food and pharmaceutical industries (Aulton et al., 1995) and was recently used as an oleogelator (Patel, Schatteman, Vos, & Dewettinck, 2013).

Considering these attractive properties, shellac gained a lot of interest for developing several capsules types such as calcium shellac microspheres prepared by emulsification-precipitation (Xue & Zhang, 2009), composite (Leick, Kott, et al., 2011) and coated liquid-filled pectinate macrocapsules (Henning, Leick, Kott, Rehage, & Suter, 2012), and microcapsules by extrusion (Xue & Zhang, 2008), spray drying and co-precipitation technique (Hamad, Stoyanov, & Paunov, 2012).

Concerning the fabrication process of millimeter scale alginate liquid-core capsules, there are

three main approaches. The first one is based on microfluidic devices, by co-extrusion and electro co-extrusion of the inner core and Na-alginate drops into a CaCl<sub>2</sub> bath to form the alginate capsules (Bremond, Santanach-Carreras, Chu, & Bibette, 2010)(Phawaphuthanon, Behnam, Koo, Pan, & Chung, 2014). The second method is based on the formation of alginate beads hydrogel followed by coating with oppositely charged polymers and finally by alginate core removal using a chelating agent (Correia, Sher, Reis, & Mano, 2013). For the third approach, called “reverse spherification”, the CaCl<sub>2</sub> droplets containing the active molecule is dropped into a sodium alginate bath to form the inner side of the membrane, and then the partially gelled capsules are transferred into a CaCl<sub>2</sub> solution to complete the reticulation process (Blandino, Macías, & Cantero, 1999). The latter method was used in the current study.

The aim of this work was to study the influence of shellac incorporation into alginate liquid-core capsules produced by simple extrusion process. Four different types of capsule shells have been synthesized: simple alginate membrane as a control, composite membrane by mixing shellac and alginate solutions, coating the alginate capsules with an additional shellac layer and coated composite capsules. The influences of shellac concentration, gelation time and mechanism (via precipitation or CaCl<sub>2</sub> reticulation) on release properties of riboflavin were investigated.

## **2. Materials and methods**

### **2.1. Materials**

Alginic acid sodium salt (Alg) with an M/G ratio of 1.56, Shellac (ShL) wax-free (flakes), glycerol ( $\geq 99.5\%$ ) and Riboflavin ( $M_w = 376.36$  g/mol) were purchased from Sigma Aldrich (Steinheim, Germany). The average alginate molecular weight  $M_v$  of  $1.69 \cdot 10^5$  g.mol<sup>-1</sup> was



calculated using the Mark–Houwink–Sakurada correlation:  $[\eta] = KM_v^\alpha$  Where  $\alpha = 0.92$  and  $k = 7.3 \cdot 10^{-5}$  (Thu et al., 1996).

Calcium chloride dihydrate ( $M_w=147.02$  g/mol) was obtained from VWR International (Leuven, Belgium), tri-sodium citrate ( $M_w= 294.09$  g/mol) from Fisher scientific (Leicestershire, United Kingdom), HCl 1 M and NaOH 1M were purchased from Sigma Aldrich.

For ShL labelling and Alg-FITC derivative synthesis, Nile red, fluorescein isothiocyanate (FITC, isomer I), N-(3-dimethylaminopropyl)-N'-ethylcarbodiimide hydrochloride (EDC), N-hydroxy sulfosuccinimide sodium salt (NHSS) and 1, 6-diaminohexane were purchased from from Sigma-Aldrich (Chemie, Steinheim, Germany).

## **2.2. Samples preparation**

### **2.2.1. Solutions preparation**

To prepare the liquid-core solution,  $\text{CaCl}_2$  (1 % wt) was solubilized into 90 % wt of glycerol ( $\eta=0.22$  Pa.s, 20 °C) to modulate the cross-linking solution density and ensure capsules spherical shape (Blandino et al., 1999). To investigate the influence of pH, cross linking solutions with different pH values (1, 3, 5) were prepared from the stock solution by adding some drops of HCl. In order to study the passive release of the obtained systems, riboflavin was solubilized in the cross-linking solutions.

Alg solution 1% wt was prepared by dispersion of the polymer powder in distilled water under stirring until complete dissolution. M2

To prepare ShL solution, the polymer was dissolved during 1h in 1.5 % wt ammonium bicarbonate solution at 50 °C to a final concentration of 12 % (w/v). The excess of ammonium salt was then removed by heating the solution at 65°C until a constant pH was reached (pH  $\approx$  7.4) and evaporated water was replaced (Frag & Leopold, 2011).

Solutions of the pure components were mixed together in the composition range 0.5% and 1-5 % wt of Alg and ShL, respectively.

### **2.2.2. Capsules preparation**

In order to prepare the liquid-filled capsules, CaCl<sub>2</sub> solution was extruded dropwise through a needle (outer diameter, 0.9 mm) into stirred Alg and Alg-ShL mixtures in order to obtain alginate and composite capsules, respectively. A dropping height of 5 cm was used to ensure the formation of spherical capsules (Leick, Henning, Degen, Suter, & Rehage, 2010). After a gelation time of 10 minutes, capsules were rinsed with distilled water to avoid external gelation (Blandino et al., 1999). Then capsules were transferred into a CaCl<sub>2</sub> (1% wt) solution to stabilize capsule membranes at the corresponding pH (1, 3,5 or water).

For the preparation of coated capsules, Alg and composite Alg-ShL capsules were transferred into a stirred shellac solution. Then, capsules were rinsed and stored into a CaCl<sub>2</sub> solution at the desired pH.

## **2.3. Characterization of capsules**

### **2.3.1. Measurements of capsule size and membrane thickness**

The external diameter and membrane thickness of capsules were performed under an optical microscope (Olympus AX70, Japan) equipped with a camera (Olympus DP70). Dp controller software (dp controller, version 2.1.1) was used for taking photos (Fig.1). Shell thickness and capsules diameter were therefore calculated using imageJ software (National Institutes of Health, Bethesda, Maryland, USA). The data for one experimental condition were calculated from values taken from 10 capsules.

For capsules fluorescence imaging, ShL was mixed with Nile red and Alg-FITC derivative was synthesized according to Zhu et al 2005 (H. Zhu, Srivastava, & McShane, 2005). Briefly, 120

mg of Alg was mixed with EDC/NHSS (50 mg/30 mg) for the activation of carbonyl groups on alginate in pH 5 sodium acetic buffer for 30 min, followed by addition of 60 mg 1, 6-diaminohexane for another 4 h. The mixture was precipitated in 2-propanol to remove unreacted diamine. The Alg-amine derivative was reacted with FITC (0.5 mg) in pH 8.5 sodium bicarbonate solution for 4 h and precipitated in acetone. Finally, the obtained Alg-FITC derivative was mixed with unlabeled Alg solution.

### **2.3.2. Release properties**

The release of riboflavin was carried out using a Uv-vis spectrophotometer Pharmacia Biotech Ultrospec 4000 (Richmond Scientific Ltd, Lancashire, U.K). Capsules were placed at 20 °C into 20 ml water at different pH values. At scheduled time intervals, the amount of released vitamin was determined from solution absorbance at 440 nm wavelength. At the end of each experiment, in order to determine the total mass initially encapsulated, 1 ml of tri-sodium citrate solution (1M) was added and capsules were sonicated at 40 kHz (Sonicator Vibra cell 75115, 500 watt, Bioblock Scientific Co) and 40% of full power for 600 s (1 s on / 1 s off) to rupture the capsule membrane.

### **2.4. ATR-FTIR spectroscopy**

Attenuated total reflectance Fourier transform infrared (ATR-FTIR) spectra of air dried solutions were acquired using a Tensor 27 mid-FTIR Bruker spectrometer (Bruker, Karlsruhe, Germany) equipped with an ATR accessory (128 scans, 4 cm<sup>-1</sup> resolution, wavenumber range : 4000 - 400 cm<sup>-1</sup>) and a DTGS detector. Spectral manipulations were performed using OPUS software (Bruker, Karlsruhe, Germany). Raw absorbance spectra were smoothed using a nine points smoothing function. Elastic baseline correction using 200 points and H<sub>2</sub>O/CO<sub>2</sub> correction were then applied. Then, spectra were centered and normalized.

## **2.5. Scanning electronic Microscopy**

Prior to analysis, capsules were frozen using liquid nitrogen and then rapidly cutted. Samples were then deposited on a carbon adhesive tab (EMS<sup>®</sup> 77825-12) at room temperature. The coverslips were coated with gold palladium for 2X100 s (Polaron SC7640, Thermo VG Scientific, England). Preparations were observed under SEM (Cambridge Stereoscan S240) at 5 kV.

## **3. Results and Discussion**

### **3.1. Feasibility of shellac incorporation into alginate matrix**

In the current study, several combinations of Alg and ShL were tested in order to control physicochemical properties of the final liquid-core matrix. Alginate capsules were obtained by dripping glycerol solution 90 % vt containing 1 or 2 % wt CaCl<sub>2</sub>. To prepare composite and coated capsules, three ShL concentrations (1, 5 and 10 % wt) and two ShL gelation mechanisms were investigated, calcium reticulation at neutral pH and acid precipitation (pH5, 3 and 1).

The different combinations, showed that the feasibility of composite and coated capsules is closely related to the concentration of ShL and calcium during capsules formation and to the mechanism of ShL precipitation.

For alginate capsules obtained with 1 % wt CaCl<sub>2</sub>, preliminary experiments demonstrated that the preparation of composite and coated capsules is possible only with 1 % wt shellac. In fact, for higher shellac concentrations, composite capsules cannot be formed and only precipitate was observed during dripping of CaCl<sub>2</sub> into Alg-ShL mixture. During the preparation of coated system we observe Alg membrane disintegration by ShL deposition on capsules surface.

In the case of ShL coating by reticulation with CaCl<sub>2</sub>, preparation is possible with 1 and 5 % wt ShL. However, the ShL layer was not stable and detached from the Alg capsule during storage. During coating with ShL 10 % wt, the Alg membrane disintegrated during the coating process.

For Alg capsules obtained with 2 % wt CaCl<sub>2</sub>, experiments revealed that composite capsules preparation is possible for ShL concentration up to 5% wt and coated capsules for all ShL concentrations. Unfortunately, during capsules coating by pH precipitation, we observed a very fast deposition of ShL generating the formation of non-uniform external layer. This variation of ShL thickness layer and structure could lead to heterogeneous mechanical and release properties. Since this type of system could be used as “liquid pearls” in molecular gastronomy or in biotechnology, we selected the systems prepared with 1% CaCl<sub>2</sub> for the subsequent characterizations. The influence of pH and temperature on physicochemical properties of capsules is studied.

From this preliminary study, we observed that coating the capsules by ShL reticulation with Ca<sup>2+</sup> lead to the formation of a uniform and smooth layer at the surface of alginate capsules compared to capsules prepared by acid ShL precipitation. In the other hand, the preparation of composite Alg-ShL capsules was closely related to the amount of ShL and Ca<sup>2+</sup>, which could be explained by the competition between ShL and alginate shellac to bind calcium ions and affect the final composite gel structure.

### **3.2. Capsules structure**

The fluorescence and optical microscopic observation of aqueous-core capsules obtained by ShL precipitation and calcium reticulation are shown in figure 3 and 4, respectively.

All capsules types exhibited a spherical shape, as a consequence of closer solutions viscosities before the encapsulation step. Since the viscosity of the dripped CaCl<sub>2</sub> solution is constant, in the other hand ShL addition did not lead to significant viscosity changes.

Concerning capsules obtained by acid precipitation (Fig. 3), the incorporation of 1% ShL in the Alg membrane resulted in a relative opaque system (fig. 3b) due to ShL precipitate formation.

For coated Alg capsules by shellac precipitation, after 1 min the ShL precipitate is randomly localized on the surface of Alg capsules and did not form a homogenous layer (Fig. 3c). However, after 10 min coating, shellac precipitate cover all the capsule surface (Fig. 3d). Even if shellac precipitation during acidification is a very fast process, 1 min is not sufficient to form a homogenous external layer.

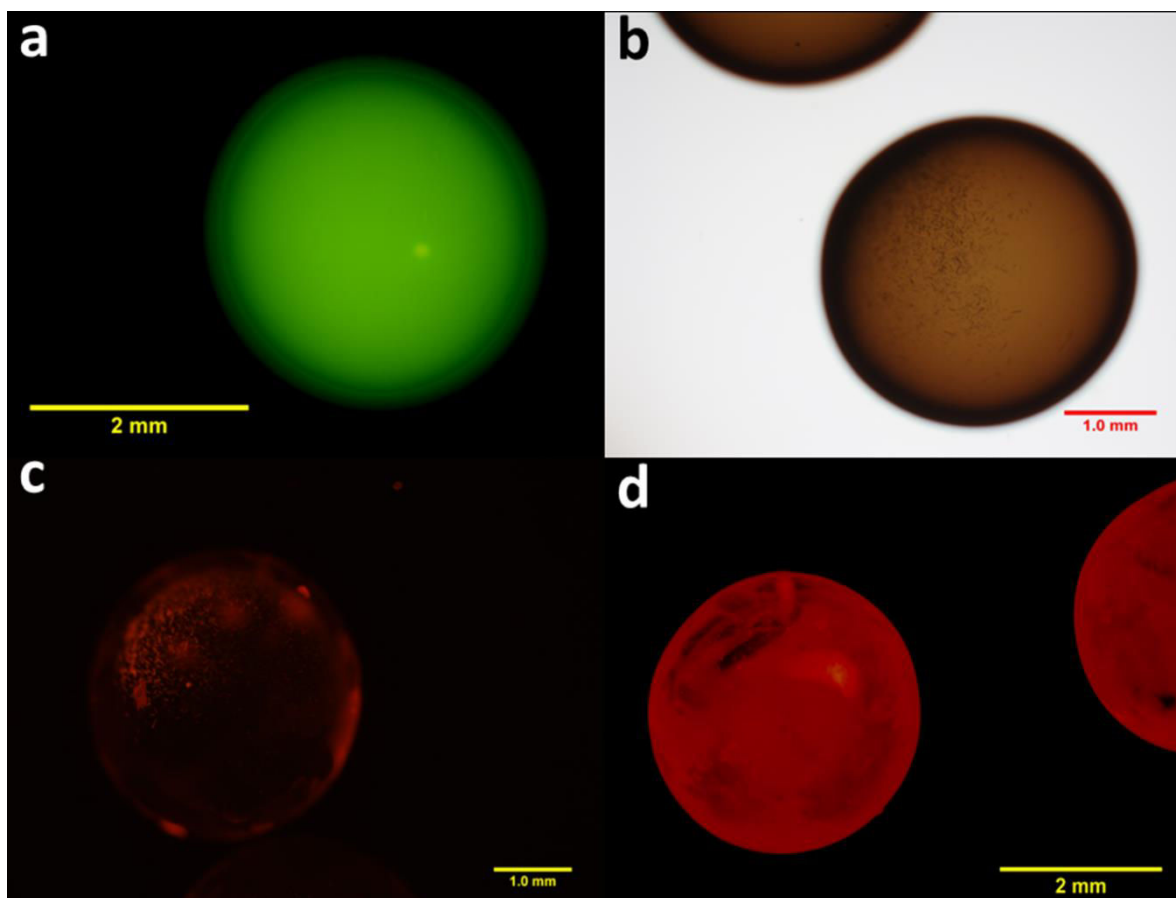


**Figure. 2.** Fluorescence images of simple Alg (a), composite Alg-ShL 1% wt (b), ShL coated Alg during 1 min (c) and 10 min (d).

Fig. 2 showed optical micrographs of simple Alg capsules, composite and coated capsules prepared by calcium reticulation at neutral pH and then incubated at different pH-values (pH1, 3 and 5).

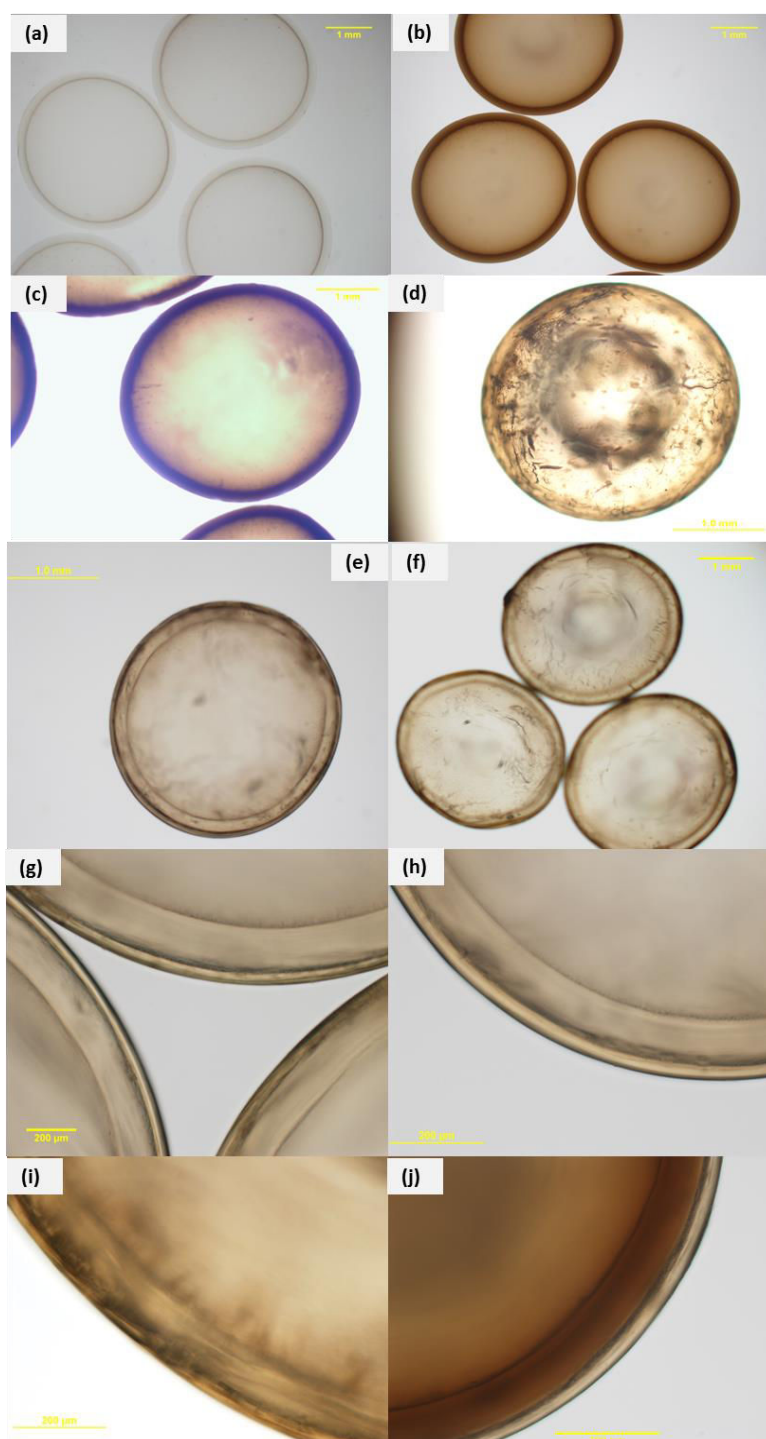


**Figure 3.** Microscopic images of simple Alg capsules at pH5 (a), composite Alg-ShL 0.5% (b), composite Alg-ShL 1% wt (c), coated Alg capsules at pH1 (c, i), pH3 (d, g) and pH5 (e, g) and coated Alg-Shl composite capsule (j).

Compared to simple Alg capsules (Fig. 3a), the incorporation of ShL resulted in opaque capsules (fig 3.b and c), and this opacity is function of ShL amount incorporation. In fact for alg-ShL 5% composite capsules, it's hard to distinguish between the membrane and core capsule due to high system opacity (figure not shown). In this case, others experimental techniques could be usefull like NMR imaging to distinguish simply the capsule membrane (Leick, Kott, et al., 2011),(Henning et al., 2012). Coating alginate capsule (Fig. 3d, e and f) resulted in a dark layer surrounding the liquid core capsules, but more distinguishable at pH3 and 5 (Fig. 3e and f) than at pH1 (Fig. 3d). From the observation of ShL coated Alg membrane (Fig. 3g, h), we can easily differentiate the ShL layer at the surface of capsules. However at pH1, even after zooming, it's still hard to distinguish between the two polymers layers (Fig. 3i). We showed also that it's possible to perform ShL coating of Alg-ShL composite capsules (Fig. 3j).

From the microscopic observation, the average diameter and membrane thickness of simple, composite and coated capsules were calculated (Table 1).



**Table 1.** Diameter and membrane thickness of Alg / ShL liquid-core capsules. Mean values and standard deviation.

Capsules	pH 1		pH 3		pH 5	
	Diameter (mm)	Membrane thickness ( $\mu\text{m}$ )	Diameter (mm)	Membrane thickness ( $\mu\text{m}$ )	Diameter (mm)	Membrane thickness ( $\mu\text{m}$ )
<b>Simple</b>	3.30 $\pm$ 0.13	206 $\pm$ 18	3.34 $\pm$ 0.24	208 $\pm$ 19	3.66 $\pm$ 0.14	305 $\pm$ 11
<b>pH precipitation</b>						
<b>Composite</b>	2.94 $\pm$ 0.12	185 $\pm$ 19	3.15 $\pm$ 0.14	205 $\pm$ 8	3.42 $\pm$ 0.10	187 $\pm$ 17
<b>Coated 1min</b>	3.20 $\pm$ 0.13	238 $\pm$ 20	3.49 $\pm$ 0.13	235 $\pm$ 17	3.48 $\pm$ 0.07	290 $\pm$ 27
<b>Coated 10 min</b>	3.29 $\pm$ 0.14	207 $\pm$ 21	3.28 $\pm$ 0.06	225 $\pm$ 10	3.52 $\pm$ 0.15	284 $\pm$ 18
<b>Calcium reticulation</b>						
<b>Simple coated</b>	2.68 $\pm$ 0.20	138 $\pm$ 17	3.03 $\pm$ 0.20	207 $\pm$ 18	3.29 $\pm$ 0.10	223 $\pm$ 19

The average diameter of capsules ranged from 3.6 to 3.3 mm and from 2.94, 3.2 and 3.29 mm to 3.42, 3.48 and 3.52 mm for composite Alg-ShL 1%, Alg capsules coated during 1 min and 10 min by ShL acid precipitation, respectively.

The diameter of alg coated capsules by Ca reticulation, ranged from 2.68 to 3.29 at pH1 and pH3, respectively.

Membrane measurements showed a pH-dependent thickness of simple Alg capsules which decrease with pH diminution (from 305 to 206  $\mu\text{m}$  at pH 5 and 1, respectively), indicating alginate hydrogel shrinking in acidic conditions (Moe, Skjaak-Braek, Elgsaeter, & Smidsroed, 1993). This reduction could be explained by potential alginate precipitation or partial a calcium

alginate conversion in alginic acid gel by protons exchange (K. I. Draget, Skjåk-Bræk, Christensen, Gåserød, & Smidsrød, 1996). In fact, the pKa values of both alginate monomers b-D-mannuronic acid (M) and a-L-guluronic acid (G) residues are of 3.38 and 3.65, respectively (K. I. Draget, Skjåk Bræk, & Smidsrød, 1994).

The membrane thickness evolution of composite Alg-ShL capsules with pH decrease was comparable to alginate capsules and the highest thickness was observed for pH5.

However, composite Alg-ShL capsules showed lower membrane thicknesses compared to simple Alg capsules. A possible explanation, is that the precipitation of shellac decreased membrane development during the gelation process. No significant differences on membrane thickness were observed between simple and coated capsules by acid precipitation during 1 and 10 minutes, respectively.

Surprisingly, ShL coated Alg capsules by Ca reticulation, exhibited a thinner membrane than simple ALg capsules over all the pH range. The double layer capsules exhibit lower membrane thickness than simple capsules and therefore Alg membrane size decrease after or during the coating process. This Alg membrane shrinking might be induced by a depletion of cross-linked calcium ions in the hydrogel as a consequence of chemical interaction between Ca and ShL as previously reported by S. Henning et al.,

Another possible explanation could be related to the physical nature of alginate and shellac layers. In fact, alginate is a hydrogel mainly composed of water, whereas shellac is a solid precipitate mainly stabilized with lower water content. Therefore during shellac layer deposition at the surface of alginate capsules, a mechanical pressure could be applied at the interface and might lead to membrane volume decrease.

In general, capsule diameter evolution depends strongly on capsule membrane thickness, since the droplet size is controlled by the intrinsic properties of the  $\text{CaCl}_2$  solution during the dripping step.

In order to investigate the internal structure of membranes, SEM was performed on cross-sections of aqueous-core capsules. The SEM micrographs of the different capsules type are shown in Fig.4 at different magnifications.

The internal surface of the alginate membrane is relatively smooth with a network structure (Fig 4.a). The air dried composite membrane Alg-ShL (Fig. 4b) showed a sponge-like membrane with an internal structure not too different from simple shellac layer (Fig 4.d) but with higher porosity. The coated capsules (Fig. 4c) showed two distinct films, Alg membrane surrounded by ShL layer. The interspace between the two membrane highlighted at high magnifications, could be related to Shellac layer detachment at capsule surface caused by the drying process during SEM experiments. In (Fig. 4e) we can observe a half of composite capsule during SEM experiments. It's interesting to note that this type of capsules maintain its structure integrity during drying and SEM analysis compared to simple alginate capsules which could be related to the difference of the physical structure between the two polymers gels.

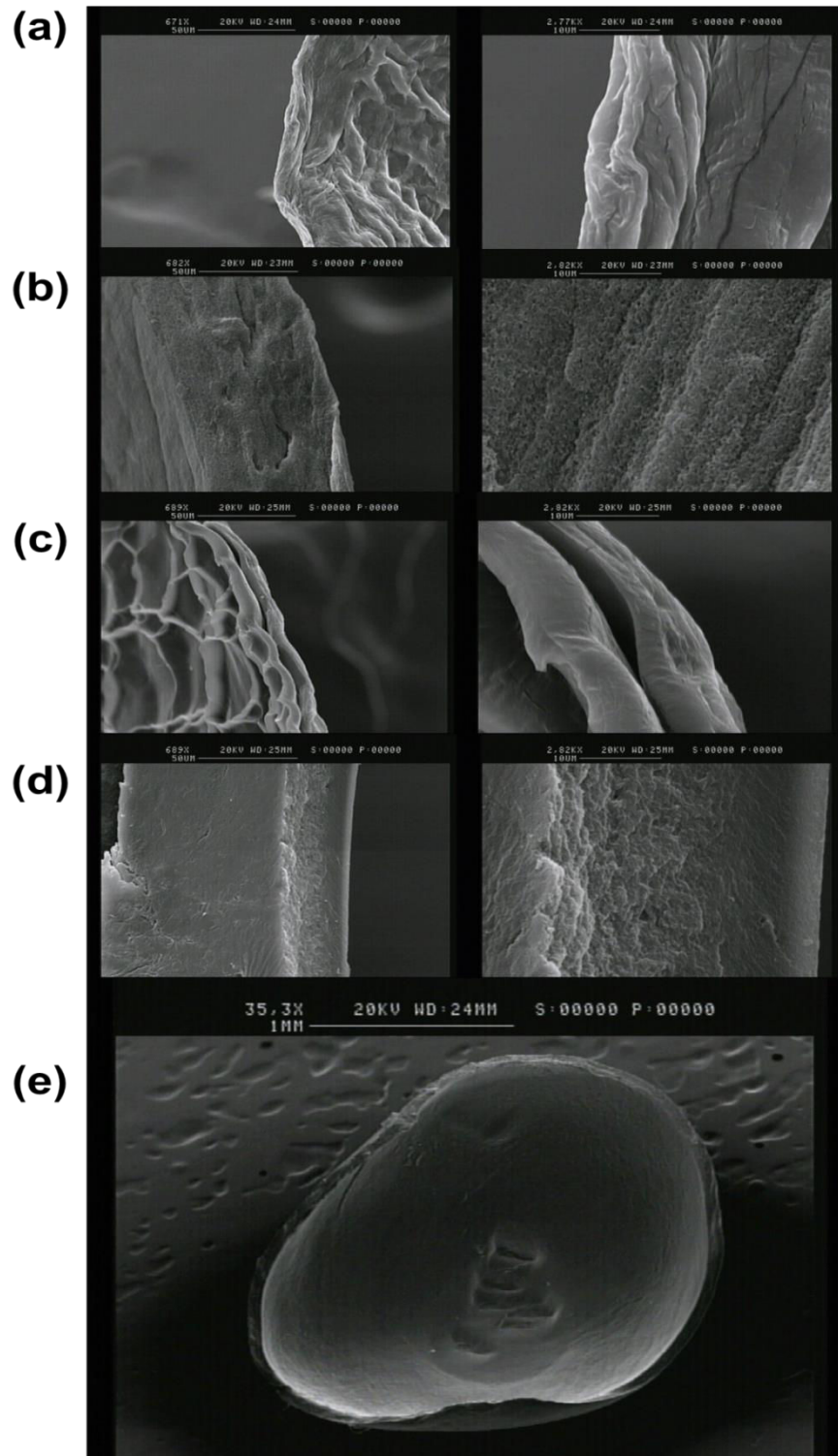


**Figure 4.** SEM images of the cross-sections of simple Alg (a), composite Alg/ShL 1% (b), coated Alg (c), ShL precipitate (d) and composite Alg/ShL capsule (e).

### 3.3. FTIR spectroscopy

The FTIR spectra of casted Alg, ShL solutions and precipitates (gel) after acidification or calcium reticulation are shown in Figure.5. All spectra displayed a band between 3000 and 3700  $\text{cm}^{-1}$  (OH stretching) .

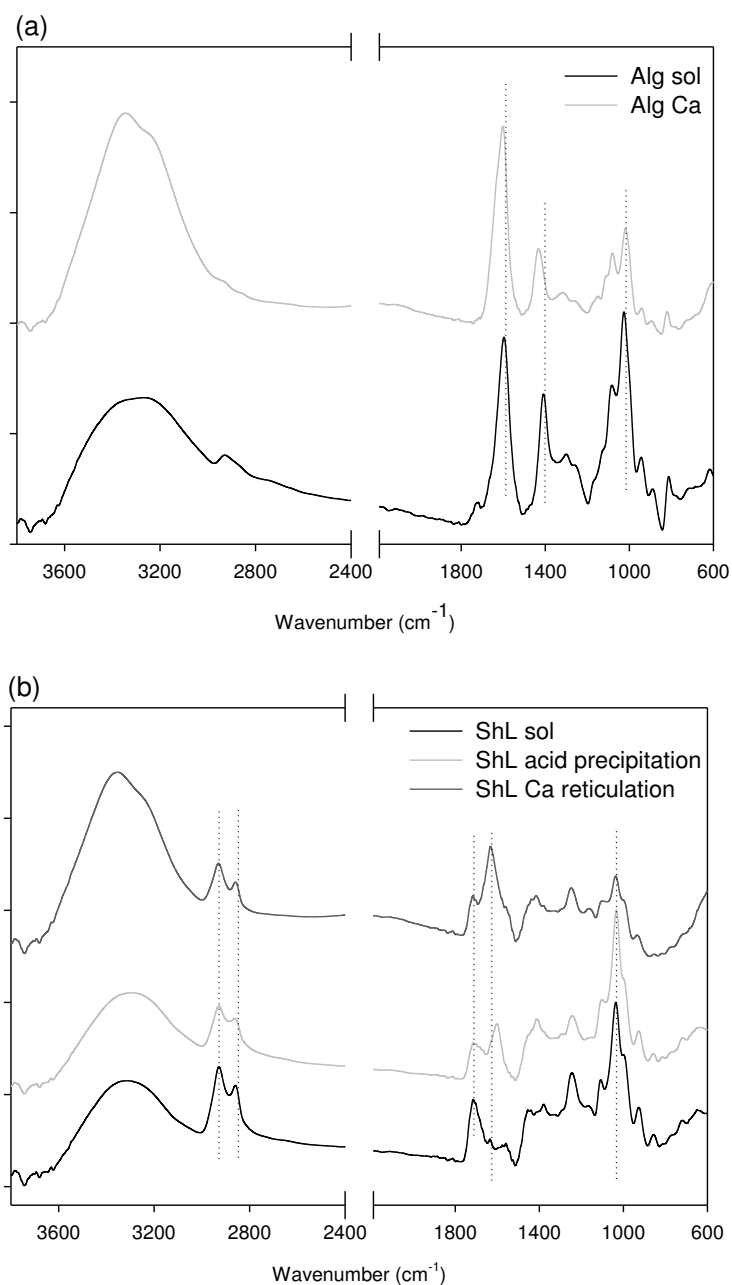


**Figure. 5.** FTIR spectra of Alg (a) and ShL (b).

The casted alginate solution and calcium alginate dried hydrogel spectra (Fig.5a) showed two characteristics peaks due to the carboxylate group; an antisymmetric stretch of C-O bond at  $1594\text{ cm}^{-1}$  and a symmetric stretch at  $1413\text{ cm}^{-1}$  Of the COO group.

The band at  $1023\text{ cm}^{-1}$  is an antisymmetric stretch (C-O-C) given by the guluronics units (Sartori, Finch, Ralph, & Gilding, 1997). The reticulation of alginate with calcium cations caused a decrease in intensity of COO<sup>-</sup> stretching peaks, and a decrease in intensity of  $1031\text{ cm}^{-1}$  peak. This indicated that an ionic bonding between calcium ion and carboxyl groups of alginate and a partial covalent bonding between calcium and oxygen atom of ether groups, respectively (Pongjanyakul & Puttipipatkachorn, 2007).

The cross-linking process caused an obvious shift to higher wavenumber and a decrease in intensity of COO<sup>-</sup> stretching peaks due to ionic exchange of the sodium in the uronic-acid residues by calcium divalent cations and, hence, a change in the charge density and the radius of the atomic weight of the cation (Voo et al., 2015).

In Fig. 5b, the FTIR spectra of dried ShL solution, acid ShL precipitate and Ca ShL are shown. The band in the area between  $3700$  and  $3000\text{ cm}^{-1}$  is a result of O-H stretching vibrations. This band present significant great intensity and has a shoulder in the spectrum of the ShL Ca.

All spectra showed two bands due to C-H stretching vibrations ( $2930$  and  $2850\text{ cm}^{-1}$ ), this bands exhibited the same intensities and same locations for all ShL samples.

However, the wavenumber region  $1700$ - $1500\text{ cm}^{-1}$  showed significant changes between the three ShL spectra. This indicates some interactions with the carboxylate groups, such as due to hydrogen bands, and calcium interaction with the carboxylate groups, for ShL acid and ShL Ca, respectively.

The intensity of the bands at  $1629$  and  $1542$  is significantly increased for ShL Ca compared to ShL solution and ShL acid precipitate.

The bands at 1629 and 1404  $\text{cm}^{-1}$  may be referred to the asymmetric and symmetric C=O stretching vibration, respectively, of the carboxylate. From changes in the spectrum it may be concluded that the mechanism of interaction is a salt formation of calcium ions and the carboxylate groups of shellac. However, the presence of the carbonyl band at 1708  $\text{cm}^{-1}$  in the calcium shellac spectrum indicates that not all carboxylic groups are involved during ShL Ca precipitate formation (Derrick, 1989).

### **3.4. Release properties**

Relative amounts of released riboflavin versus time elapsed after capsules preparation were plotted in Figure 6 and 7 for different pH and membrane capsules structure. Riboflavin release kinetic showed the same profile for all capsules types with an exponential phase followed by stationary phase which reflects the equilibrium state. The riboflavin diffusion from simple, composite and coated capsules by ShL acid precipitation at different pH-values is shown in Fig. 6.

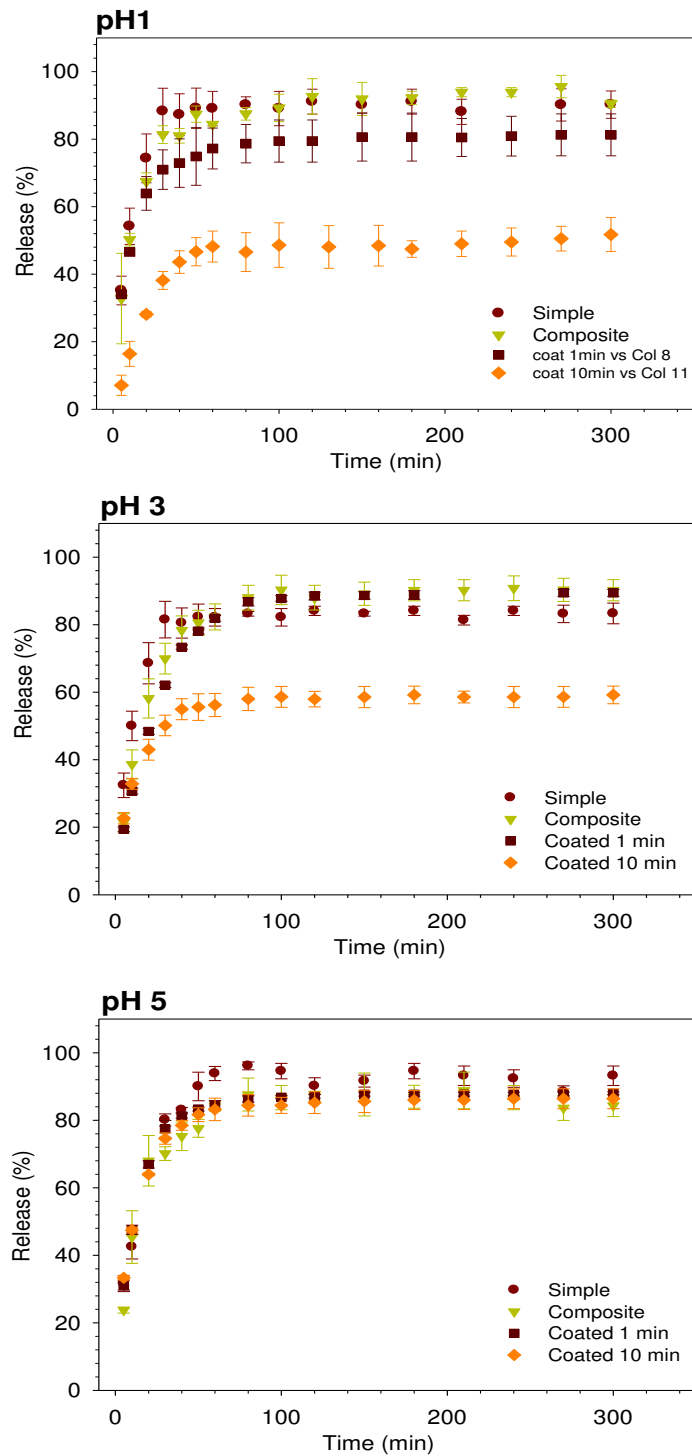


**Figure 6.** Riboflavin release from simple Alg, Alg-ShL composite and coated capsules during 1 and 10 min via ShL acid precipitation at different pH-values.



For all capsules types and pH-values the equilibrium release state was achieved after 80 min. However, the percentage of released riboflavin depends considerably on capsule types (membrane architecture) and pH-values.

In fact, at pH1, simple and composite Alg-ShL capsules didn't show significant differences where the final release percentage where about 90% approximatively. Coating capsules during 1 min resulted in a final release percentage of 80%. However, this amount was not significantly different from the released amount from simple and composite capsules. This observation could be explained by the nonhomogeneous ShL deposition at the surface of Alg capsules as previously discussed (Fig. 2c). Coating the capsules during 10 min, resulted in a significantly decrease of the total amount of riboflavin released after 300 min (51.8 %).

At pH3, simple, composite and coated capsules showed the same riboflavin rate and final amount. However, for coated capsules during 10 min, the final amount of riboflavin was 59.2 %. At pH5, all capsules types showed the same diffusion profile and the total amounts of released riboflavin after 100 min were not significantly different for all capsules types.

Concerning riboflavin release from coated capsules by ShL calcium reticulation (Fig. 7a), the final amount of released vitamin at pH 3 and 5 (91.5 and 83.5 %, respectively) was not significantly different, however at pH1 the final released amount didn't exceed 40% after 5 hours.

The coated capsules were heated at 60°C below the glass transition temperature of ShL during 30 minutes into a riboflavin solution, then capsules were washed and transferred into the release media (pH5, 3 and 1). The resulted capsules showed a better retention than unheated matrix (Fig. 7b). In fact, the final amounts of released vitamin at pH1, 3 and 5 were 10.8, 48.3 and 63.2 %, respectively.

The high retention efficiency of heated liquid-core, could be related to the structural changes in the shellac layer during heating. In fact ShL is a thermoplastic polymer, therefore sticky

polymer precipitate is formed at this temperature, which result in a dense network with lower porosity than unheated capsules. (Pearnchob & Bodmeier, 2003)

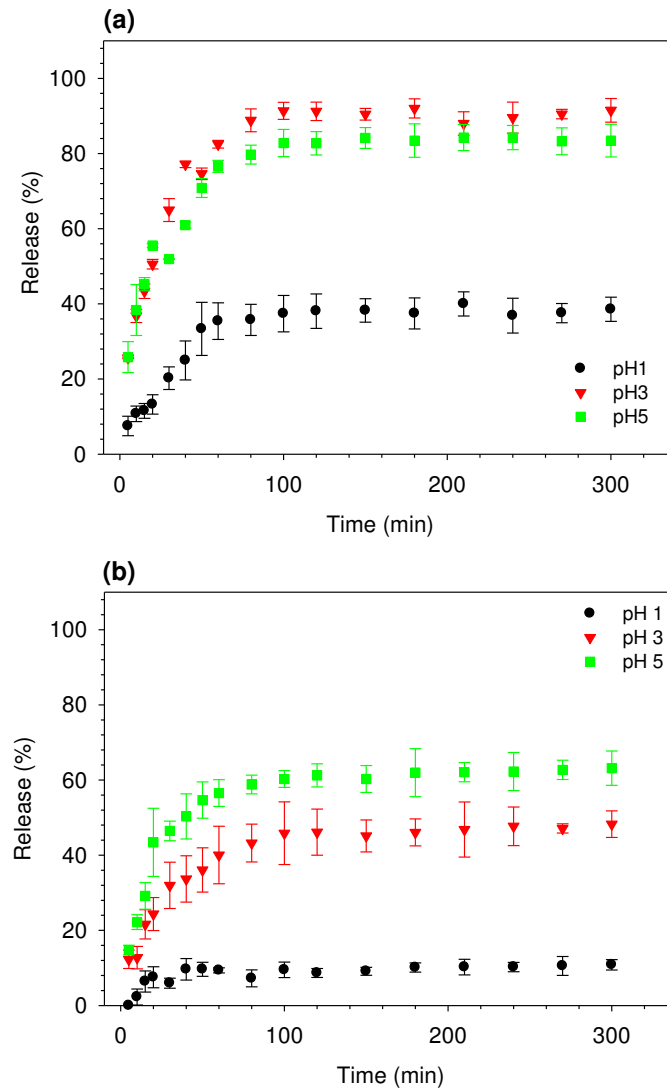


**Figure 7.** Riboflavin release from unheated coated capsules by ShL calcium reticulation (a) and after heating (b).

#### **4. Conclusion**

In conclusion, the influence of ShL incorporation on structure and permeability of Alg liquid-core capsules produced by reverse spherification was investigated. The membrane architecture was controlled by the preparation of simple Alg membrane, mixing ShL and Alg solutions to produce composite system or coating the Alg capsules with an additional ShL layer. The influence of preparation pH, ShL concentration and shellac preparation mechanism (acid precipitation or calcium reticulation) were studied.

The Optical and fluorescence microscopy highlighted different capsules and membranes architectures and SEM the obtained internal membrane structures.

Compared to simple and composite capsules, coated capsules displayed a retarded release of the entrapped riboflavin vitamin. However, the retention efficiency of the coated capsules was closely related to the preparation mechanism of the external ShL layer. In fact ShL calcium reticulation lead to a higher vitamin retention for the entire pH range.

This type of matrix could be useful for developing macro and micro-capsules with pH- sensitive release behavior. For example, the design of pH sensitive system for oral drug delivery applications (J. H. Park, Saravanakumar, Kim, & Kwon, 2010)(Qiu & Park, 2012), like the encapsulation of low molecular weight drugs which target the intestines (pH 7.4) to ensure their retention and avoid their undesirable early release during their passage through the stomach (pH 1.2). However, further investigations under buffered environments and physiological conditions are necessary for drug delivery applications.

#### **Acknowledgments**

COOKAL and GYMNOKIDI companies and ANRT French Agency are acknowledged for their financial support (project N° 312/2012). Justine Paoli from the Medical School of Nancy (Microscopy services) is thanks for performing SEM images.

## ***Conclusion générale et perspectives***

Dans ce travail de thèse, les propriétés physicochimiques de capsules d'alginate à cœur liquide ont été étudiées et modifiées par incorporation de biopolymères. Ces capsules trouvent des applications dans plusieurs domaines et notamment dans la cuisine moléculaire : perles gastronomiques 'COOKAL'. La fonctionnalité de ce système biphasique (gel/liquide) complexe dépend considérablement de sa perméabilité et stabilité mécanique et chimique. Ces capsules millimétriques à cœur liquide ou 'Perles' sont préparées par sphérification inverse qui consiste en une extrusion goutte à goutte d'un mélange (contenant du chlorure de calcium) dans un bain de gélification à base d'alginate. Un agent épaississant est généralement ajouté à la solution de  $\text{CaCl}_2$  afin de permettre la formation de capsules sphériques et de limiter leur déformation par le cisaillement du bain de gélification.

Dans un premier travail, on s'est donc naturellement intéressé au rôle que peut jouer le polymère utilisé pour ajuster la viscosité de la solution de  $\text{CaCl}_2$  sur les propriétés finales des capsules. Le module de Young de la membrane des capsules a été corrélé aux propriétés viscoélastiques d'hydrogels plans d'alginate obtenues par rhéologie oscillatoire aux faibles amplitudes et la perméabilité de la membrane a été évaluée par suivi de la cinétique de diffusion de la rouge cochenille, riboflavine et BSA. Cette étude a démontré l'importance de la composition du cœur liquide, ce qui peut donner de nouvelles idées afin d'ajuster les propriétés physicochimiques de macro et microcapsules en modulant les interactions cœur-membrane.

Dans ce travail, la charge du polymère utilisé pour ajuster la viscosité de la solution de chlorure de calcium affecte les propriétés finales des capsules. Néanmoins plusieurs autres paramètres doivent être étudiés, tels que la masse moléculaire du polymère. En effet, l'utilisation de molécules de faible masse moléculaire pourrait fragiliser les capsules par diffusion de part et d'autre de la membrane des capsules. En revanche, des polymères de grandes tailles, peuvent également affecter la stabilité de la membrane et causer la rupture des capsules par application

d'une force de traction en cas de gonflement du polymère dans des conditions spécifiques (nature du solvant, pH...).

Dans un second travail, la stabilité et la perméabilité des capsules ont été contrôlées par une simple incorporation d'un mélange protéique (caséinate de sodium) dans la membrane d'alginate. Les capsules composites ont montré un renforcement des propriétés mécaniques et une libération pH-dépendante de la molécule encapsulée. Ce profil de libération est expliqué par des interactions électrostatiques entre le caséinate de sodium et la molécule encapsulée à  $\text{pH} < 4$ .

L'incorporation de biopolymères dans la membrane d'alginate est une alternative intéressante pour modifier les propriétés finales des capsules à cœur liquide. Cependant, la gélification de l'alginate en présence de ces biopolymères doit être étudiée, par exemple par gélification lente de l'alginate en présence et en absence du second biopolymère et suivi de la transition sol-gel par rhéologie.

Pour des applications en biotechnologie, la biocompatibilité des biopolymères incorporés dans la matrice d'alginate doit être étudiée. La biodégradabilité ainsi que les propriétés de gonflement de l'hydrogel composite (alginate/biopolymère) doivent également être caractérisées.

La stratégie générale utilisée dans cette étude peut être utile pour développer de nouveaux types de microcapsules pour des applications de libération contrôlée par incorporation de polymères dans la coque des capsules susceptibles d'interagir dans certaines conditions ( $T^{\circ}\text{C}$ , pH,...) avec le principe actif encapsulé.

Comme application directe à cette étude, des microsphères à base d'alginate et de caséinate de sodium ont été développées en utilisant un équipement basé sur une technologie de buse vibrante combinée à un potentiel électrostatique. Trois types de systèmes ont été synthétisés :

microsphères simples (alginate), composites (alginate/caséinate de sodium) et composites enrobées par une couche de caséinate de sodium. L'efficacité des microsphères pour l'élimination de colorants azoïques (rouge cochenille et noir amido) a été évaluée. Ce système efficace à pH acide, trouve des applications dans l'élimination de colorants à partir de rejets industriels (textile, plasturgie, etc...) par un mécanisme d'adsorption.

Dans un dernier travail, la gomme laque qui est un additif alimentaire (E904) issu de la sécrétion d'une cochenille asiatique (*Kerria lacca*) a été incorporée dans la membrane d'alginate ou comme revêtement externe. L'optimisation de l'architecture des capsules alginate/gomme laque a permis d'améliorer les propriétés barrières de la membrane d'alginate vis-à-vis des molécules de faible masse moléculaire.

La faisabilité de l'enrobage des capsules par de la gomme laque est étroitement liée aux conditions expérimentales (concentration en gomme laque et en  $\text{CaCl}_2$ ), et les résultats ont démontré une réduction du volume de l'hydrogel d'alginate qui peut être lié aux différences physiques entre le gel d'alginate et le précipité de gomme (mobilité moléculaire, ratio polymère/solvant dans le gel...). Il semblerait donc que l'étape d'enrobage induise une contrainte mécanique à la surface des capsules et conduise à l'expulsion d'un certain volume d'eau de la membrane. Ces changements structuraux de la membrane peuvent également être liés à une compétition entre les deux polymères pour fixer les cations calcium. Une étude donc plus approfondie de cet aspect serait intéressante.

En conclusion, ce travail de thèse a permis de modifier les propriétés physicochimiques des capsules à cœur liquide à base d'hydrogel d'alginate par incorporation de biopolymères. Les systèmes développés peuvent également être utilisés dans différents domaines et extrapolés à une échelle micrométrique afin de s'adapter à une gamme d'applications plus large.

## ***Références bibliographiques***



- Alessandri, K., Sarangi, B. R., Gurchenkov, V. V., Sinha, B., Kie's sling, T. R., Fetler, L., ... others. (2013). Cellular capsules as a tool for multicellular spheroid production and for investigating the mechanics of tumor progression in vitro. *Proceedings of the National Academy of Sciences*, *110*(37), 14843–14848.
- Aravindhan, R., Fathima, N. N., Rao, J. R., & Nair, B. U. (2007). Equilibrium and thermodynamic studies on the removal of basic black dye using calcium alginate beads. *Colloids and Surfaces A: Physicochemical and Engineering Aspects*, *299*(1), 232–238.
- Atsuki, K., & Tomoda, Y. (1926). Studies on seaweeds of Japan I. The chemical constituents of Laminaria. *J. Soc. Chem. Ind. Japan*, *29*, 509–517.
- Aulton, M., Cole, G., & Hogan, J. (1995). *Pharmaceutical Coating Technology*. Taylor & Francis.
- Banat, I. M., Nigam, P., Singh, D., & Marchant, R. (1996). Microbial decolorization of textile-dyecontaining effluents: A review. *Bioresource Technology*, *58*(3), 217–227.
- Bartkowiak, A., & Hunkeler, D. (2000). Alginate–Oligochitosan Microcapsules. II. Control of Mechanical Resistance and Permeability of the Membrane. *Chemistry of Materials*, *12*(1), 206–212.
- Ben Messaoud, G., Sánchez-González, L., Jacquot, A., Probst, L., & Desobry, S. (2015). Alginate/sodium caseinate aqueous-core capsules: a pH-responsive matrix. *Journal of Colloid and Interface Science*, *440*, 1–8.
- Best, J. P., Neubauer, M. P., Javed, S., Dam, H. H., Fery, A., & Caruso, F. (2013). Mechanics of pH-responsive hydrogel capsules. *Langmuir*, *29*(31), 9814–9823.
- Birnbaum, S., Pendleton, R., Larsson, P.-O., & Mosbach, K. (1981). Covalent stabilization of alginate gel for the entrapment of living whole cells. *Biotechnology Letters*, *3*(8), 393–400. <http://doi.org/10.1007/BF01134097>
- Blandino, A., Macías, M., & Cantero, D. (1999). Formation of calcium alginate gel capsules: influence of sodium alginate and CaCl<sub>2</sub> concentration on gelation kinetics. *Journal of Bioscience and Bioengineering*, *88*(6), 686–689.
- Boeris, V., Farruggia, B., & Picó, G. (2010). Chitosan-bovine serum albumin complex formation: a model to design an enzyme isolation method by polyelectrolyte precipitation. *Journal of Chromatography. B, Analytical Technologies in the Biomedical and Life Sciences*, *878*(19), 1543–1548. <http://doi.org/10.1016/j.jchromb.2010.04.008>
- Braccini, I., & Pérez, S. (2001). Molecular Basis of Ca<sup>2+</sup>-Induced Gelation in Alginates and Pectins: The Egg-Box Model Revisited. *Biomacromolecules*, *2*(4), 1089–1096. <http://doi.org/10.1021/bm010008g>
- Breguet, V., Gugerli, R., Perneti, M., von Stockar, U., & Marison, I. W. (2005). Formation of Microcapsules from Polyelectrolyte and Covalent Interactions. *Langmuir*, *21*(21), 9764–9772. <http://doi.org/10.1021/la0512796>
- Bremond, N., Santanach-Carreras, E., Chu, L.-Y., & Bibette, J. (2010). Formation of liquid-core capsules having a thin hydrogel membrane: liquid pearls. *Soft Matter*, *6*(11), 2484–2488.
- Caruso, F., Caruso, R. A., & Möhwald, H. (1998). Nanoengineering of inorganic and hybrid hollow spheres by colloidal templating. *Science*, *282*(5391), 1111–1114.
- Caruso, F., Caruso, R. A., & Möhwald, H. (1999). Production of hollow microspheres from nanostructured composite particles. *Chemistry of Materials*, *11*(11), 3309–3314.
- Cellesi, F., Weber, W., Fussenegger, M., Hubbell, J. A., & Tirelli, N. (2004). Towards a fully synthetic substitute of alginate: optimization of a thermal gelation/chemical cross-linking scheme (“tandem” gelation) for the production of beads and liquid-core capsules. *Biotechnology and Bioengineering*, *88*(6), 740–749.

- Chan, E.-S., Lee, B.-B., Ravindra, P., & Poncelet, D. (2009). Prediction models for shape and size of ca-alginate macrobeads produced through extrusion–dripping method. *Journal of Colloid and Interface Science*, 338(1), 63–72. <http://doi.org/10.1016/j.jcis.2009.05.027>
- Chang, T. M. S. (2005). Therapeutic applications of polymeric artificial cells. *Nature Reviews Drug Discovery*, 4(3), 221–235. <http://doi.org/10.1038/nrd1659>
- Chen, L., Remondetto, G. E., & Subirade, M. (2006). Food protein-based materials as nutraceutical delivery systems. *Trends in Food Science & Technology*, 17(5), 272–283.
- Cheong, S. H., Park, J. K., Kim, B. S., & Chang, H. N. (1993). Microencapsulation of yeast cells in the calcium alginate membrane. *Biotechnology Techniques*, 7(12), 879–884. <http://doi.org/10.1007/BF00156366>
- Ching, S. H., Bansal, N., & Bhandari, B. (2015). Alginate gel particles- a review of production techniques and physical properties. *Critical Reviews in Food Science and Nutrition*, 0. <http://doi.org/10.1080/10408398.2014.965773>
- Ching, S. H., Bhandari, B., Webb, R., & Bansal, N. (2015). Visualizing the interaction between sodium caseinate and calcium alginate microgel particles. *Food Hydrocolloids*, 43, 165–171.
- Chiou, M.-S., Ho, P.-Y., & Li, H.-Y. (2004). Adsorption of anionic dyes in acid solutions using chemically cross-linked chitosan beads. *Dyes and Pigments*, 60(1), 69–84.
- Correia, C. R., Sher, P., Reis, R. L., & Mano, J. F. (2013). Liquified chitosan–alginate multilayer capsules incorporating poly(L-lactic acid) microparticles as cell carriers. *Soft Matter*, 9(7), 2125–2130. <http://doi.org/10.1039/C2SM26784E>
- Cortez, C., Tomaskovic-Crook, E., Johnston, A. P. R., Scott, A. M., Nice, E. C., Heath, J. K., & Caruso, F. (2007). Influence of size, surface, cell line, and kinetic properties on the specific binding of A33 antigen-targeted multilayered particles and capsules to colorectal cancer cells. *ACS Nano*, 1(2), 93–102. <http://doi.org/10.1021/nn700060m>
- Crini, G. (2005). Recent developments in polysaccharide-based materials used as adsorbents in wastewater treatment. *Progress in Polymer Science*, 30(1), 38–70. <http://doi.org/10.1016/j.progpolymsci.2004.11.002>
- Crini, G. (2006). Non-conventional low-cost adsorbents for dye removal: A review. *Bioresource Technology*, 97(9), 1061–1085.
- Daly, M. M., & Knorr, D. (1988). Chitosan-Alginate Complex Coacervate Capsules: Effects of Calcium Chloride, Plasticizers, and Polyelectrolytes on Mechanical Stability. *Biotechnology Progress*, 4(2), 76–81. <http://doi.org/10.1002/btpr.5420040205>
- Davis, T. A., Volesky, B., & Mucci, A. (2003). A review of the biochemistry of heavy metal biosorption by brown algae. *Water Research*, 37(18), 4311–4330. [http://doi.org/10.1016/S0043-1354\(03\)00293-8](http://doi.org/10.1016/S0043-1354(03)00293-8)
- Decher, G., & Hong, J.-D. (1991). Buildup of ultrathin multilayer films by a self-assembly process, 1 consecutive adsorption of anionic and cationic bipolar amphiphiles on charged surfaces. In *Makromolekulare Chemie. Macromolecular Symposia* (Vol. 46, pp. 321–327). Wiley Online Library. Retrieved from <http://onlinelibrary.wiley.com/doi/10.1002/masy.19910460145/full>
- Decher, G., & Hong, J. D. (1991). Buildup of ultrathin multilayer films by a self-assembly process: II. Consecutive adsorption of anionic and cationic bipolar amphiphiles and polyelectrolytes on charged surfaces. *Berichte Der Bunsengesellschaft Für Physikalische Chemie*, 95(11), 1430–1434.
- Decher, G., Hong, J. D., & Schmitt, J. (1992). Buildup of ultrathin multilayer films by a self-assembly process: III. Consecutively alternating adsorption of anionic and cationic polyelectrolytes on charged surfaces. *Thin Solid Films*, 210, 831–835.

- De Geest, B. G., Déjugnat, C., Prevot, M., Sukhorukov, G. B., Demeester, J., & De Smedt, S. C. (2007). Self-Rupturing and Hollow Microcapsules Prepared from Biopolyelectrolyte-Coated Microgels. *Advanced Functional Materials*, 17(4), 531–537. <http://doi.org/10.1002/adfm.200600198>
- De Geest, B. G., Déjugnat, C., Sukhorukov, G. B., Braeckmans, K., De Smedt, S. C., & Demeester, J. (2005). Self-Rupturing Microcapsules. *Advanced Materials*, 17(19), 2357–2361. <http://doi.org/10.1002/adma.200401951>
- De Geest, B. G., Déjugnat, C., Verhoeven, E., Sukhorukov, G. B., Jonas, A. M., Plain, J., ... De Smedt, S. C. (2006). Layer-by-layer coating of degradable microgels for pulsed drug delivery. *Journal of Controlled Release*, 116(2), 159–169. <http://doi.org/10.1016/j.jconrel.2006.06.016>
- De Geest, B. G., De Koker, S., Demeester, J., De Smedt, S. C., & Hennink, W. E. (2009). Pulsed in vitro release and in vivo behavior of exploding microcapsules. *Journal of Controlled Release: Official Journal of the Controlled Release Society*, 135(3), 268–273. <http://doi.org/10.1016/j.jconrel.2009.01.017>
- De Geest, B. G., Koker, S. D., Demeester, J., Smedt, S. C. D., & Hennink, W. E. (2010). Self-exploding capsules. *Polymer Chemistry*, 1(2), 137–148. <http://doi.org/10.1039/B9PY00287A>
- De Geest, B. G., McShane, M. J., Demeester, J., De Smedt, S. C., & Hennink, W. E. (2008). Microcapsules Ejecting Nanosized Species into the Environment. *Journal of the American Chemical Society*, 130(44), 14480–14482. <http://doi.org/10.1021/ja806574h>
- De Geest, B. G., Stubbe, B. G., Jonas, A. M., Van Thienen, T., Hinrichs, W. L. J., Demeester, J., & De Smedt, S. C. (2006). Self-exploding lipid-coated microgels. *Biomacromolecules*, 7(1), 373–379. <http://doi.org/10.1021/bm0507296>
- De Geest, B. G., Vandenbroucke, R. E., Guenther, A. M., Sukhorukov, G. B., Hennink, W. E., Sanders, N. N., ... De Smedt, S. C. (2006). Intracellularly Degradable Polyelectrolyte Microcapsules. *Advanced Materials*, 18(8), 1005–1009. <http://doi.org/10.1002/adma.200502128>
- Degen, P., Zwar, E., Schulz, I., & Rehage, H. (2015). Magneto-responsive alginate capsules. *Journal of Physics: Condensed Matter*, 27(19), 194105.
- Delcea, M., Möhwald, H., & Skirtach, A. G. (2011). Stimuli-responsive LbL capsules and nanoshells for drug delivery. *Advanced Drug Delivery Reviews*, 63(9), 730–747.
- Derrick, M. (1989). Fourier Transform Infrared Spectral Analysis of Natural Resins Used in Furniture Finishes. *Journal of the American Institute for Conservation*, 28(1), 43–56. <http://doi.org/10.2307/3179466>
- Donath, E., Sukhorukov, G. B., Caruso, F., Davis, S. A., & Möhwald, H. (1998). Novel hollow polymer shells by colloid-templated assembly of polyelectrolytes. *Angewandte Chemie International Edition*, 37(16), 2201–2205.
- Donati, I., Holtan, S., Mørch, Y. A., Borgogna, M., Dentini, M., & Skjåk-Braek, G. (2005). New hypothesis on the role of alternating sequences in calcium-alginate gels. *Biomacromolecules*, 6(2), 1031–1040.
- Dupuy, B., Arien, A., & Minnot, A. P. (1994). FT-IR of membranes made with alginate/polylysine complexes. Variations with the mannuronic or guluronic content of the polysaccharides. *Artificial Cells, Blood Substitutes and Biotechnology*, 22(1), 71–82.
- Draget, K. I., Skjåk-Braek, G., Christensen, B. E., Gåserød, O., & Smidsrød, O. (1996). Swelling and partial solubilization of alginic acid gel beads in acidic buffer. *Carbohydrate Polymers*, 29(3), 209–215. [http://doi.org/10.1016/0144-8617\(96\)00029-X](http://doi.org/10.1016/0144-8617(96)00029-X)

- Draget, K. I., Skjåk Bræk, G., & Smidsrød, O. (1994). Alginic acid gels: the effect of alginate chemical composition and molecular weight. *Carbohydrate Polymers*, 25(1), 31–38. [http://doi.org/10.1016/0144-8617\(94\)90159-7](http://doi.org/10.1016/0144-8617(94)90159-7)
- Draget, K. I., Skjåk-Bræk, G., & Stokke, B. T. (2006). Similarities and differences between alginic acid gels and ionically crosslinked alginate gels. *Food Hydrocolloids*, 20(2–3), 170–175. <http://doi.org/10.1016/j.foodhyd.2004.03.009>
- Draget, K. I., Smidsrød, O., & Skjåk-Bræk, G. (2005). Alginates from Algae. In *Biopolymers Online*. Wiley-VCH Verlag GmbH & Co. KGaA. Retrieved from <http://onlinelibrary.wiley.com/doi/10.1002/3527600035.bpol6008/abstract>
- Drury, J. L., & Mooney, D. J. (2003). Hydrogels for tissue engineering: scaffold design variables and applications. *Biomaterials*, 24(24), 4337–4351. [http://doi.org/10.1016/S0142-9612\(03\)00340-5](http://doi.org/10.1016/S0142-9612(03)00340-5)
- Eiselt, P., Lee, K. Y., & Mooney, D. J. (1999). Rigidity of Two-Component Hydrogels Prepared from Alginate and Poly(ethylene glycol)–Diamines. *Macromolecules*, 32(17), 5561–5566.
- Elçin, Y. M. (1995). Encapsulation of urease enzyme in xanthan-alginate spheres. *Biomaterials*, 16(15), 1157–1161.
- Elzoghby, A. O., El-Fotoh, W. S. A., & Elgindy, N. A. (2011). Casein-based formulations as promising controlled release drug delivery systems. *Journal of Controlled Release*, 153(3), 206–216.
- Ertesvåg, H., & Valla, S. (1998). Biosynthesis and applications of alginates. *Polymer Degradation and Stability*, 59(1–3), 85–91. [http://doi.org/10.1016/S0141-3910\(97\)00179-1](http://doi.org/10.1016/S0141-3910(97)00179-1)
- Farag, Y., & Leopold, C. S. (2011). Development of shellac-coated sustained release pellet formulations. *European Journal of Pharmaceutical Sciences: Official Journal of the European Federation for Pharmaceutical Sciences*, 42(4), 400–405. <http://doi.org/10.1016/j.ejps.2011.01.006>
- Farris, S., Schaich, K. M., Liu, L., Piergiovanni, L., & Yam, K. L. (2009). Development of polyion-complex hydrogels as an alternative approach for the production of bio-based polymers for food packaging applications: a review. *Trends in Food Science & Technology*, 20(8), 316–332. <http://doi.org/10.1016/j.tifs.2009.04.003>
- Fernandes, P. A. L., Delcea, M., Skirtach, A. G., Möhwald, H., & Fery, A. (2010). Quantification of release from microcapsules upon mechanical deformation with AFM. *Soft Matter*, 6(9), 1879–1883. <http://doi.org/10.1039/C002564J>
- Fischer, F. G., & Dörfel, H. (1955). Die polyuronsäuren der braunalgen (Kohlenhydrate der Algen I). *Hoppe-Seyler's Zeitschrift Für Physiologische Chemie*, 302(1-2), 186–203.
- Fu, H., Liu, Y., Adrià, F., Shao, X., Cai, W., & Chipot, C. (2014). From Material Science to Avant-Garde Cuisine. The Art of Shaping Liquids into Spheres. *The Journal of Physical Chemistry B*, 118(40), 11747–11756.
- Gattás-Asfura, K. M., & Stabler, C. L. (2009). Chemoselective Cross-Linking and Functionalization of Alginate via Staudinger Ligation. *Biomacromolecules*, 10(11), 3122–3129. <http://doi.org/10.1021/bm900789a>
- George, M., & Abraham, T. E. (2006). Polyionic hydrocolloids for the intestinal delivery of protein drugs: Alginate and chitosan — a review. *Journal of Controlled Release*, 114(1), 1–14. <http://doi.org/10.1016/j.jconrel.2006.04.017>
- Grant, G. T., Morris, E. R., Rees, D. A., Smith, P. J., & Thom, D. (1973). Biological interactions between polysaccharides and divalent cations: the egg-box model. *FEBS Letters*, 32(1), 195–198.

- Hamad, S. A., Stoyanov, S. D., & Paunov, V. N. (2012). Triggered cell release from shellac–cell composite microcapsules. *Soft Matter*, 8(18), 5069–5077. <http://doi.org/10.1039/C2SM07488E>
- Hameed, B. H., Din, A. M., & Ahmad, A. L. (2007). Adsorption of methylene blue onto bamboo-based activated carbon: kinetics and equilibrium studies. *Journal of Hazardous Materials*, 141(3), 819–825.
- Haug, A. (1964). *Composition and Properties of Alginates*. N.T.H. Trykk.
- Haug, A., Larsen, B., & Smidsrød, O. (1966). A Study of the Constitution of Alginic Acid by Partial Acid Hydrolysis. *Acta Chemica Scandinavica*, 20, 183–190. <http://doi.org/10.3891/acta.chem.scand.20-0183>
- Haug, A., Larsen, B., & Smidsrød, O. (1967a). Alkaline Degradation of Alginate. *Acta Chemica Scandinavica*, 21, 2859–2870. <http://doi.org/10.3891/acta.chem.scand.21-2859>
- Haug, A., Larsen, B., & Smidsrød, O. (1967b). Studies on the Sequence of Uronic Acid Residues in Alginic Acid. *Acta Chemica Scandinavica*, 21, 691–704. <http://doi.org/10.3891/acta.chem.scand.21-0691>
- Haug, A., Myklestad, S., Larsen, B., & Smidsrød, O. (1967). Correlation between Chemical Structure and Physical Properties of Alginates. *Acta Chemica Scandinavica*, 21, 768–778. <http://doi.org/10.3891/acta.chem.scand.21-0768>
- Haug, A., & Smidsrød, O. (1965). Fractionation of Alginates by Precipitation with Calcium and Magnesium Ions. *Acta Chemica Scandinavica*, 19, 1221–1226. <http://doi.org/10.3891/acta.chem.scand.19-1221>
- Haug, A., Smidsrød, O., Högdahl, B., Øye, H. A., Rasmussen, S. E., Sunde, E., & Sørensen, N. A. (1970). Selectivity of Some Anionic Polymers for Divalent Metal Ions. *Acta Chemica Scandinavica*, 24, 843–854. <http://doi.org/10.3891/acta.chem.scand.24-0843>
- Henning, S., Leick, S., Kott, M., Rehage, H., & Suter, D. (2012). Sealing liquid-filled pectinate capsules with a shellac coating. *Journal of Microencapsulation*, 29(2), 147–155.
- Heyman, B., De Vos, W. H., Van der Meeren, P., & Dewettinck, K. (2014). Gums tuning the rheological properties of modified maize starch pastes: Differences between guar and xanthan. *Food Hydrocolloids*, 39, 85–94. <http://doi.org/10.1016/j.foodhyd.2013.12.024>
- Hirst, E. L., Jones, J. K. N., & Jones, W. O. (1939). 389. The structure of alginic acid. Part I. *Journal of the Chemical Society (Resumed)*, (0), 1880–1885. <http://doi.org/10.1039/JR9390001880>
- Hoffman, A. S. (2012). Hydrogels for biomedical applications. *Advanced Drug Delivery Reviews*, 64, Supplement, 18–23. <http://doi.org/10.1016/j.addr.2012.09.010>
- Hong, J. D., Lowack, K., Schmitt, J., & Decher, G. (1993). Layer-by-layer deposited multilayer assemblies of polyelectrolytes and proteins: from ultrathin films to protein arrays. In *Trends in Colloid and Interface Science VII* (pp. 98–102). Springer. Retrieved from <http://link.springer.com/chapter/10.1007/BFb0118482>
- Ho, Y. S., & McKay, G. (1999). Pseudo-second order model for sorption processes. *Process Biochemistry*, 34(5), 451–465. [http://doi.org/10.1016/S0032-9592\(98\)00112-5](http://doi.org/10.1016/S0032-9592(98)00112-5)
- Hu, S.-H., Tsai, C.-H., Liao, C.-F., Liu, D.-M., & Chen, S.-Y. (2008a). Controlled rupture of magnetic polyelectrolyte microcapsules for drug delivery. *Langmuir: The ACS Journal of Surfaces and Colloids*, 24(20), 11811–11818. <http://doi.org/10.1021/la801138e>
- Iler, R. K. (1966). Multilayers of colloidal particles. *Journal of Colloid and Interface Science*, 21(6), 569–594.
- Jeon, O., Bouhadir, K. H., Mansour, J. M., & Alsberg, E. (2009). Photocrosslinked alginate hydrogels with tunable biodegradation rates and mechanical properties. *Biomaterials*, 30(14), 2724–2734. <http://doi.org/10.1016/j.biomaterials.2009.01.034>

- Kim, J.-W., Utada, A. S., Fernández-Nieves, A., Hu, Z., & Weitz, D. A. (2007). Fabrication of monodisperse gel shells and functional microgels in microfluidic devices. *Angewandte Chemie*, *119*(11), 1851–1854.
- King, A. H. (1983). Brown seaweed extracts (alginates). *Food Hydrocolloids*, *2*, 115–188.
- Kosaraju, S. L. (2005). Colon targeted delivery systems: review of polysaccharides for encapsulation and delivery. *Critical Reviews in Food Science and Nutrition*, *45*(4), 251–258. <http://doi.org/10.1080/10408690490478091>
- Koyama, K., & Seki, M. (2004a). Cultivation of yeast and plant cells entrapped in the low-viscous liquid-core of an alginate membrane capsule prepared using polyethylene glycol. *Journal of Bioscience and Bioengineering*, *97*(2), 111–118. [http://doi.org/10.1016/S1389-1723\(04\)70177-2](http://doi.org/10.1016/S1389-1723(04)70177-2)
- Koyama, K., & Seki, M. (2004b). Evaluation of mass-transfer characteristics in alginate-membrane liquid-core capsules prepared using polyethylene glycol. *Journal of Bioscience and Bioengineering*, *98*(2), 114–121. [http://doi.org/10.1016/S1389-1723\(04\)70251-0](http://doi.org/10.1016/S1389-1723(04)70251-0)
- Kuo, C. K., & Ma, P. X. (2001). Ionically crosslinked alginate hydrogels as scaffolds for tissue engineering: part 1. Structure, gelation rate and mechanical properties. *Biomaterials*, *22*(6), 511–521.
- Lagergren, S. *Zur Theorie der sogenannten Absorption gelöster Stoffe, Kungliga Svenska Vetenskapsakad, Handlingar 24, (1898) 1–39.*
- Lawrie, G., Keen, I., Drew, B., Chandler-Temple, A., Rintoul, L., Fredericks, P., & Grøndahl, L. (2007). Interactions between alginate and chitosan biopolymers characterized using FTIR and XPS. *Biomacromolecules*, *8*(8), 2533–2541.
- Lee, K. H., Shin, S. J., Park, Y., & Lee, S.-H. (2009). Synthesis of Cell-Laden Alginate Hollow Fibers Using Microfluidic Chips and Microvascularized Tissue-Engineering Applications. *Small*, *5*(11), 1264–1268. <http://doi.org/10.1002/smll.200801667>
- Lee, K. Y., & Mooney, D. J. (2012). Alginate: properties and biomedical applications. *Progress in Polymer Science*, *37*(1), 106–126.
- Lee, K. Y., Rowley, J. A., Eiselt, P., Moy, E. M., Bouhadir, K. H., & Mooney, D. J. (2000). Controlling Mechanical and Swelling Properties of Alginate Hydrogels Independently by Cross-Linker Type and Cross-Linking Density. *Macromolecules*, *33*(11), 4291–4294. <http://doi.org/10.1021/ma9921347>
- Legrand, P., Benoit, J.-P., Briançon, S., Fattal, E., Fessi, H., & Passirani, C. (2007). Sphéroïdes et formes vectorisées. *Pharmacie Galénique: Formulation et Technologie Pharmaceutique*, 221–250.
- Leick, S., Henning, S., Degen, P., Suter, D., & Rehage, H. (2010). Deformation of liquid-filled calcium alginate capsules in a spinning drop apparatus. *Physical Chemistry Chemical Physics: PCCP*, *12*(12), 2950–2958. <http://doi.org/10.1039/b921116k>
- Leick, S., Kemper, A., & Rehage, H. (2011). Alginate/poly-L-lysine capsules: mechanical properties and drug release characteristics. *Soft Matter*, *7*(14), 6684–6694. <http://doi.org/10.1039/C1SM05676J>
- Leick, S., Kott, M., Degen, P., Henning, S., Päsler, T., Suter, D., & Rehage, H. (2011). Mechanical properties of liquid-filled shellac composite capsules. *Physical Chemistry Chemical Physics*, *13*(7), 2765–2773. <http://doi.org/10.1039/C0CP01803A>
- Leong, J.-Y., Tey, B.-T., Tan, c., & Chan, E.-S. (2015). Nozzleless Fabrication of Oil-Core Biopolymeric Microcapsules by the Interfacial Gelation of Pickering Emulsion Templates. *ACS Applied Materials & Interfaces*. Retrieved from <http://pubs.acs.org/doi/abs/10.1021/acsami.5b04486>

- Lertsutthiwong, P., Noomun, K., Jongaroonngamsang, N., Rojsitthisak, P., & Nimmannit, U. (2008). Preparation of alginate nanocapsules containing turmeric oil. *Carbohydrate Polymers*, 74(2), 209–214. <http://doi.org/10.1016/j.carbpol.2008.02.009>
- Lim, F., & Sun, A. M. (1980). Microencapsulated islets as bioartificial endocrine pancreas. *Science (New York, N.Y.)*, 210(4472), 908–910.
- Limmatvapirat, S., Limmatvapirat, C., Luangtana-anan, M., Nunthanid, J., Oguchi, T., Tozuka, Y., ... Puttipipatkachorn, S. (2004). Modification of physicochemical and mechanical properties of shellac by partial hydrolysis. *International Journal of Pharmaceutics*, 278(1), 41–49. <http://doi.org/10.1016/j.ijpharm.2004.02.030>
- Liu, L., Wan, Y., Xie, Y., Zhai, R., Zhang, B., & Liu, J. (2012). The removal of dye from aqueous solution using alginate-halloysite nanotube beads. *Chemical Engineering Journal*, 187, 210–216.
- Lund, W. (1994). *Suspensions. The pharmaceutical codex: principles and practice of pharmaceutics*. London: The Pharmaceutical Press.
- Lu, T., Xiang, T., Huang, X.-L., Li, C., Zhao, W.-F., Zhang, Q., & Zhao, C.-S. (2015). Post-crosslinking towards stimuli-responsive sodium alginate beads for the removal of dye and heavy metals. *Carbohydrate Polymers*, 133, 587–595. <http://doi.org/10.1016/j.carbpol.2015.07.048>
- Madene, A. (2006). *Etude des Transferts d'Arômes Encapsulés dans une Matrice Alimentaire type Génoise*. Institut National Polytechnique de Lorraine. Retrieved from [http://pegase.scd.inpl-nancy.fr/theses/2006\\_MADENE\\_A.pdf](http://pegase.scd.inpl-nancy.fr/theses/2006_MADENE_A.pdf)
- Madene, A., Jacquot, M., Scher, J., & Desobry, S. (2006). Flavour encapsulation and controlled release – a review. *International Journal of Food Science & Technology*, 41(1), 1–21. <http://doi.org/10.1111/j.1365-2621.2005.00980.x>
- Mahmoodi, N. M. (2011). Equilibrium, kinetics, and thermodynamics of dye removal using alginate in binary systems. *Journal of Chemical & Engineering Data*, 56(6), 2802–2811.
- Martins, E., Renard, D., Davy, J., Marquis, M., & Poncelet, D. (2015). Oil core microcapsules by inverse gelation technique. *Journal of Microencapsulation*, 32(1), 86–95. <http://doi.org/10.3109/02652048.2014.985342>
- Mei, L., Xie, R., Yang, C., Ju, X.-J., Wang, J.-Y., Zhang, Z., & Chu, L.-Y. (2013). Bio-inspired mini-eggs with pH-responsive membrane for enzyme immobilization. *Journal of Membrane Science*, 429, 313–322.
- Mei, L., Xie, R., Yang, C., Ju, X.-J., Wang, W., Wang, J.-Y., & Chu, L.-Y. (2013). pH-responsive Ca-alginate-based capsule membranes with grafted poly (methacrylic acid) brushes for controllable enzyme reaction. *Chemical Engineering Journal*, 232, 573–581.
- Mele, E., Fragouli, D., Ruffilli, R., Gregorio, G. L. D., Cingolani, R., & Athanassiou, A. (2013). Complex architectures formed by alginate drops floating on liquid surfaces. *Soft Matter*, 9(27), 6338–6343. <http://doi.org/10.1039/C3SM27847F>
- Moe, S. T., Skjaak-Braek, G., Elgsaeter, A., & Smidsroed, O. (1993). Swelling of covalently crosslinked alginate gels: influence of ionic solutes and nonpolar solvents. *Macromolecules*, 26(14), 3589–3597.
- Mørch, Y. A., Donati, I., Strand, B. L., & Skjåk-Braek, G. (2006). Effect of Ca<sup>2+</sup>, Ba<sup>2+</sup>, and Sr<sup>2+</sup> on alginate microbeads. *Biomacromolecules*, 7(5), 1471–1480. <http://doi.org/10.1021/bm060010d>
- Motornov, M., Roiter, Y., Tokarev, I., & Minko, S. (2010). Stimuli-responsive nanoparticles, nanogels and capsules for integrated multifunctional intelligent systems. *Progress in Polymer Science*, 35(1–2), 174–211. <http://doi.org/10.1016/j.progpolymsci.2009.10.004>

- Ngah, W. W., Teong, L. C., & Hanafiah, M. (2011). Adsorption of dyes and heavy metal ions by chitosan composites: A review. *Carbohydrate Polymers*, 83(4), 1446–1456.
- Nigam, S. C., Tsao, I.-F., Sakoda, A., & Wang, H. Y. (1988). Techniques for preparing hydrogel membrane capsules. *Biotechnology Techniques*, 2(4), 271–276.
- Nussinovitch, A., Gershon, Z., & Nussinovitch, M. (1996). Liquid-core hydrocolloid capsules. *Food Hydrocolloids*, 10(1), 21–26.
- Ong, H.-Y., Lee, B.-B., Radzi, A. M., Zakaria, Z., & Chan, E.-S. (2015). A comparative study on liquid core formulation on the diameter on the alginate capsules. In *AIP Conference Proceedings* (Vol. 1674, p. 020009). AIP Publishing. <http://doi.org/10.1063/1.4928826>
- Paques, J. P., van der Linden, E., van Rijn, C. J. M., & Sagis, L. M. C. (2014). Preparation methods of alginate nanoparticles. *Advances in Colloid and Interface Science*, 209, 163–171. <http://doi.org/10.1016/j.cis.2014.03.009>
- Park, J. H., Saravanakumar, G., Kim, K., & Kwon, I. C. (2010). Targeted delivery of low molecular drugs using chitosan and its derivatives. *Advanced Drug Delivery Reviews*, 62(1), 28–41. <http://doi.org/10.1016/j.addr.2009.10.003>
- Park, J. K., & Chang, H. N. (2000). Microencapsulation of microbial cells. *Biotechnology Advances*, 18(4), 303–319.
- Patel, A. R., Remijn, C., Cabero, A. M., Heussen, P. C. M., Hoorn, J. W. M. S. ten, & Velikov, K. P. (2013). Novel All-Natural Microcapsules from Gelatin and Shellac for Biorelated Applications. *Advanced Functional Materials*, 23(37), 4710–4718. <http://doi.org/10.1002/adfm.201300320>
- Patel, A. R., Schatteman, D., Vos, W. H. D., & Dewettinck, K. (2013). Shellac as a natural material to structure a liquid oil-based thermo reversible soft matter system. *RSC Advances*, 3(16), 5324–5327.
- Patel, A. V., Pusch, I., Mix-Wagner, G., & Vorlop, K. D. (2000). A novel encapsulation technique for the production of artificial seeds. *Plant Cell Reports*, 19(9), 868–874. <http://doi.org/10.1007/s002990000223>
- Pawar, S. N., & Edgar, K. J. (2012). Alginate derivatization: A review of chemistry, properties and applications. *Biomaterials*, 33(11), 3279–3305. <http://doi.org/10.1016/j.biomaterials.2012.01.007>
- Pearchob, N., & Bodmeier, R. (2003). Dry polymer powder coating and comparison with conventional liquid-based coatings for Eudragit) RS, ethylcellulose and shellac. *European Journal of Pharmaceutics and Biopharmaceutics: Official Journal of Arbeitsgemeinschaft Für Pharmazeutische Verfahrenstechnik e.V.*, 56(3), 363–369.
- Perez-Ameneiro, M., Vecino, X., Barbosa-Pereira, L., Cruz, J. M., & Moldes, A. B. (2014). Removal of pigments from aqueous solution by a calcium alginate–grape marc biopolymer: A kinetic study. *Carbohydrate Polymers*, 101, 954–960.
- Phawaphuthanon, N., Behnam, S., Koo, S. Y., Pan, C.-H., & Chung, D. (2014). Characterization of core–shell calcium-alginate macrocapsules fabricated by electro-coextrusion. *International Journal of Biological Macromolecules*, 65, 267–274.
- Pillai, C. K. S., Paul, W., & Sharma, C. P. (2009). Chitin and chitosan polymers: Chemistry, solubility and fiber formation. *Progress in Polymer Science*, 34(7), 641–678. <http://doi.org/10.1016/j.progpolymsci.2009.04.001>
- Pongjanyakul, T., & Puttipipatkachorn, S. (2007). Xanthan-alginate composite gel beads: molecular interaction and in vitro characterization. *International Journal of Pharmaceutics*, 331(1), 61–71. <http://doi.org/10.1016/j.ijpharm.2006.09.011>
- Qiu, Y., & Park, K. (2012). Environment-sensitive hydrogels for drug delivery. *Advanced Drug Delivery Reviews*, 64, 49–60.



- Ren, P.-W., Ju, X.-J., Xie, R., & Chu, L.-Y. (2010). Monodisperse alginate microcapsules with oil core generated from a microfluidic device. *Journal of Colloid and Interface Science*, *343*(1), 392–395.
- Robinson, T., Chandran, B., & Nigam, P. (2002). Removal of dyes from an artificial textile dye effluent by two agricultural waste residues, corncob and barley husk. *Environment International*, *28*(1–2), 29–33. [http://doi.org/10.1016/S0160-4120\(01\)00131-3](http://doi.org/10.1016/S0160-4120(01)00131-3)
- Robinson, T., McMullan, G., Marchant, R., & Nigam, P. (2001). Remediation of dyes in textile effluent: a critical review on current treatment technologies with a proposed alternative. *Bioresource Technology*, *77*(3), 247–255. [http://doi.org/10.1016/S0960-8524\(00\)00080-8](http://doi.org/10.1016/S0960-8524(00)00080-8)
- Rocher, V., Bee, A., Siaugue, J.-M., & Cabuil, V. (2010). Dye removal from aqueous solution by magnetic alginate beads crosslinked with epichlorohydrin. *Journal of Hazardous Materials*, *178*(1), 434–439.
- Rocher, V., Siaugue, J.-M., Cabuil, V., & Bee, A. (2008). Removal of organic dyes by magnetic alginate beads. *Water Research*, *42*(4–5), 1290–1298. <http://doi.org/10.1016/j.watres.2007.09.024>
- Rolland, L., Santanach-Carreras, E., Delmas, T., Bibette, J., & Bremond, N. (2014). Physicochemical properties of aqueous core hydrogel capsules. *Soft Matter*, *10*(48), 9668–9674.
- Rosiak, J. M., & Yoshii, F. (1999). Hydrogels and their medical applications. *Nuclear Instruments and Methods in Physics Research Section B: Beam Interactions with Materials and Atoms*, *151*(1–4), 56–64. [http://doi.org/10.1016/S0168-583X\(99\)00118-4](http://doi.org/10.1016/S0168-583X(99)00118-4)
- Sabra, W., Zeng, A. P., & Deckwer, W. D. (2001). Bacterial alginate: physiology, product quality and process aspects. *Applied Microbiology and Biotechnology*, *56*(3-4), 315–325.
- Sankalia, M. G., Mashru, R. C., Sankalia, J. M., & Sutariya, V. B. (2007). Reversed chitosan–alginate polyelectrolyte complex for stability improvement of alpha-amylase: Optimization and physicochemical characterization. *European Journal of Pharmaceutics and Biopharmaceutics*, *65*(2), 215–232. <http://doi.org/10.1016/j.ejpb.2006.07.014>
- Sartori, C., Finch, D. S., Ralph, B., & Gilding, K. (1997). Determination of the cation content of alginate thin films by FTi.r. spectroscopy. *Polymer*, *38*(1), 43–51. [http://doi.org/10.1016/S0032-3861\(96\)00458-2](http://doi.org/10.1016/S0032-3861(96)00458-2)
- Sato, K., Hoshina, S., & Anzai, J. (2011). Preparation of polyelectrolyte giant capsules using cross-linked alginate gels as core material. *Polymer Bulletin*, *68*(3), 891–900. <http://doi.org/10.1007/s00289-011-0670-1>
- Schmidt, E., & Vocke, F. (1926). Zur Kenntnis der Polyglykuronsäuren (I.). *Berichte Der Deutschen Chemischen Gesellschaft (A and B Series)*, *59*(7), 1585–1588. <http://doi.org/10.1002/cber.19260590735>
- Shah, R. K., Kim, J.-W., Agresti, J. J., Weitz, D. A., & Chu, L.-Y. (2008). Fabrication of monodisperse thermosensitive microgels and gel capsules in microfluidic devices. *Soft Matter*, *4*(12), 2303–2309.
- Shen, H., Shi, H., Xie, M., Ma, K., Li, B., Shen, S., ... Jin, Y. (2013). Biodegradable chitosan/alginate BSA-gel-capsules for pH-controlled loading and release of doxorubicin and treatment of pulmonary melanoma. *Journal of Materials Chemistry B*, *1*(32), 3906–3917.

- Shilpa, A., Agrawal, S. S., & Ray, A. R. (2003). Controlled Delivery of Drugs from Alginate Matrix. *Journal of Macromolecular Science, Part C: Polymer Reviews*, 43(2), 187–221. <http://doi.org/10.1081/MC-120020160>
- Shin, S.-J., Park, J.-Y., Lee, J.-Y., Park, H., Park, Y.-D., Lee, K.-B., ... Lee, S.-H. (2007). “On the Fly” Continuous Generation of Alginate Fibers Using a Microfluidic Device. *Langmuir*, 23(17), 9104–9108. <http://doi.org/10.1021/la700818q>
- Skj, G., Grasdalen, H., Larsen, B., & others. (1986). Monomer sequence and acetylation pattern in some bacterial alginates. *Carbohydrate Research*, 154(1), 239–250.
- Smidsrød, O. (1974). Molecular basis for some physical properties of alginates in the gel state. *Faraday Discussions of the Chemical Society*, 57(0), 263–274. <http://doi.org/10.1039/DC9745700263>
- Smidsrød, O., & Skjåk-Braek, G. (1990). Alginate as immobilization matrix for cells. *Trends in Biotechnology*, 8(3), 71–78.
- Stanford, E. C. . (1881). British patent.
- Stanford, E. C. C. (1883). Algin: A New Substance Obtained from Some of the Commoner Species of Marine Algæ. *Scientific American*, 16, 6323–6324.
- Stendahl, J. C., Rao, M. S., Guler, M. O., & Stupp, S. I. (2006). Intermolecular forces in the self-assembly of peptide amphiphile nanofibers. *Advanced Functional Materials*, 16(4), 499–508.
- Stephen, A. M., & Phillips, G. O. (2006). *Food Polysaccharides and Their Applications*. CRC Press.
- Still, T., Sainidou, R., Retsch, M., Jonas, U., Spahn, P., Hellmann, G. P., & Fytas, G. (2008). The “Music” of Core–Shell Spheres and Hollow Capsules: Influence of the Architecture on the Mechanical Properties at the Nanoscale. *Nano Letters*, 8(10), 3194–3199. <http://doi.org/10.1021/nl801500n>
- Stokke, B. T., Draget, K. I., Smidsrød, O., Yuguchi, Y., Urakawa, H., & Kajiwarra, K. (2000). Small-Angle X-ray Scattering and Rheological Characterization of Alginate Gels. 1. Ca–Alginate Gels. *Macromolecules*, 33(5), 1853–1863. <http://doi.org/10.1021/ma991559q>
- Sukhorukov, G. B., Volodkin, D. V., Günther, A. M., Petrov, A. I., Shenoy, D. B., & Möhwald, H. (2004). Porous calcium carbonate microparticles as templates for encapsulation of bioactive compounds. *Journal of Materials Chemistry*, 14(14), 2073–2081.
- Taqiuddin, E., & Amiji, M. (2004). Enzyme immobilization in novel alginate–chitosan core-shell microcapsules. *Biomaterials*, 25(10), 1937–1945.
- Thu, B., Bruheim, P., Espevik, T., Smidsrød, O., Soon-Shiong, P., & Skjåk-Braek, G. (1996). Alginate polycation microcapsules. I. Interaction between alginate and polycation. *Biomaterials*, 17(10), 1031–1040.
- Topuz, F., Henke, A., Richtering, W., & Groll, J. (2012). Magnesium ions and alginate do form hydrogels: a rheological study. *Soft Matter*, 8(18), 4877–4881. <http://doi.org/10.1039/C2SM07465F>
- Tumarkin, E., & Kumacheva, E. (2009). Microfluidic generation of microgels from synthetic and natural polymers. *Chemical Society Reviews*, 38(8), 2161–2168.
- Vandamme, T., Poncelet, D., & Subra-Paternault, P. (2007). Microencapsulation: des sciences aux technologies.
- Vecino, X., Devesa-Rey, R., Cruz, J. M., & Moldes, A. B. (2015). Study of the physical properties of calcium alginate hydrogel beads containing vineyard pruning waste for dye removal. *Carbohydrate Polymers*, 115, 129–138. <http://doi.org/10.1016/j.carbpol.2014.08.088>

- Verma, G., & Hassan, P. A. (2013). Self-assembled materials: design strategies and drug delivery perspectives. *Physical Chemistry Chemical Physics*, *15*(40), 17016–17028.
- Voo, W.-P., Lee, B.-B., Idris, A., Islam, A., Tey, B.-T., & Chan, E.-S. (2015). Production of ultra-high concentration calcium alginate beads with prolonged dissolution profile. *RSC Advances*, *5*(46), 36687–36695. <http://doi.org/10.1039/C5RA03862F>
- Walstra, P., Jenness, R., & others. (1984). *Dairy chemistry & physics*. John Wiley & Sons. Retrieved from <http://www.cabdirect.org/abstracts/19860407993.html>
- Wang, J.-Y., Jin, Y., Xie, R., Liu, J.-Y., Ju, X.-J., Meng, T., & Chu, L.-Y. (2011). Novel calcium-alginate capsules with aqueous core and thermo-responsive membrane. *Journal of Colloid and Interface Science*, *353*(1), 61–68.
- Wee, null, & Gombotz, null. (1998). Protein release from alginate matrices. *Advanced Drug Delivery Reviews*, *31*(3), 267–285.
- Whitesides, G. M. (2006). The origins and the future of microfluidics. *Nature*, *442*(7101), 368–373.
- Xue, J., & Zhang, Z. (2008). Preparation and characterization of calcium-shellac spheres as a carrier of carbamide peroxide. *Journal of Microencapsulation*, *25*(8), 523–530.
- Xue, J., & Zhang, Z. (2009). Physical, structural, and mechanical characterization of calcium-shellac microspheres as a carrier of carbamide peroxide. *Journal of Applied Polymer Science*, *113*(3), 1619–1625. <http://doi.org/10.1002/app.30090>
- Ye, S., Wang, C., Liu, X., & Tong, Z. (2005). Deposition temperature effect on release rate of indomethacin microcrystals from microcapsules of layer-by-layer assembled chitosan and alginate multilayer films. *Journal of Controlled Release*, *106*(3), 319–328. <http://doi.org/10.1016/j.jconrel.2005.05.006>
- Zelzer, M., Todd, S. J., Hirst, A. R., McDonald, T. O., & Ulijn, R. V. (2012). Enzyme responsive materials: design strategies and future developments. *Biomaterials Science*, *1*(1), 11–39. <http://doi.org/10.1039/C2BM00041E>
- Zhang, F., Wu, Q., Chen, Z.-C., Zhang, M., & Lin, X.-F. (2008). Hepatic-targeting microcapsules construction by self-assembly of bioactive galactose-branched polyelectrolyte for controlled drug release system. *Journal of Colloid and Interface Science*, *317*(2), 477–484. <http://doi.org/10.1016/j.jcis.2007.09.065>
- Zhu, H., Srivastava, R., Brown, J. Q., & McShane, M. J. (2005). Combined physical and chemical immobilization of glucose oxidase in alginate microspheres improves stability of encapsulation and activity. *Bioconjugate Chemistry*, *16*(6), 1451–1458. <http://doi.org/10.1021/bc050171z>
- Zhu, H., Srivastava, R., & McShane, M. J. (2005). Spontaneous Loading of Positively Charged Macromolecules into Alginate-Templated Polyelectrolyte Multilayer Microcapsules. *Biomacromolecules*, *6*(4), 2221–2228. <http://doi.org/10.1021/bm0501656>
- Zhu, M.-L., Li, Y.-L., Zhang, Z.-M., & Jiang, Y. (2015). Preparation and properties of stretchable and tough alginate/polyacrylamide hollow capsules. *RSC Advances*, *5*(42), 33262–33268. <http://doi.org/10.1039/C5RA03465E>

## **Structuration et contrôle de l'architecture de capsules à coeur liquide à base d'hydrogel d'alginate par association de biopolymères.**

### **Résumé:**

Cette thèse a pour objectif d'étudier les propriétés physico-chimiques de capsules à cœur liquide à base d'hydrogel d'alginate et de contrôler leur perméabilité et propriétés mécaniques par ajout des biopolymères. Ces capsules millimétriques sont préparées par un procédé de sphérification inverse par extrusion goutte à goutte d'une solution de chlorure de calcium dans un bain de gélification à base d'alginate. Dans un premier travail, l'influence des polymères utilisés pour contrôler la viscosité du cœur liquide (agent épaississant) lors de la préparation des capsules sur la perméabilité et la stabilité mécanique de la membrane d'alginate a été étudiée. Les propriétés mécaniques des capsules ont été corrélées avec les propriétés viscoélastiques d'hydrogels d'alginate caractérisés par rhéologie oscillatoire aux faibles amplitudes. Un second travail, a consisté à élaborer des capsules composites avec une membrane de caséinate de sodium/alginate qui présentent une meilleure stabilité et une libération pH-dépendante d'un colorant utilisé comme molécule modèle. Comme perspective à cette étude, des hydrogels sphériques (microsphères) à base d'alginate et de caséinate de sodium, avec différentes architecture ont été développés et leur efficacité a été testée sur trois colorants anioniques. Ce type de système trouve des applications dans l'élimination des colorants à partir des rejets industriels par un mécanisme d'adsorption. Enfin, l'influence de l'incorporation de la gomme laque dans la membrane ou comme revêtement externe a permis de mettre en évidence une amélioration des propriétés barrières vis-à-vis de molécules de faible masse moléculaire (riboflavine dans ce cas). Les capsules à base d'alginate ont un large spectre d'utilisation allant de la cuisine moléculaire à la biotechnologie ce qui nécessite une meilleure compréhension et contrôle de leurs propriétés physicochimiques en fonction de l'application visée.

***Mots-clés:** Capsules à cœur liquide; hydrogel d'alginate; biopolymères; sphérification inverse; propriétés mécaniques; perméabilité.*

### **Abstract:**

The aim of this thesis is to study the physicochemical properties of alginate liquid-core capsules and to control their permeability and mechanical properties by biopolymers blending. These millimeter-scale size capsules are prepared by a reverse spherification process by dripping a solution of calcium chloride into an alginate gelling bath. In a first work, the influence of polymers used to control capsule liquid-core viscosity (thickening agent) during capsules preparation on permeability and mechanical stability of the alginate membrane was investigated. The mechanical properties of capsules were correlated with viscoelastic properties of plane alginate hydrogels characterized by small amplitude oscillatory shear rheology. In a second work, composite capsules with a membrane of sodium caseinate / alginate were developed and showed improved stability and pH-dependent release of a dye used as a model molecule. As perspective to this study, composite alginate/sodium caseinate microspheres with different architectures were developed and their effectiveness was tested against three anionic dyes. This type of system has applications in the removal of dyes from industrial wastewater by an adsorption mechanism. Finally, the influence of shellac incorporation in alginate membrane or as an external coating layer resulted in enhanced physicochemical properties and decreased membrane permeability against low molecular weight molecules (riboflavin in this case). Alginate capsules have a wide range of applications ranging from molecular gastronomy to biotechnology which requires a better understanding and control of their physicochemical properties according to the target application.

***Keywords:** liquid-core capsules; alginate hydrogel; biopolymers; reverse spherification; mechanical properties, permeability*